

1988

## The effect of antecedent wetness on flow instability during infiltration into layered soil /

David Mark Edelstein  
*University of Massachusetts Amherst*

Follow this and additional works at: <https://scholarworks.umass.edu/theses>

---

Edelstein, David Mark, "The effect of antecedent wetness on flow instability during infiltration into layered soil /" (1988). *Masters Theses 1911 - February 2014*. 3405.  
Retrieved from <https://scholarworks.umass.edu/theses/3405>

This thesis is brought to you for free and open access by ScholarWorks@UMass Amherst. It has been accepted for inclusion in Masters Theses 1911 - February 2014 by an authorized administrator of ScholarWorks@UMass Amherst. For more information, please contact [scholarworks@library.umass.edu](mailto:scholarworks@library.umass.edu).

UMASS/AMHERST



312066014839473

The Effect of Antecedent Wetness  
on Flow Instability During  
Infiltration into  
Layered Soil

A Thesis Presented

by

David Mark Edelstein

Submitted to the Graduate School of the  
University of Massachusetts in partial fulfillment  
of the requirements for the degree of

MASTER OF SCIENCE

February 1988

Department of Plant and Soil Sciences

The Effect of Antecedent Wetness  
on Flow Instability During  
Infiltration into  
Layered Soil

A Thesis Presented

by

David Mark Edelstein

Approved as to style and content by:

*Daniel Hillel*

-----  
Daniel Hillel, Chairperson of Committee

*Haim Gunner*

-----  
Haim Gunner, Member

*David Ostendorf*

-----  
David Ostendorf, Member

*John Baker*

-----  
John Baker, Department Head

Department of Plant and Soil Science

## Acknowledgements

This thesis does not represent the work of one lone student studying soil processes in a vacuum. The intellectual and emotional support of many people fill these pages, and it is my great pleasure to be able to thank them.

Dr. Daniel Hillel has been my adviser during my studies at the University of Massachusetts, guiding me through this study of unstable flow. Dr. Hillel has never missed an opportunity to challenge my perseverance and test my intellectual maturity, and I am grateful to him for adding this structure to my thought.

My thesis committee is composed of two men I admire greatly, Dr. David Ostendorf and Dr. Haim Gunner. While taking Dr. Ostendorf's hydrology course, I watched him discover a mathematical order in the chaos of nature. To my great relief, he was also able to find order in the chaotic early versions of this thesis. Dr. Gunner has worked continually to assuage my fears and anxieties as I undertook this project. I believe that he personifies the much loved Yiddish word, "mensch."

My partner in the soil physics lab, Ralph Baker, made much of the experimentation and thought described in this thesis possible. There is no idea or work in this project that he did not help to create, and he wrote computer programs to evaluate results which would still be raw data



without such programs. I thank him for his patience in working with a very headstrong lab partner.

I have never been comfortable working around computers, but Dr. Robert Gonter, Trina Hosmer, and Pat Kochin of the University Computing Center made it possible for me to do so. Dr. Gonter wrote two programs I needed desperately, and did it with such aplomb as to impress me that there is great art in computer science. Trina Hosmer gave me hours of her time to organize pages of raw data into a statistical framework, and actually got me to understand how to get the computer to analyze my data for me; I feel as though I have been introduced to one of higher education's great mysteries. Pat Kochin helped me with the word processing which made the writing of this paper almost painless, even for a person who does not know how to type.

Emotional support is a wonderful thing at times of great stress, and I am thankful that the people I love came through with plenty of it. My parents, grandparents, and brothers have withstood nearly thirty years of idiosyncratic behavior from me, and are satisfied with whatever achievements I can claim as their reward. Theirs has been a difficult task, but never a thankless one: my gratitude to them is as great as my love for them.

Friends also listened to the moans and groans of this agonized degree candidate. My roommates, Karen Wesler and Elyse Holsberg, have provided me with a high quality home

life for the past year and a half. I have also been strengthened in hope and resolve through the kindness of Michael Inserra and Ginny Davis.

## Abstract

### The Effect of Antecedent Wetness on Flow Instability During Infiltration into Layered Soil

February, 1988

David Mark Edelstein, B.A., Harvard College  
M.A., University of Massachusetts

Directed by: Professor Daniel I. Hillel

Flow instability has been cited as a possible cause of accelerated groundwater pollution. Instability takes the form of narrow, rapidly moving streams of water referred to as "fingers." An approximately two dimensional cell was filled with layers of sand, wetting front patterns during infiltration into the cell were observed, and the hydraulic properties of the sands were tested. A layer of fine textured sand overlying a layer of coarse textured sand can cause fingers in the coarse textured layer. Uniform antecedent wetness can prevent the appearance of fingers in the same sequence of layers. If wetness varies horizontally, fingers may form in the driest regions. If wetness varies with depth, fingers will form in dry regions but not in wet regions, regardless of whether wetness increases or decreases with depth. The width and speed of fingers can be correlated to the soil's mean particle size and initial wetness, which affect the following hydraulic



properties of the soil: height of capillary rise,  
sorptivity, diffusivity, and conductivity.

## Table of Contents

Acknowledgements.....	iii
Abstract.....	vi
List of Tables.....	x
Table of Figures.....	xi

Chapter	Page
I. Introduction	1
A. Research objective.....	1
B. Relevance.....	1
C. Present approach.....	3
II. Literature Review.....	6
A. Overview of the problem.....	6
B. Laboratory experiments.....	6
C. Field experiments.....	10
D. Theoretical considerations.....	11
III. Methods and Materials.....	19
A. Cell construction and packing.....	19
B. Water delivery and experimental procedure...	26
C. Soil hydraulic properties.....	30
IV. Results.....	37
A. Uniform initial wetness experiments.....	37
B. Variable initial wetness experiments.....	63
C. Point source infiltration experiments.....	70

D.	Hydraulic properties.....	91
V.	Discussion.....	99
A.	Uniform initial wetness experiments.....	99
B.	Variable initial wetness experiments.....	103
C.	Point source experiments.....	107
D.	Hydraulic properties.....	109
VI.	Conclusions.....	113
Appendices		
A.	Quality Control.....	115
B.	Sorptivity Data and Programs.....	117
C.	Conductivity Program.....	122
	Bibliography.....	127

## List of Tables

Table	Page
4.1 Layered soil infiltration experiments.....	39
4.2 Point source infiltration experiments.....	72
4.3 Conductivity.....	96
4.4 Diffusivity and Sorptivity.....	97
ANOVA 1: Density.....	115
ANOVA 2: Wetness.....	116
A.1 Sorptivity Data.....	117

## Table of Figures

Figure	Page
3.1 The packed experimental cell in support structure with Mariotte device.....	28
4.1 Run 1, 19% of actual size.....	40
4.2 Run 2, 19% of actual size.....	41
4.3 Run 3, 19% of actual size.....	42
4.4 Run 4, 19% of actual size.....	43
4.5 Run 5, 19% of actual size.....	44
4.6 Run 6, 19% of actual size.....	45
4.7 Run 7, 19% of actual size.....	46
4.8 Run 8, 19% of actual size.....	47
4.9 Run 9, 19% of actual size.....	48
4.10 Run 10, 19% of actual size.....	49
4.11 Run 11, 19% of actual size.....	50
4.12 Run 12, 19% of actual size.....	51
4.13 Initial wetness vs. finger width, layered soil experiments.....	52
4.14 Initial wetness vs. finger speed, layered soil experiments.....	53
4.15 Finger width vs. finger speed, layered soil experiments.....	54
4.16 Regression of $(\text{time})^{1/2}$ vs. cumulative infiltration in layered soil experiments in an air dry condition.....	55
4.17 Regression of $(\text{time})^{1/2}$ vs. cumulative infiltration in layered soil experiments at first incremental increase in initial wetness.....	56
4.18 Regression of $(\text{time})^{1/2}$ vs. cumulative infiltration in layered soil experiments,	



second incremental increase in initial wetness.....	57
4.19 Regression of (time) <sup>1/2</sup> vs. cumulative infiltration in layered soil experiments, final incremental increase in initial wetness.....	58
4.20 Multiple stepwise regression, ln (finger width) in layered soil experiments..	59
4.21 Multiple stepwise regression, ln (finger speed) in layered soil experiments..	60
4.22 Run 13, 19% of actual size.....	65
4.23 Run 14, 19% of actual size.....	66
4.24 Run 15, 19% of actual size.....	67
4.25 Run 16, 19% of actual size.....	68
4.26 Run 17, 19% of actual size.....	73
4.27 Run 18, 19% of actual size.....	74
4.28 Run 19, 19% of actual size.....	75
4.29 Run 20, 19% of actual size.....	76
4.30 Run 21, 19% of actual size.....	77
4.31 Run 22, 19% of actual size.....	78
4.32 Run 23, 19% of actual size.....	79
4.33 Run 24, 19% of actual size.....	80
4.34 Run 25, 19% of actual size.....	81
4.35 Run 26, 19% of actual size.....	82
4.36 Flux vs. finger width, point source experiments.....	83
4.37 Flux vs. finger speed, point source experiments.....	84
4.38 Initial wetness vs. finger width, point source experiments.....	85

4.39	Multiple stepwise regression, ln (finger width), point source experiments....	86
4.40	Initial wetness vs. finger speed, point source experiments.....	87
4.41	Finger width vs. finger speed, point source experiments.....	88
4.42	Multiple stepwise regression, ln (finger speed) in point source experiments..	89
4.43	Soil moisture characteristic curve for 1.00-2.00 mm sand.....	92
4.44	Soil moisture characteristic curve for .500-.710 mm sand.....	93
4.45	Soil moisture characteristic curve for .355-.500 mm sand.....	94
4.46	Soil moisture characteristic curve for .047-.105 mm sand.....	95

## I. Introduction

### A. Research objective

Our investigation focuses on the movement of liquids in layered soils by unstable flow. In such a situation, the wetting front could break into "fingers" or "pipes." Water might then move through such fingers at the faster rate associated with the saturated conductivity of the least restrictive, rather than the most restrictive, soil layer.

Conversely, the presence of small amounts of initial moisture has been predicted to stabilize the wetting front and eliminate fingering. If this were true, it would be important to determine what had been changed by the addition of water to the coarse sublayer.

### B. Relevance

Water movement in soil is of vital interest to both agricultural and environmental planners. Agronomists hope to maintain the balance between soil air and soil water so that crops can attain maximum growth in a soil that is well aerated without being droughty. Environmentalists are concerned with the many pollutants which can dissolve in

water and with the soil's ability to remove these pollutants before they enter the food chain.

Unfortunately, it is very difficult to follow water movement, whether below the soil surface or in the atmosphere. As a result, certain assumptions are made about the general behavior of water in response to the forces acting on it and to the hydraulic properties of porous media. Using models based on such assumptions, agronomists plan irrigation schedules while environmentalists predict the fate and impact of water-borne wastes.

A basic feature of such predictive models pertains to the shape of the wetting front, which is the boundary formed between soil already moistened by infiltrating water and the drier soil below this boundary. The idealized condition is that percolating water forms a horizontal, planar wetting front which proceeds downward through the soil at a rate related to the saturated conductivity of the most restrictive layer (e.g., Hanks and Bowers, 1962).

Newer models, however, have attempted to include the possibility that the wetting front may be neither planar nor horizontal. Soil water may actually travel in "preferred pathways" (Horton and Wierenga, 1986), which include such morphological features as animal borings or root channels, as well as pathways which may be created by instabilities in the wetting front itself.

Such fingers might drain the root zone, drawing water away from crops and down to the water table more quickly than expected. Fingers could also transport pollutants to the groundwater (Hillel, 1986). Instead of the "living filter" of the soil having a chance to work on the pollutants long enough to reduce their impact, waste would be transported intact and at high speed to the water table. Some layered soils are predicted (Philip, 1975a) to produce these instability fingers. Laboratory models of soils where a fine textured soil layer overlies a more conductive coarse textured soil layer have been observed to produce fingers which are not correlated to distinctive soil features in the sublayer. Since 350 soil series in the United States alone have such a layering sequence (Hill and Parlange, 1972), flow instability could be an important problem in the prediction of water movement if indeed the laboratory models accurately reflect natural systems.

### C. Present approach

This paper attempts to examine the fingering behavior of water in soil profiles with fine over coarse layers, and to consider this behavior in the light of what is known about the hydraulic properties of the layers involved. In particular, the effect of antecedent moisture on fingering will be examined as a special case. Since soil hydraulic



properties are affected by changes in soil wetness, it seems possible that the impact of changes in soil wetness on fingering may illuminate the relationship between a soil's hydraulic properties and fingering.

These experiments are meant to resolve some of the issues between the existing theories of flow instability. The primary issue of contention is the role of soil moisture. It remains unclear whether fingering flow is enhanced, eliminated, or unaffected by soil moisture. Answering this question may help to illustrate the role of soil hydraulic properties in promoting fingering flow, as all soil hydraulic properties bear some relationship to soil wetness.

Then there is the issue of the root causes and the persistence of instability. Once fingering flow has begun, will it provide a pathway for any later flow, will it dissipate through horizontal spreading, and can it be interrupted by a change in soil properties farther down the profile? If an initially moist soil layer can stabilize the flow, can a lower, dryer region within that layer destabilize the flow later?

This approach can be summarized as an attempt to answer three questions: (1) under what conditions will instability fingers be produced in layered soil; (2) what effect will initial moisture in the sublayer have on flow instability; (3) if increasing the initial moisture of the sublayer has

any effect on wetting front appearance, can the change be correlated to soil hydraulic properties?

## II. Literature Review

### A. Overview of the problem

Infiltration of liquids into soils is a common natural phenomenon, but it is a physical process of daunting complexity to those who have attempted to define it mathematically. Philip (1957a-e) made a classic contribution in five papers devoted to infiltration into a uniform soil of uniform initial wetness. In spite of all accomplished since, infiltration into layered soils remains an elusive problem.

### B. Laboratory experiments

The experiments of Miller and Gardner (1962) demonstrated that either a coarse or a fine layer could act as a barrier to flow. A coarse sublayer is a barrier because it is hardly conductive when dry, and will not accept water until tensions at the interface with the more restrictive layer above it are low enough to allow the coarse material's smallest continuous pores to fill. The fine sublayer acts as a barrier because even when wet, its pores are too small to conduct the water at the potential rate that the upper layer could supply.

In both cases, tensions at the textural interface are reduced, lowering the moisture gradient between the surface and that interface. This reduces the driving force for water flow through the toplayer. Therefore, the infiltration rate is reduced.

Miller and Gardner (1962) noticed flow instability in their experiments where a soil covered a sand layer. They referred to the preferred pathways created by this layering as "channels," and commented that as long as the channels persisted, infiltration remained slow overall. They posited that these channels were created by heterogeneities in the superlayer forming point sources of water at the low tensions created by the sand barrier. They suggested that the reason that the channels did not spread laterally upon entering the sand was the extremely low conductivity of the dry sand. Since they were examining infiltration, and not wetting front speed, Miller and Gardner (1962) saw the appearance of "channels" as restrictive, rather than permissive.

Unstable flow has since been examined specifically in the laboratory on several occasions (Hill and Parlange, 1972; White et al, 1977; Diment and Watson, 1985; Glass and Steenhuis, 1984). As yet, neither theoretical nor empirical approaches to the problem have provided a sufficient basis for predicting its occurrence in the field. The various theoretical approaches rely on conflicting assumptions, and

the empirical studies have not been comprehensive enough to allow generalization.

Laboratory experimentation has thus far supported the contention that flow instability in layered soils is restricted to soils where a fine layer overlies a layer of coarse, dry sand. The experiments of Hill and Parlange (1972) were all carried out with coarse sands as the sublayer. Diment and Watson (1985) carried out a series of experiments at moisture levels of  $0.02 \text{ cm}^3\text{cm}^{-3}$  or less. They found that fingering was suppressed in cases of soil water redistribution in uniform profiles where  $O_i$  was  $0.02 \text{ cm}^3\text{cm}^{-3}$ . It was also suppressed in cases where a layer of fine material overlay a coarser layer at that same initial moisture content. In their experiments, too, breakaway fingers were only produced in coarse dry sands. They conjectured a relationship between a soil's diffusivity (defined as  $K/c$  where  $K$  is the soil conductivity and  $c=dO/dh$ ) and the tendency of fingers to spread out and form a more or less planar wetting front. They suggested that any water content above  $0.05 \text{ cm}^3\text{cm}^{-3}$  would suppress fingering, and that the sharp, non-diffuse wetting front required by Philip's (1975a) model could not form in soils wetter than this.

Other experiments have been done which reveal fingering, but they have been performed either with washed air dry sand or in a Hele-Shaw cell. White et al. (1977)



sought to prove Philip's (1975b) theory that a positive pressure gradient with depth (i.e., pressure increasing with depth) would produce instability of a predictable wavelength. This was found to be true in Hele-Shaw cells, but fingers produced in coarse sands did not conform to the predicted wavelength. They were unable to produce recognizable fingers in homogeneous fine sand. Conceding that the Green-Ampt model was inaccurate for predicting instability in soils, they restricted later experiments (1977) to Hele-Shaw cells, which do provide the necessary non-diffuse wetting front, and found that Philip's (1975b) model held in such a case.

Glass and Steenhuis (1984), using well-washed, monodisperse sands, also found that fine-textured over coarse-textured layering could produce fingers in the coarse layer. Maintaining ponding in these systems over long periods, they determined that fingers could persist for some time, and even after infiltration had ceased and lateral spreading had occurred, the original finger channels remained preferred pathways during subsequent applications of water.

In their experiments involving uniform initial wetness in the coarse sublayer, Glass and Steenhuis regarded the wetting fronts produced as unstable in spite of the fact that these fronts moved slowly and no breakaway fingers were produced. The justification for this view is that

perturbations in these fronts tended to grow with time, rather than dissipate. They came to regard the interface between the layers as a series of point sources of water, delivering streams of water to the lower layer. Where these streams were close enough to or wide enough to overlap, flow appears stable. Where they do not overlap, either because the point sources are widely separated or because the sublayer resists spreading, fingers are produced.

### C. Field experiments

Experimental work involving field soils has suggested the existence of preferred pathways associated with unstable flow in layered soils (Starr et al., 1978). The soil used in this case had a layer of fine sandy loam overlying a gravelly coarse sand, with a layer of clay beneath the sand. This suggests two possible causes of instability: fine over coarse layering, and air entrapment below the wetting front. Dyes and chemical tracers indicated that the infiltrating water did break into streams in the layer of gravelly coarse sand. If unstable flow did indeed occur in this case, much laboratory work needs to be done to explain how a phenomenon that had been associated with idealized geometries, textural homogeneity, and extreme dryness could occur under field conditions. In practical terms, the common feature of the field and laboratory studies has been the fact that the

coarse layer is not actually a typical, polydisperse soil layer but a layer of sand of a rather narrow particle, and hence pore, size range.

#### D. Theoretical considerations

The advent of the computer age has made the problem of layered soils more accessible. Hanks and Bowers (1962) developed a computer simulation of infiltration into soils with various layering sequences. They concluded, on the basis of this model, that whether a soil had a fine horizon overlying a coarse one, or a coarse horizon overlying a fine one, it was the fine layer which would ultimately control the infiltration rate. In the first case, the coarse lower layer could only conduct what the finer layer would transmit. In the second, the fine layer would provide a barrier to flow through the coarse layer, and water could only enter the soil as a whole as fast as the restrictive layer could absorb it. They predicted reduced infiltration for both cases of layered soils compared to a uniform soil of the same texture as the upper layer.

There are several theories of flow instability in soils, which contradict one another to a greater or lesser extent. Some are strictly mathematical, while others are partly empirical.

Flow instability along the interface between oil and water has concerned petroleum engineers for some time (Hagoot, 1974). Unstable flow in porous media had already been modelled in the laboratory using a Hele-Shaw cell (Saffman and Taylor, 1958). Such studies formed the basis for a theory of unstable flow of water in soil (Philip, 1975a). Some of the simplifying methods of the earlier models were used in the mathematical analyses of the problem.

Raats (1973) attempted to develop a single criterion that would determine whether soil conditions would lead to flow instability. His model related instability to wetting front acceleration with depth. Acceleration would occur, according to Raats, if the pressure head at the soil surface were smaller than the pressure head at the wetting front. He then outlined five situations where this disparity could occur: 1) the soil is water repellent; 2) air is trapped and compressed below the wetting front; 3) infiltration occurs at a rate slower than that allowed by the saturated conductivity of a texturally homogeneous layer of the soil infiltrated; 4) a fine textured layer overlies a coarse textured one; 5) the conductivity of the soil increases with depth.

It is important to notice the role that conductivity plays in Raats' analysis, because although he relates instability to a difference in pressure head, he perceives



the build-up or loss of pressure as related to the soil's saturated conductivity. Further, he suggests that initial moisture plays a destabilizing role by increasing a soil's conductivity. In a soil where the wetting front is accelerating, increased initial wetness seems likely to make the wetting front accelerate even more.

The theory of Raats (1973) suggests that acceleration will occur if the wetting front reaches a more conductive region than the one it is crossing at any particular time. As a result, Raats predicts unstable flow in soils where a fine layer overlies a coarse layer, especially if the coarse layer is wet. Wetness increases soil conductivity, so, according to Raats, an increase in wetness alone may also be a cause of unstable flow, as it may accelerate the wetting front. This was a crucial issue examined in our research.

Philip (1975a) rejects Raats' criterion for wetting front instability. Applying the techniques of hydrodynamic stability analysis (Lin, 1955) to the Green-Ampt model of soil, Philip (1975a) concludes that instability occurs when the pressure gradient behind the wetting front opposes gravitationally driven flow. He particularly notes that instability cannot occur except where the flow is gravitationally driven, that is, during vertical downward infiltration.

In spite of his different approach to the problem, Philip (1975a) finds that, in cases that conform to the



Green-Ampt model (i.e., cases where 1) there is a constant potential at the wetting front; 2) conductivity and volumetric wetness are uniform behind the wetting front; 3) the wetting front is so distinct that the conductivity and wetness functions are discontinuous at the wetting front) Raats (1973) correctly identified instability producing situations. He only elaborates that instability caused by applying water to the soil surface at a non-ponding rate is a special case of wetting front redistribution when the air entry pressure of the soil is less than the wetting front moisture potential. He is also more ambiguous about the role of initial moisture in unstable flow, as he expresses his criterion for instability in terms of conductivities behind the wetting front, rather than ahead of it as Raats does. Philip also finds that although Raats correctly identified some instability producing situations, his mathematics were not always correct.

Philip (1975a), using the Green-Ampt model of a delta function soil, states that instability will occur if the pressure gradient between the soil surface and the wetting front opposes flow. In a layered soil, this results in the expression:

$$h_L > -(r-1)L \quad (2.1)$$

where  $h_L$  is the tension at the interface between the layers,  $r$  is the ratio of the conductivity of the lower layer behind the wetting front to the conductivity of the upper layer

behind the wetting front, and  $L$  is the depth of the interface. Because of his use of the Green-Ampt model, Philip (1975a) disregards the possibility that the moisture of the lower layer plays any role in flow stability. The question of the effect of antecedent moisture remains open.

Philip (1975a) also points to limitations of his own analysis, particularly its reliance on the Green-Ampt model. He notes that in real soils, sharp, or "non-diffuse," wetting fronts are produced by a combination of convection and "diffusion," or lateral spreading, while his analysis calls for a situation where a "fingered," or "diffuse," wetting front is produced by a resistance to, or a negation of, lateral spreading. He suggests that a more accurate model would take lateral movement into account.

More recently, Milly (1985) investigated this problem from the point of view of the second derivative of the soil's hydraulic conductivity as a function of soil volumetric wetness. Instability was indicated when this derivative was negative on the interval from  $O_i$  to  $O_{sat}$ . Milly concludes that water flow through porous media is generally stable, but may become unstable through a layer of coarse material that conforms closely to the Green-Ampt model. This approach also disregards the effect of initial soil moisture.

Milly (1985) arrives at the criterion:

$$c \leq 1 \qquad (2.2a)$$

from

$$K = K_{\text{sat}} N^c \quad (2.2b)$$

where  $K$  is the conductivity of the soil at any given wetness,  $K_{\text{sat}}$  is the saturated conductivity of the soil,  $N$  is the soil's relative saturation, and  $c$  is a constant. This criterion finds instability in any soil with  $c \leq 1$ , regardless of the value of  $N$ . No soils actually meet the criterion  $c \leq 1$ ;  $c$  has only been found to be unity in fragmented sandstone, according to Mualem (1976).

Diment et al. (1982) attempted to solve this problem. Including forces which would dissipate the energy of an extremely sharp ("Green-Ampt") wetting front as a basis for both theoretical and numerical analysis, they find that these forces would, except under exceptionally dry conditions, take over to close the gaps between incipient fingers. Although they find some trend toward instability in a case of very widely spaced fingers, Diment and Watson (1983) state that any moisture content greater than  $.05 \text{ cm}^3 \text{ cm}^{-3}$  generally prevents unstable flow. They explain experimental findings of flow instability as a laboratory artifact caused by the use of air dry sands (Hill and Parlange, 1972). Attention should be drawn to the fact that the Diment et al. (1972) model is based on a single, non-hysteretic soil-moisture characteristic curve. Curves more descriptive of coarse sands might yield a higher limit of soil moisture for flow instability.

Diment and Watson (1983) examined the issue of initial water in terms of a matrix which they solved numerically. Their numerical solution could not tolerate wetnesses below  $0.05 \text{ cm}^3\text{cm}^{-3}$ , and within this range of wetnesses predicted no instability. They concluded that this was a threshold wetness:

$$\theta_i = 0.05 \text{ cm}^3\text{cm}^{-3} \quad (2.3)$$

Our experiments are meant to resolve some of the issues between these theories. The first question is whether unstable flow can occur in a medium where particle size uniformity is less than that described by Milly (1985). This could include any medium from coarse sands to fine-grained soil.

The next issue of contention is the role of soil moisture. It remains unclear whether fingering flow is enhanced, eliminated, or unaffected by soil moisture. Answering this question may help to illustrate the role of soil hydraulic properties in promoting fingering flow, as all soil hydraulic properties bear some relationship to soil wetness. A corollary issue is whether Diment and Watson (1983) did in fact discover a threshold value for fingering at  $0.05 \text{ cm}^3\text{cm}^{-3}$ .

Finally there is the issue of persistence of instability. Once fingering flow has begun, does it provide a pathway for subsequent flow, and how long will it persist? Will it dissipate through horizontal spreading, and can it



be interrupted by a change in soil properties farther down the profile? If an initially moist soil can stabilize the flow, as Diment and Watson (1983) predict, can a lower, dryer region within that layer destabilize the flow later?

Answering these questions may also shed provide a clue as to whether or not unstable flow is likely to be widespread in nature. Milly's (1985) criterion calls for an unusual porous medium, while Diment and Watson (1983) state that instability depends on low soil moistures which are not typical of natural soils, but must be produced in the laboratory. Philip (1975a) does recognize that he is calling for an idealized wetting front in his model, but makes no statement about the type of medium necessary to produce unstable flow in the field. Raats (1973) also makes no statement of limitation on the likelihood of his model applying to the natural world.

### III. Methods and Materials

#### A. Cell construction and packing

In order to observe wetting front instability patterns, we built a cell approximating a two-dimensional system (Fig. 3.1). We considered it desirable that the cell not leak, and that the cell it permit dismantling and sampling after each experiment. At least one wall of the cell was to be transparent, so that we could observe the wetting front pattern as it developed.

The dimensions of our cell were were similar to those of Hill and Parlange (1972), with a length of 75 cm and a thickness of 2.5 cm. However, we increased the vertical dimension (height) from 30 cm to 58.4 cm. The added height was intended to provide more time for observing the persistence of the flow pattern, as well as the effect of more than two soil layers.

The chamber's frame was built of three sections of steel rectangular tubing measuring 1.27 cm x 2.54 cm (outside dimension) with a 0.159 cm wall thickness. A section of this material 80 cm long formed the bottom of the frame, while two 58.4 cm lengths were welded to it, one at each end, forming a rectangular U shape. The 1.27 cm thickness faced the inside of the cell, while the broader 2.54 cm side faced the cell's outside walls.



A series of holes measuring 0.318 cm in diameter and spaced 2.54 cm apart along the frame's bottom rail provided drainage. Water could run through these holes, and then along the hollow inside of the bottom tube, to two outlet tubes at one end of the frame. The tubes were positioned one above the other. Each tube had an inside diameter of 0.635 cm.

Holes 0.794 cm in diameter were drilled through the 2.54 cm face of the frame at intervals of 10.2 cm. These holes matched holes in a 60 cm x 83 cm aluminum plate (0.635 cm thick), which served as the cell back, and in two 60 cm x 83 cm panes of 1.27 cm plexiglass, which provided an observation window. To prevent leakage, gaskets of 0.635 cm thick closed cell foam rubber were positioned between the frame and the plates with which it was in contact. Nuts, bolts and lock washers with a threaded surface diameter of 0.635 cm held this sandwich of plexiglass plates, gaskets, frame and aluminum plate together (Fig. 3.1).

The large internal volume of the cell necessitated the use of such substantial materials for the cell walls. The cell generally contained 11.5 kg of soil or sand, and the pressure exerted by this material when the model was standing upright caused the cell walls to bulge. Excessive bulging might interfere with both the uniformity of the packed soil and the condition of two-dimensionality. This necessitated the use of thicker materials to minimize

bulging. While the aluminum plate and 2.54 cm thickness of plexiglass did not eliminate bulging completely, they reduced it sufficiently to permit satisfactory packing.

Published data (Hill and Parlange, 1972) indicated that unstable flow could be achieved in a two layer system where very fine sand (0.05-0.10 mm in diameter) overlies a coarse sand (0.5-1.0 mm in diameter). A similar two layer system was used by Diment and Watson (1985). This particle size ratio became the basis for our experiments.

We performed our initial experiments with a coarse layer of material from a sand and gravel pit which was retained between a No. 40 (0.425 mm mesh) and a No. 18 (1.00 mm mesh) sieve after hand sieving. The fine layer was material from the B horizon of an Agawam very fine sandy loam retained between a No. 300 (0.047 mm mesh) and a No. 140 (0.105 mm mesh) sieve after two minutes of shaking on a portable sieve shaker.

After this initial phase, we subjected the soil materials to a much more thorough sieving and cleaning. Three coarse sublayer fractions were created: (1) very coarse sand, retained between a No. 18 (1.00 mm mesh) and a No. 10 (2.00 mm mesh) sieve (2) coarse sand, retained between a No. 35 (0.500 mm mesh) and a No. 25 (0.710 mm mesh) sieve and (3) medium sand, retained between a No. 45 (0.355 mm mesh) and a No. 35 (0.500 mm mesh) sieve. We obtained all fractions by shaking the sand on a portable sieve

shaker for a period of six minutes. Fractions were then washed at least twice under a pressurized stream of tap water. The fine layer continued to be the Agawam very fine sand retained between a No. 300 and a No. 140 sieve, but it too was now subjected to six minutes rather than two minutes of mechanical sieving. Once these fractions were sieved and washed, we used them repeatedly over the course of these experiments to help standardize the textures of layers from one trial to the next.

Because non-planar wetting fronts can result from soil heterogeneities within layers as well as from flow instability, it was important that the sand be packed as uniformly as possible into the cells. Wetting front irregularities could then be ascribed to spontaneous flow instability rather than to pre-existing macropores forming preferred pathways.

To prevent layering and bedding in the sublayer, the cell was assembled horizontally without the front pane of plexiglass. Sand was distributed uniformly over the aluminum plate between the three sides of the frame and the piston, a section of rectangular tubing that fit snugly inside the frame. This served to prevent the formation of vertical non uniformities which might interfere with the progress of the wetting front after the cell was stood upright. The sand was smoothed to form a shallow layer that filled the region bounded by the frame and the piston. The

double sheets of plexiglass were placed over the frame to close the cell, and the entire container was bolted together.

We then vibrated the system to insure a high, uniform bulk density. Vibration has been shown to pack granular materials to a uniform density even when the materials are somewhat moist, though the highest densities are achieved when the materials are either saturated or dry (Felt, 1958). Because of the size of the cell, we needed a large vibrating table (VIBCO Model US-900) to pack the sand. We packed the cell horizontally (i.e., with the aluminum plate on the surface of the vibrating table) for thirty seconds to distribute sand throughout the cell and reduce the bulging of the plastic wall. The cell was subsequently vibrated in an upright position (i.e., with the bottom of the frame on the vibrating surface) for one minute if the sand were dry and for two minutes if the sand were moist. We deemed the additional vibration time for the latter necessary because moist sand grains appear to move into position more slowly than dry ones, possibly due to the surface tension effect of the moisture.

We ran several tests to determine whether there was a significant variation in density within the cell. Three cells of each particle size and each level of wetness were set up and then dismantled after vibration. We obtained samples at the same four locations each time and measured



for bulk density. While no chamber was perfectly uniform, differences between locations alone did not seem great enough to cause fingering flow. A statistical discussion of significant differences is contained in Appendix 1.

The method for insuring uniform wetness was based on that described by Diment and Watson (1985). We weighed a mass of 10 kg of coarse sand (enough for one experiment), and then added enough water to achieve the desired wetness by mass. After thoroughly mixing sand and water together by stirring, we poured the moist sand into a large plastic bag, where it was further stirred by pouring the sand from one part of the bag to another. We then sealed the bag for 36 hours to allow the moisture further opportunity to distribute through the sand. Upon packing as described above, acceptably uniform wetnesses were achieved. Tests were carried out simultaneously with tests for density, with 10 wetness samples taken per cell. A statistical analysis of this data is again provided in Appendix 1.

After the sublayer had been packed, we introduced the overlying fine material through the open top of the cell. A tremi tube was used to insure that a homogeneous mixture of particle sizes would be achieved, as this unwashed material still retained some particles smaller than .047 mm. After the 1500 g of this material were in the cell, we tamped and levelled it repeatedly until further tamping did not reduce the layer thickness. Tamping was employed, rather than

vibration, to prevent the migration of small particles into the large pores of the sublayer, which would have blurred the interface between the layers. Uniform packing of this layer was achieved, as demonstrated by the planar wetting front formed by water infiltrating into this layer. This straight wetting front showed that no non-uniform barriers or express routes existed within the upper soil layer.

In experiments where the coarse layer was initially wet, it was difficult to discern the shape of the wetting front unless the infiltrating water were dyed. Dyeing the water itself proved to be unsatisfactory as much of the dye was retained by the fine layer, and did not reach the lower layer where an unstable front might develop. Instead, we mixed dry acid red dye powder with 200 g of the fine material, and placed it directly on top of the coarse layer, with the remaining 1300 g of fine material added on top. Acid red was chosen as it is known to be an anionic dye which tends to follow the wetting front closely (Corey,1968). While there was concern that the dye could itself cause fingering by making the infiltrating water more dense than the water held in the lower layer (Bachmat and Elrick,1970), this did not prove to be the case, as the initially wet experiments, where this effect might have been expected to become more important, did not develop fingers.



## B. Water delivery and experimental procedure

In order to have a clearly defined boundary condition, as well as to prevent possible unstable flow due to redistribution rather than soil layering, the model operated from the condition of continuous shallow ponding of constant depth. This would also served to ensure that wetness throughout the fine layer would be uniform.

Preliminary trials indicated that 500 ml of water would provide a sufficient excess to be a starting point for a 1.0 cm ponding depth. This initial quantity of water was poured on the soil surface by hand from a beaker. Since it was important to prevent scouring of the fine layer which might disrupt the wetting front, the soil was shielded twice. Directly on the surface of the soil, an aluminum screen held soil particles in place. Above this screen, a shield of thin plastic with slots cut in the bottom reduced the velocity of water as it was poured into the cell. The result was a planar wetting front with no scouring of the surface.

To maintain a constant 1 cm head, we installed a Mariotte device after the initial 500 ml application of water. We removed the plastic shield from the cell, and placed the T-shaped delivery end of the Mariotte bottle just above the soil surface. The horizontal part of the T acted to shield the soil surface from water released from the

device. This horizontal tube was closed with one hole stoppers at each end, but open along its upper surface so that the depth of water in the tube would match the ponded depth of water on the soil. When the water level was sufficiently reduced, air would rise up the vertical part of the tube and release water until the 1.0 cm depth was regained. The tube was calibrated at 50 ml intervals to allow measurement of cumulative infiltration against time.

After packing the cell with the coarse material by vibration, and creating a fine layer packed by tamping, we moved the cell from the vibration table to the laboratory bench. While the packed chamber was, to some extent, free standing, we created a support structure to hold it upright. This structure, made of light gauge angle iron, was fitted around the cell and extended above the top of the cell. This structure also provided a convenient framework for attaching the Mariotte device to the cell (Fig 3.1).

A person standing behind the cell on the laboratory bench applied the initial 500 ml of water. As water was poured from the beaker, the beaker was moved along the length of the cell to provide uniform wetting. We used tap water, rather than de-aired water, as the process of applying water in this fashion would have reaerated de-aired water in any case. Distilled water was also deemed unnecessary because no major chemical or structural changes were anticipated in view of the soil's coarse texture.

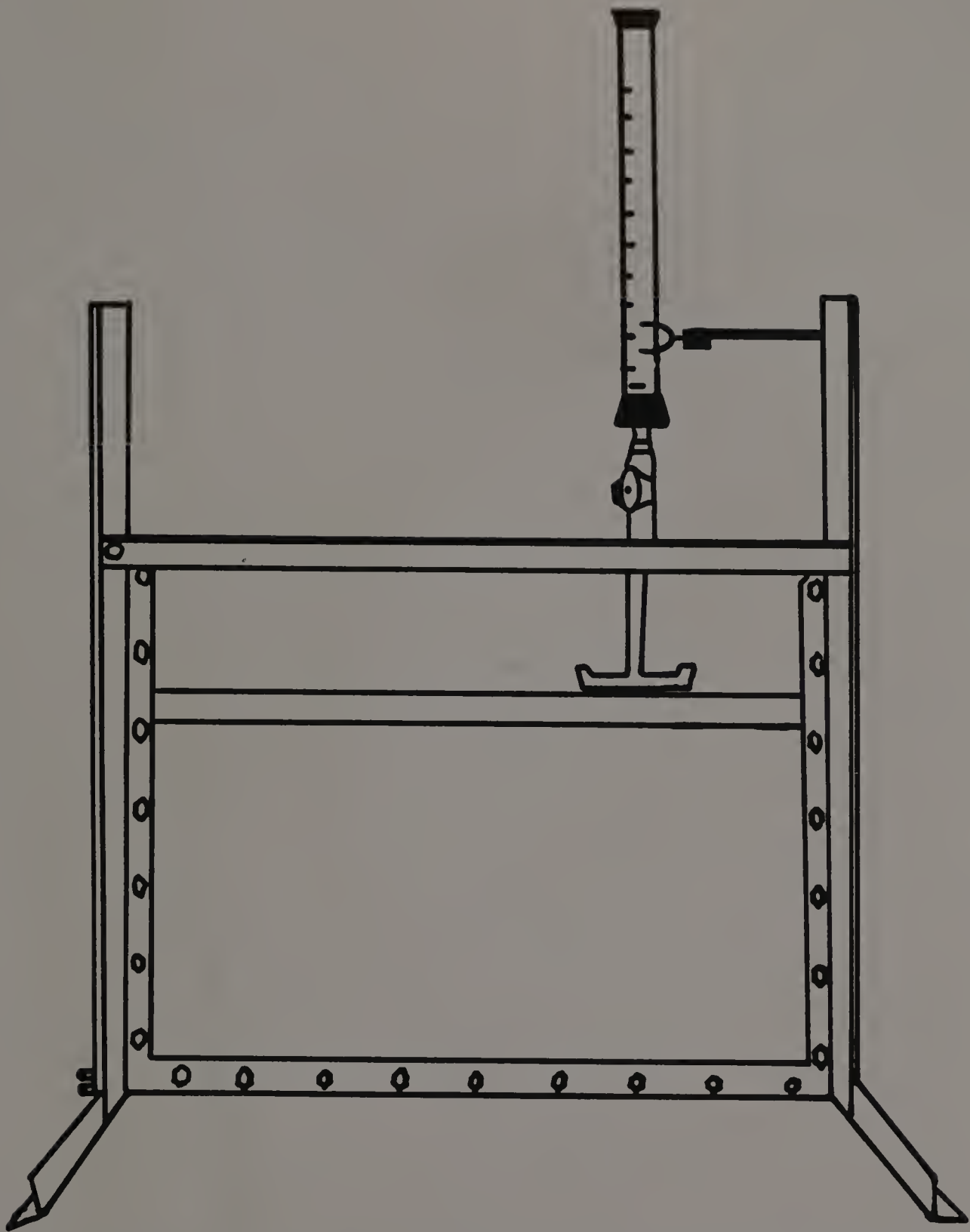


Fig. 3.1: The packed experimental cell in support structure with Mariotte device.

At the moment that ponding began, we started a laboratory clock. This allowed the measurement of the wetting process against time. Periodically during the experiment, we took photographs and drew lines over the transparent window of the cell showing the location and appearance of the wetting front, and the times of these photos and tracings were noted. Mariotte readings at these times were also recorded. We re-filled the Mariotte device as necessary until some portion of the wetting front reached the bottom of the cell, at which time we ended the experiment. We then removed the Mariotte device and support structure, placed the cell on its aluminum back plate, and removed the front plexiglass sheets. In this position, any further sampling by region could be performed as necessary.

In experiments where a burette was used to model water delivery from a point source, the procedure was adjusted to account for the fact that the burette was replacing the restrictive upper layer in this model. While the coarse layer was packed as usual, there was no upper layer. Instead of ponding water at the soil surface, the burette became the water source. Constant flow rates were maintained manually by adjusting the valve on the burette. The experiment was considered to have begun when the first drop of water emerged from the tip of the burette; after that time, the same experimental procedure was followed as for the layered soil experiments.

### C. Soil hydraulic properties

Because the relationship between soil wetness and matric potential can be used as a basis for estimating other hydraulic properties, it was essential to determine this relationship. Our task was complicated by the need to obtain the absorption, rather than the desorption, relationship between wetness and potential, as our instability experiments only involved absorption.

We were able to obtain this curve for the coarse materials by a simple method where suction and wetness were related directly to the height of capillary rise in a column filled with the sand fraction in question. A column was built of stacked lucite rings of various heights, each having an inside diameter of 2.62 cm and an outside diameter of 6.30 cm. The rings were stacked so that several measurements could be made in the wetted region of the column. The stack was aligned and held together by a metal strap that ran under the bottom of the stack and was bolted tight at the top. The composite tube was filled with sand through a Tremi tube, and vibrated on the vibrating table to assure uniform packing of the column (see II.A).

The column was then placed in water deep enough to cover the bottom ring and allowed to equilibrate for one week, sufficient time for capillary rise to stop. After



this time, the column was dismantled section by section and tested for moisture content. Each wet sample was weighed and then dried in a microwave oven until it reached a constant weight. The section location and water content were then graphed to show how much water was absorbed at a particular soil tension.

Obtaining a soil moisture characteristic curve for the finer material was somewhat more complicated, as pores in a material that fine were likely to have the potential to raise water to a level far in excess of the column height. For this material, the method described by Bouma et al., (1974) was employed. Saturated Tempe cells were attached to water columns supplied from burettes. The burettes were closed with a rubber stopper at the top, but had a sidearm open to the atmosphere, so they acted as Marriotte devices. Atmospheric pressure was established in the system at the location of the sidearm. One hundred grams of the fine material were added to the Tempe cell, which was then closed. A plastic tube on top of the Tempe cell prevented evaporation but could be opened to release any build up of air pressure. Gradually, the sidearm was raised from 150 cm below the level of the soil (150 cm tension) to the level of the Tempe cell (atmospheric pressure, 0 tension). At each step, the amount of water entering the soil was visible by the change of water level in the burette. Again, the relationship between the amount of water absorbed and the



tension applied formed the soil moisture characteristic curve in the absorbing direction.

Saturated conductivity was measured by the "constant head" method in a Soiltest Model K-600 conductivity column. Soil materials were packed into the column and vibrated (see II. A) to obtain uniform density. A de-aired water source was attached to an inlet tube at the bottom of the column, and the soil was slowly infiltrated from beneath and allowed to saturate overnight. In this way, air entrapment between soil pores could be minimized.

After saturation was complete, the water source was raised to provide some small constant head. Constant head was maintained by a bubble tube below the water surface of the water source, so that atmospheric pressure would be held to a known elevation until the water ran out. The outflow from the test column was measured against time, and the conductivity determined by Darcy's law:

$$K=(QL)/(AH) \quad (3.1)$$

where Q is the outflow per unit time, L is the length of the soil column, A is the column area, and H is the pressure difference.

Unsaturated conductivity was estimated by the model of Mualem (1976), where conductivity K is defined by equation 2.2, with c given by:

$$c=2+n+2/y \quad (3.2)$$

where  $n$  is a tortuosity factor, and  $y$  is the pore size distribution index. The tortuosity factor  $n$  was found by Mualem (1976) to be equal to 0.5, while  $y$  is defined as the slope of the line which results from a plot of  $\ln(N)$  against  $\ln(h)$ , for all  $h$  greater than the soil's air entry value, where  $h$  is the matric potential of the soil. The  $N$  vs.  $h$  relationship were determined from the soil moisture characteristic curve by the use of a computer program, Etafit, listed in Appendix 3, which performs a Golden Section Search based upon the algorithm given by Mualem (1976).

Sorptivity and diffusivity, each a combination of soil conductivity and matric potential, were approximated by the method of Bruce and Klute (1956). Sorptivity is defined as:

$$S=I t^{-1/2} \quad (3.3)$$

where  $I$  is cumulative infiltration and  $t$  is time, while diffusivity is defined as:

$$D=K(\theta) dh/d\theta \quad (3.4)$$

where  $K(\theta)$  is conductivity as a function of volumetric wetness and  $dh/d\theta$  is the first derivative of matric potential with respect to wetness.

While this method does not provide definitive results over the full range of soil moisture, it can give reasonable results at levels of moisture well below saturation, which was the major concern in these experiments. The use of this fairly simple method made possible an attempt to obtain some

data about these hydraulic properties directly, rather than extrapolating all such results from the soil moisture characteristic.

Material from each type of coarse sublayer and the fine overlying material were tested for diffusivity,  $D$ , and sorptivity,  $S$ . It has been suggested that both properties are associated with finger width (Hill and Parlange, 1972; Diment and Watson, 1982).

Each soil material was packed into a flat rectangular box made of 1.27 cm plexiglass. The inside dimensions of the box were 45.6 cm x 9.70 cm x 0.98 cm, the small dimension representing the box height. A reservoir of water was attached to one end of the box, and filled with water until the water level was halfway up the height of the box. Timing began as water infiltrated the soil horizontally. The water level was maintained manually during infiltration. After the wetting front had progressed between 25 cm and 35 cm, a set of metal blades separated by wooden spacers was plunged through the soil, coming to rest against the rubber pad on the floor of the box. Samples were obtained by removing the sides of the box, and pushing samples out from between the blades into weighing cans. Samples were weighed to the nearest milligram, dried overnight, and weighed again to the nearest milligram. Distances of each soil section from the water inlet were measured. These distances, divided by the square root of the total time of the

experiment, formed the Boltzmann transform designated by the symbol B.

When the volumetric moisture content and B of each sample had been determined, and each test repeated three times, a moisture vs. B curve could be fit through the test points using the ICSFKU least squares cubic spline from the IMSL fortran program library. This curve formed the basis of the calculations necessary to determine D and S. S was the area under the B( $\theta$ ) curve, integrated using the DCSQDU routine from the IMSL library. The axes were then interchanged by a second program, which fitted the smooth curve with the exact spline program ICSCCU (IMSL), so that the limits of integration could be adjusted, giving an S to  $\theta$  relationship. Integrating from air dryness to  $\theta_{sat}$  in the second program produced the same S value as the integration performed by the first program, as would be expected if the areas under the curves were the same, as they should have been.

D was calculated by the method of Clothier et al (1983). Their method relates diffusivity and sorptivity by the equation:

$$D=p(p+1)S^2\{(1-N)^{p-1} - (1-N)^{2p}\}/2(\theta_{sat}-\theta_n)^2 \quad (3.5)$$

where S is sorptivity from air dryness to saturation, N is relative saturation,  $\theta_n$  is irreducible moisture content, and p is a fitting function defined as:

$$p=(B_{wf}-N)/N \quad (3.6)$$

where  $B_{wf}$  is the value of  $B$  at the wetting front.



## IV. Results

### A. Uniform initial wetness experiments

The first twelve experiments presented here are examples of studies involving infiltration into layered soils where the overlying layer is 1.5 kg of 0.047 mm to 0.105 mm sand, packed to a depth of approximately 6 cm and a bulk density of  $1.41 \text{ g/cm}^3$ , and the lower layer is 10 kg of uniformly wet coarse sand. The depth of the lower layer varied from 40 cm to 42 cm, while the bulk density varied from  $1.34 \text{ g/cm}^3$  to  $1.60 \text{ g/cm}^3$ . These experiments were designed to address the question of the circumstances under which fingering will occur in layered sands, and whether moistening a sand layer in which fingering is known to occur otherwise will promote or discourage fingering. We also examined the relationship between cumulative infiltration and the square root of time for each of these experiments.

The following twelve figures are tracings made of the wetting front during infiltration. Numbers on the left side of the figure indicate the time, in minutes after ponding, when the tracing was made. Each experiment is identified by a run number and the date on which we performed the experiment in Table 4.1. Following the experimental tracings are graphs indicating the relationships between the various experimental conditions and finger width, finger

speed, and cumulative infiltration.

Table 4.1

## Layered Soil Infiltration Experiments

Run number	date	Mean Particle Size (mm)	$\theta_i$ (%)	Finger Width (cm)	Finger Speed (cm/min)
1	6/22/87	1.50	0.377	1.17	13.05
2	7/13/87		1.67	1.53	8.43
3	7/17/87		3.17	2.63	2.98
4	6/25/87		4.41	*	2.53
5	5/14/87	0.600	0.266	2.45	10.11
6	6/26/87		0.666	1.84	9.11
7	5/27/87		1.56	5.40	1.81
8	6/2/87		2.94	*	1.68
9	6/3/87	0.425	0.267	4.62	4.28
10	7/10/87		0.931	3.17	5.72
11	6/8/87		1.46	5.34	1.65
12	6/16/87		2.27	*	1.43

\* indicates fingers not discernible; speed is velocity of wetting front as a whole.

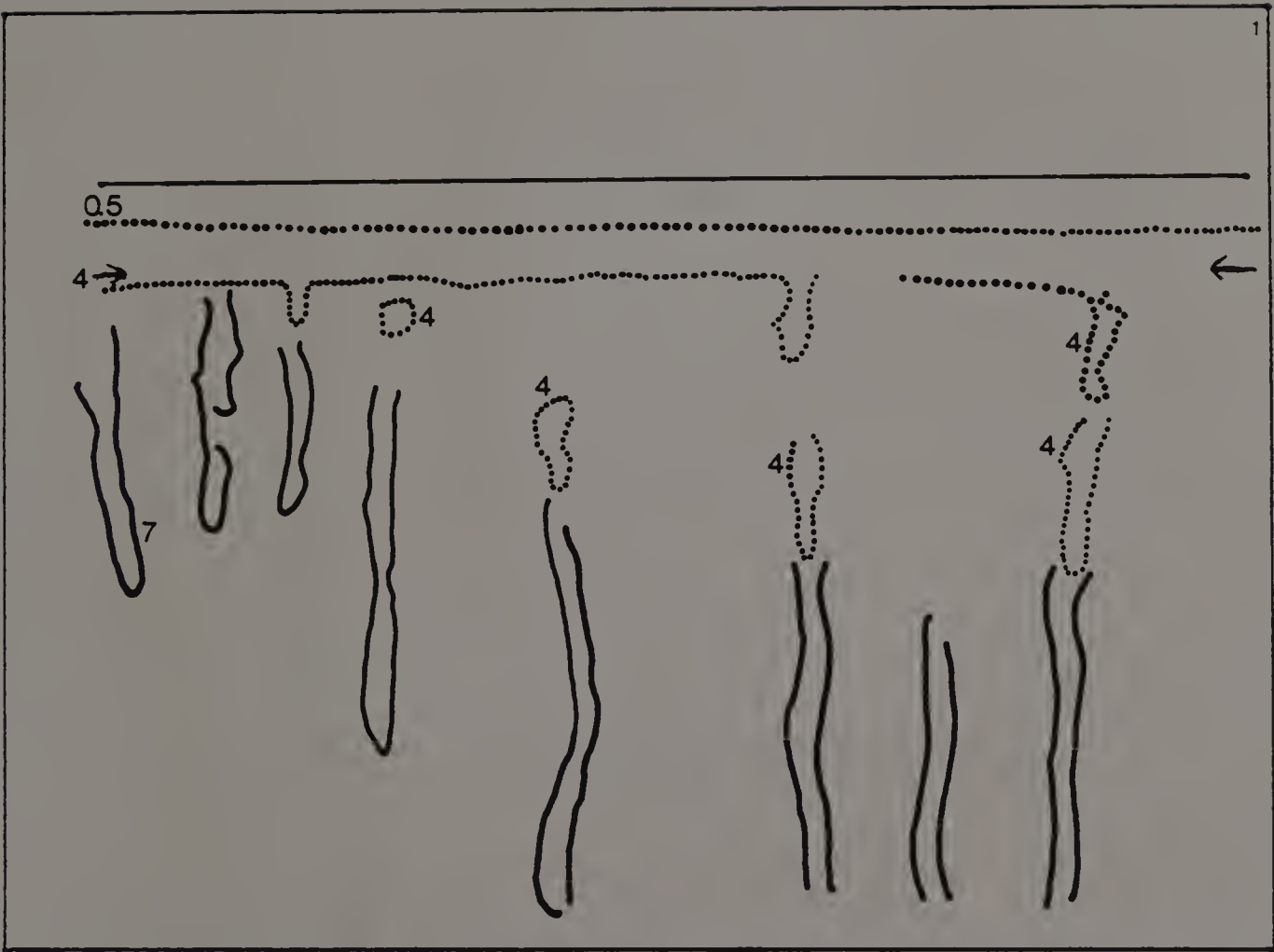


Fig. 4.1: Run 1, 19% of actual size. Straight line indicates soil surface. Arrows indicate position of interface. Numbers indicate time after ponding in minutes.

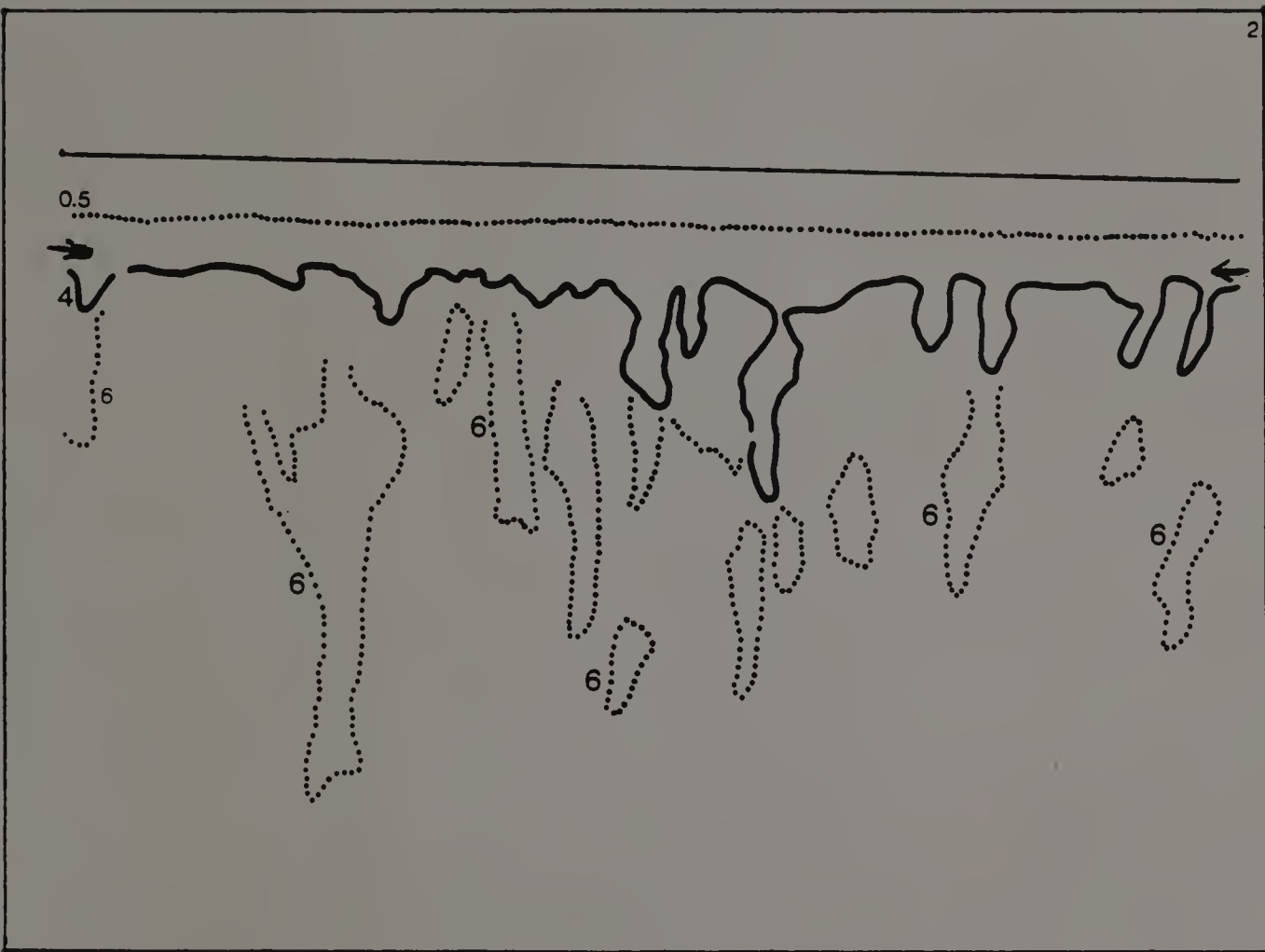


Fig. 4.2: Run 2, 19% of actual size. Straight line indicates soil surface. Arrows indicate position of interface. Numbers indicate time after ponding in minutes.



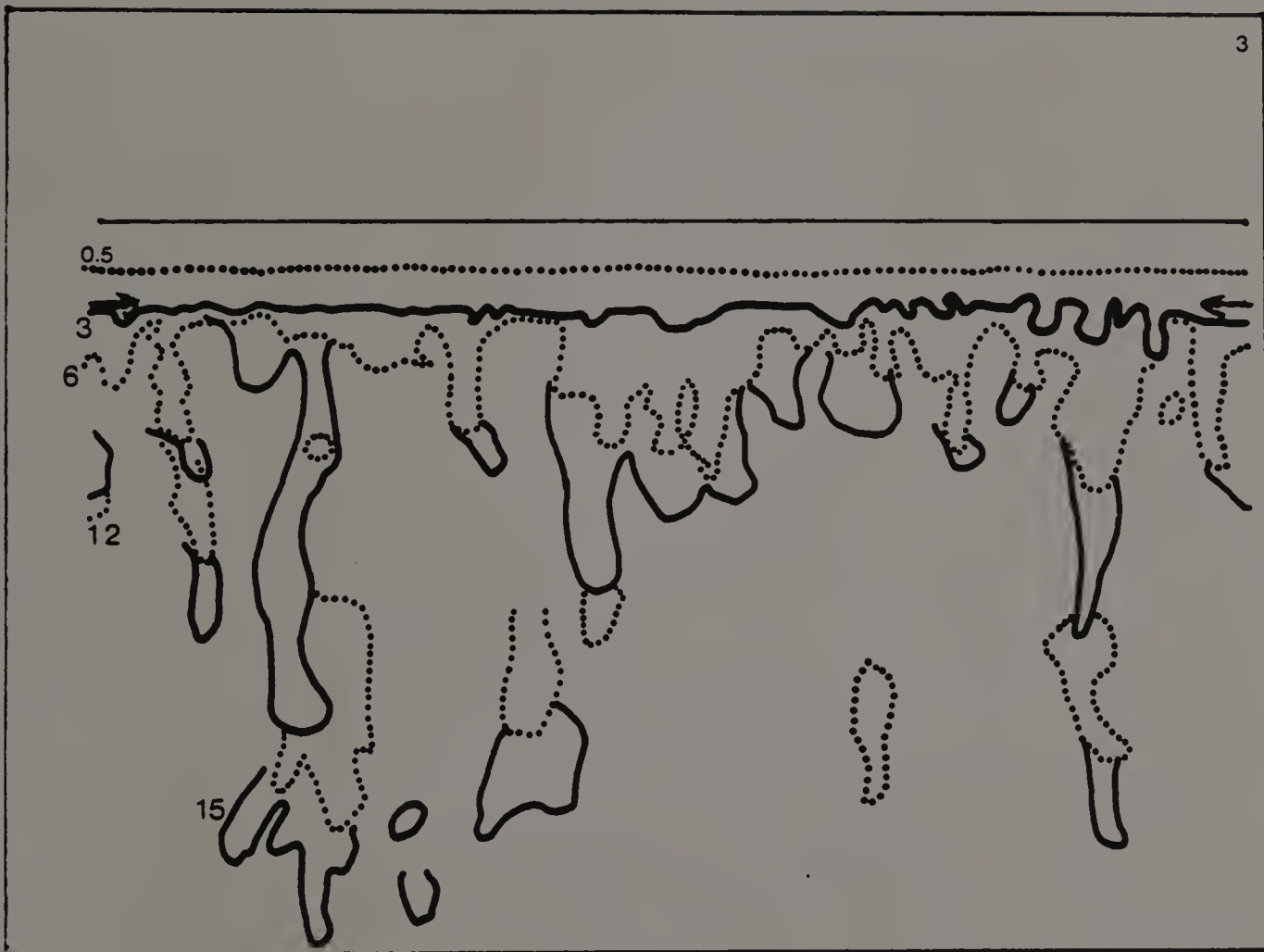


Fig. 4.3: Run 3, 19% of actual size. Straight line indicates soil surface. Arrows indicate position of interface. Numbers indicate time after ponding in minutes.

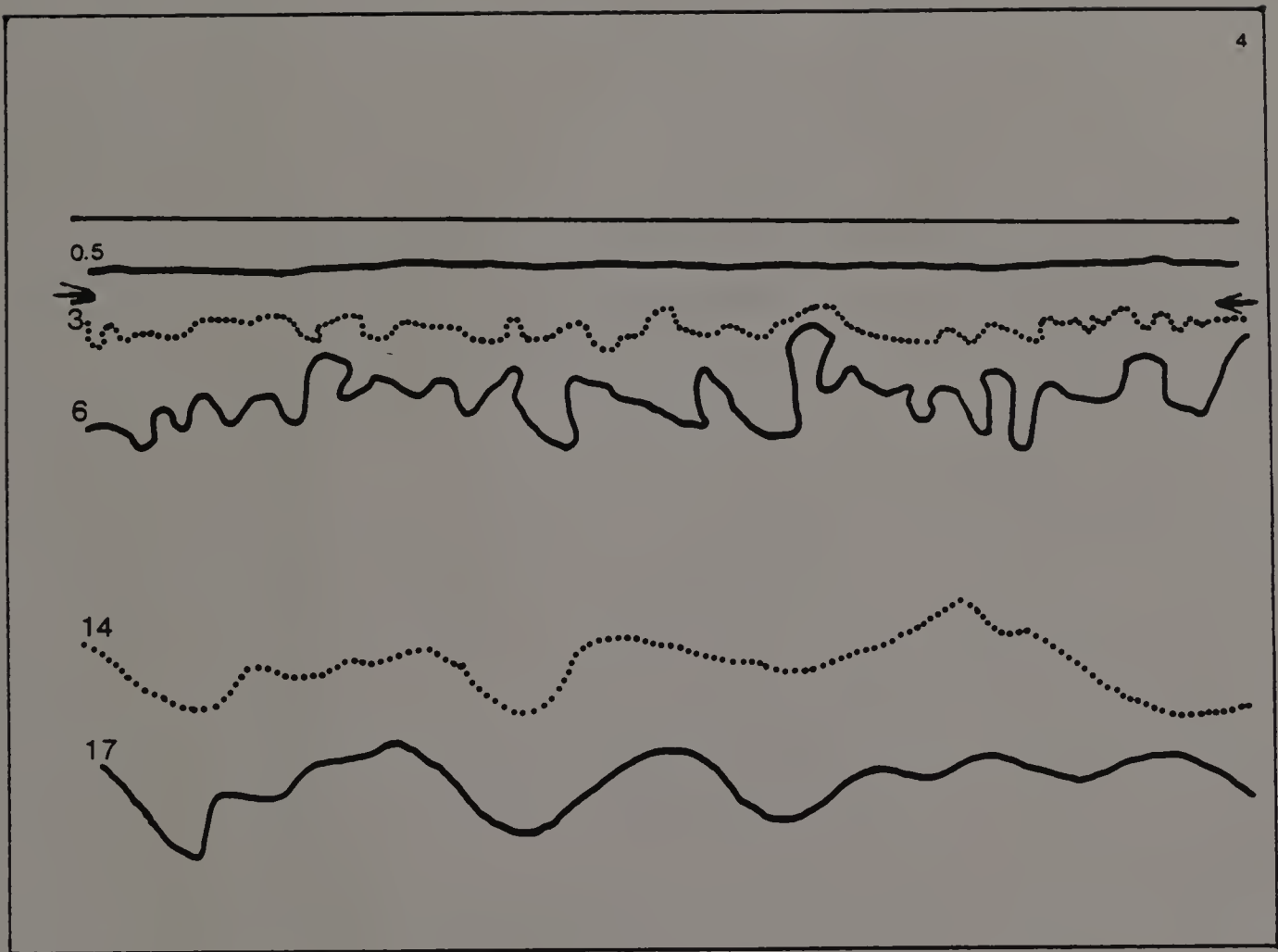


Fig. 4.4: Run 4, 19% of actual size. Straight line indicates soil surface. Arrows indicate position of interface. Numbers indicate time after ponding in minutes.

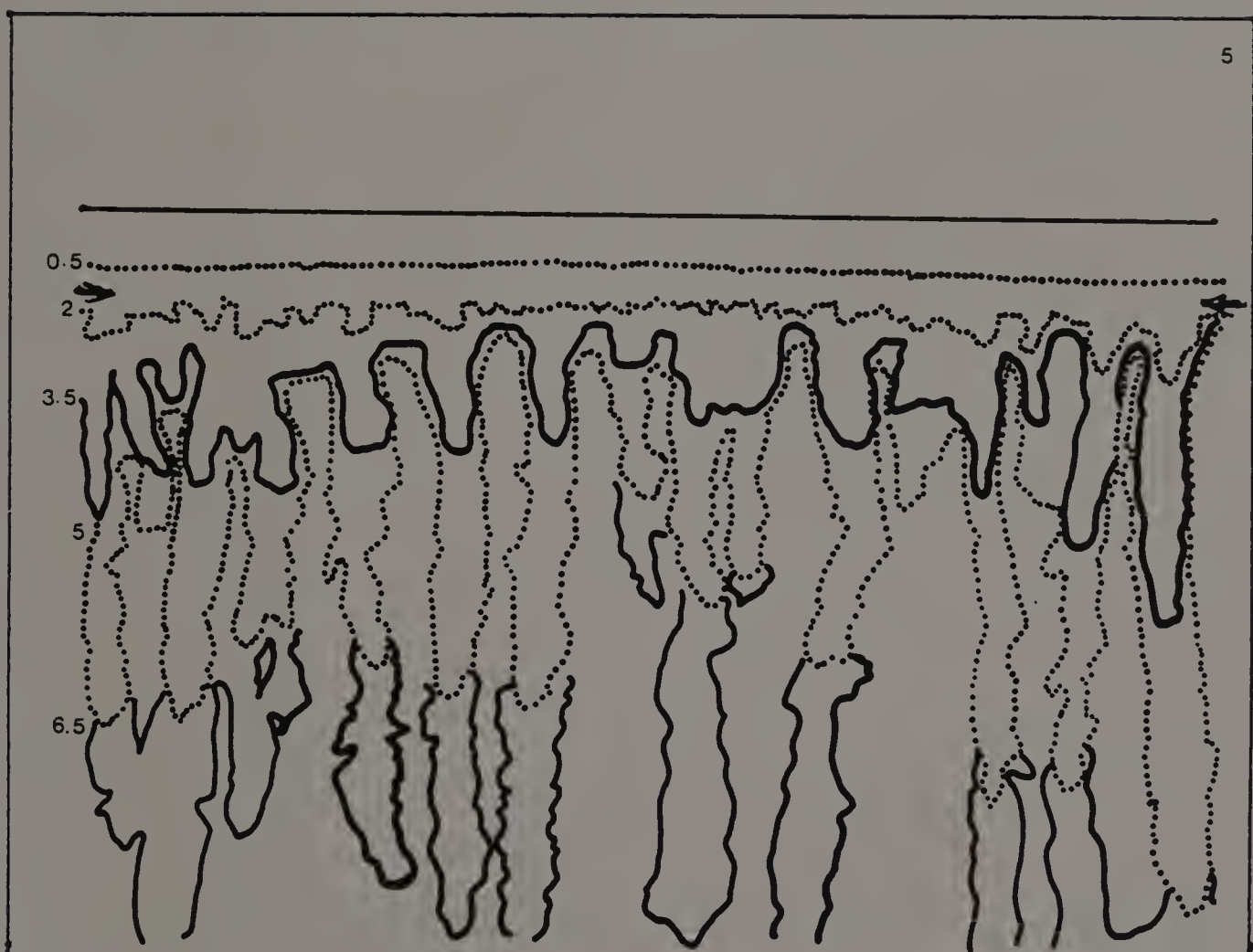


Fig 4.5: Run 5, 19% of actual size. Straight line indicates soil surface. Arrows indicate position of interface. Numbers indicate time after ponding in minutes.

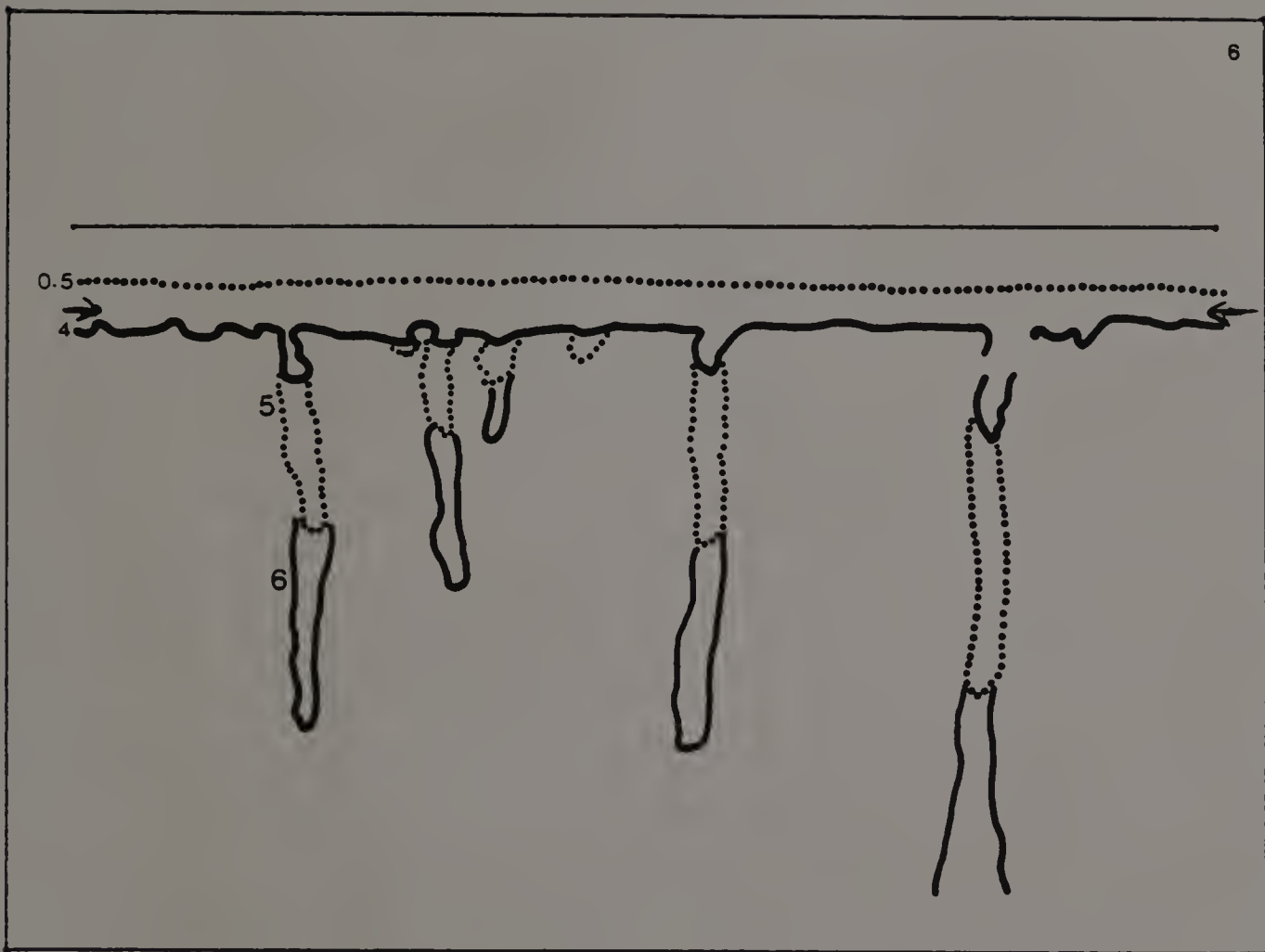


Fig. 4.6: Run 6, 19% of actual size. Straight line indicates soil surface. Arrows indicate position of interface. Numbers indicate time after ponding in minutes.

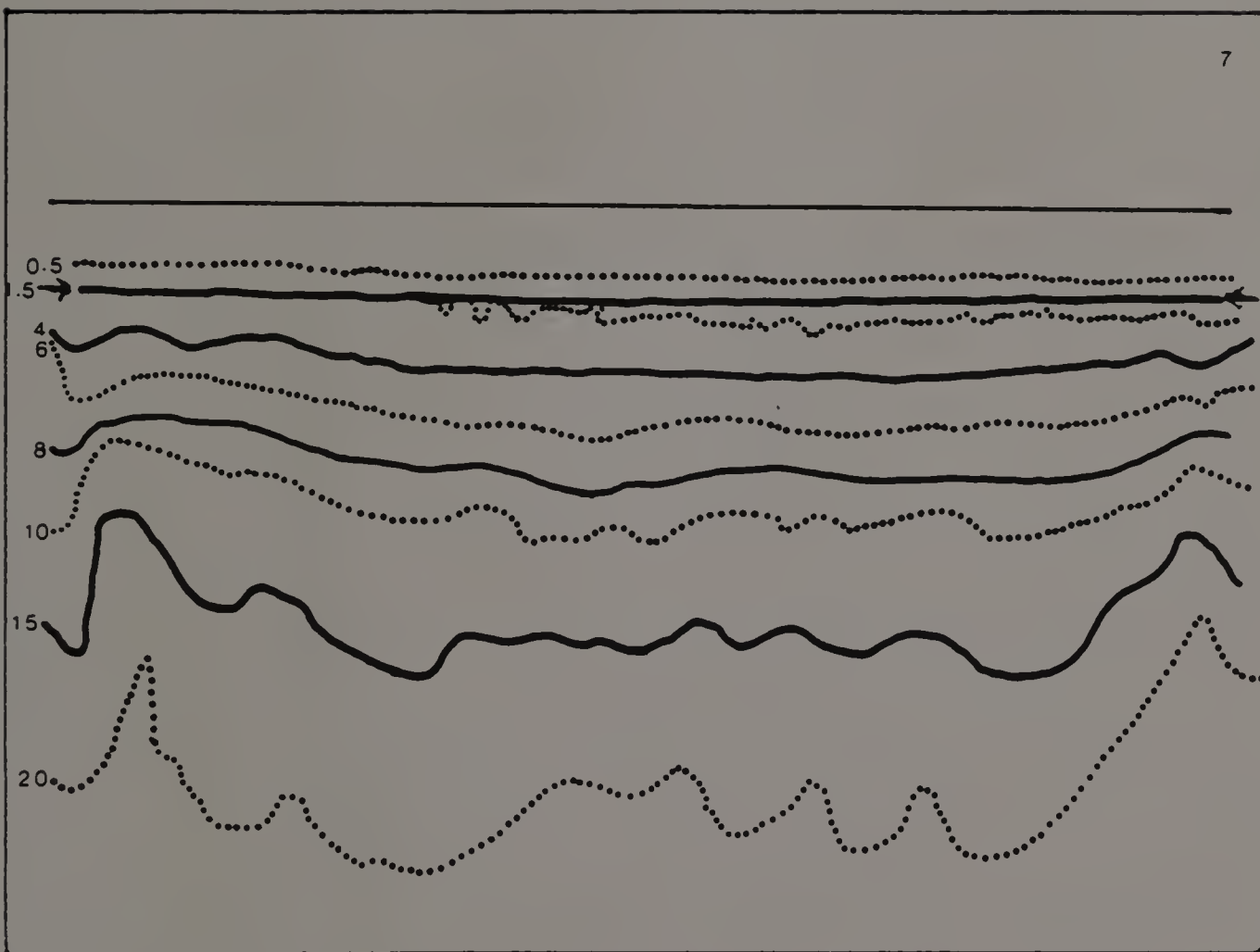


Fig. 4.7: Run 7, 19% of actual size. Straight line indicates soil surface. Arrows indicate position of interface. Numbers indicate time after ponding in minutes.



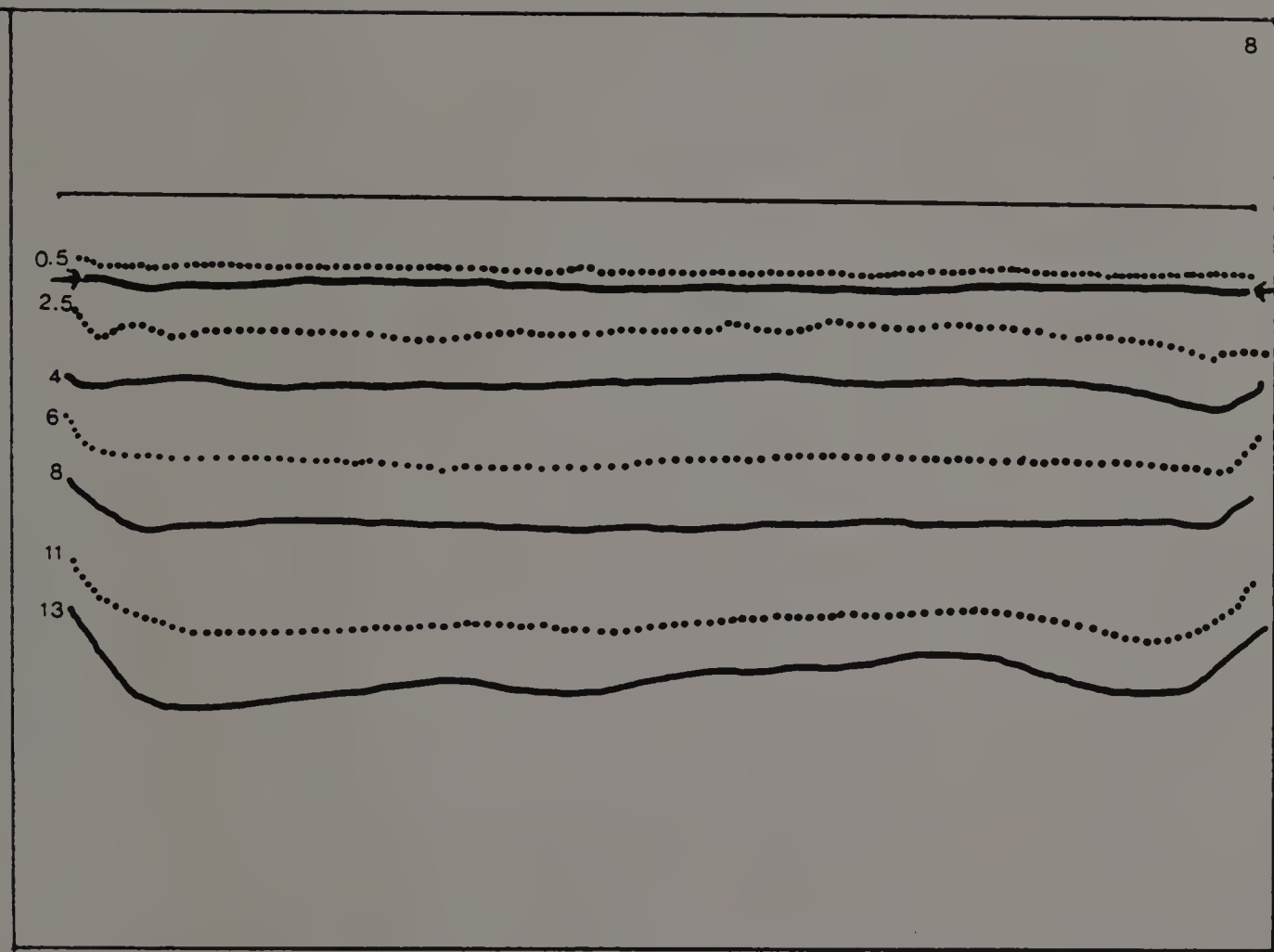


Fig. 4.8: Run 8, 19% of actual size. Straight line indicates soil surface. Arrows indicate position of interface. Numbers indicate time after ponding in minutes.

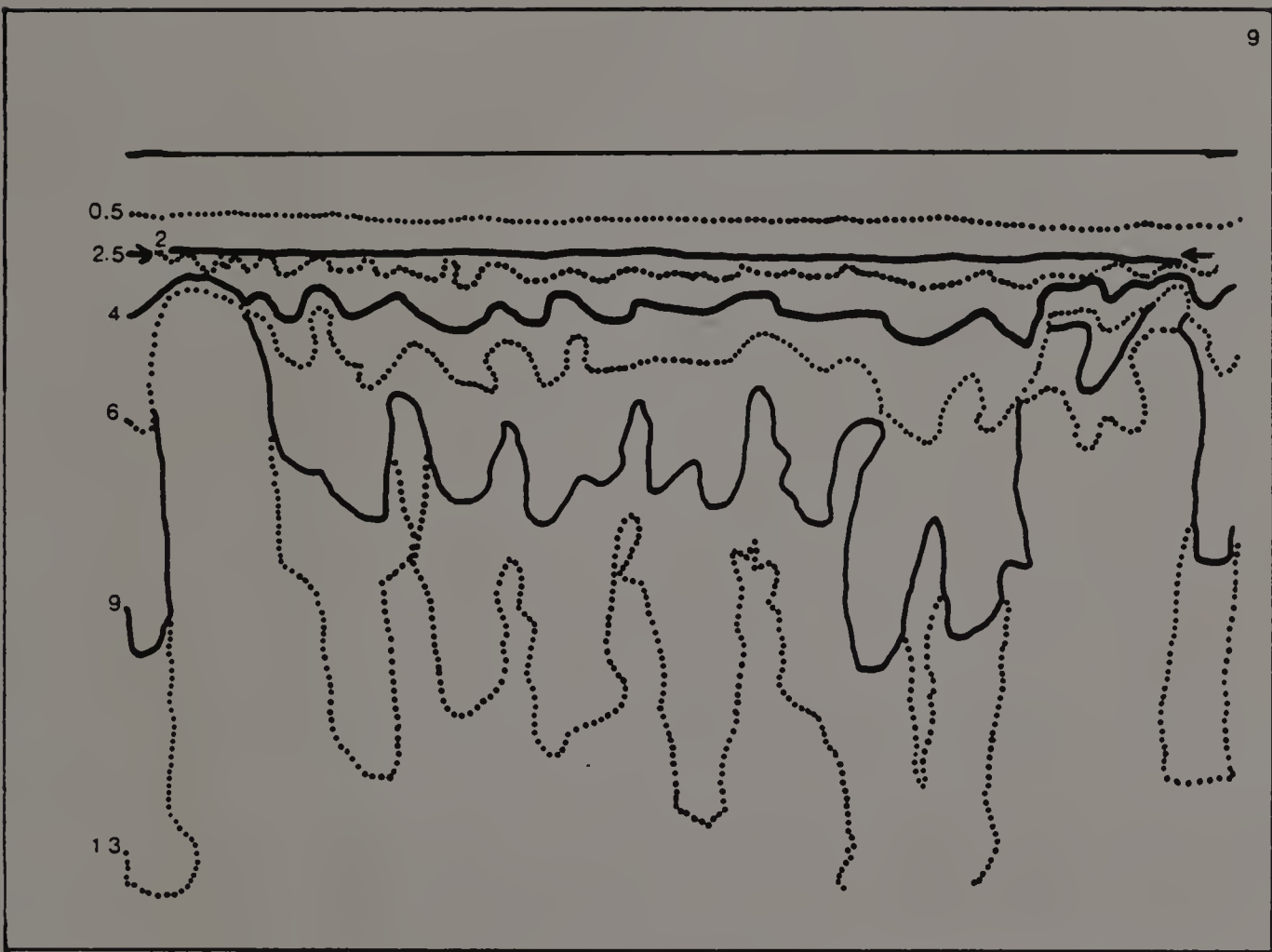


Fig. 4.9: Run 9, 19% of actual size. Straight line indicates soil surface. Arrows indicate position of interface. Numbers indicate time after ponding in minutes.

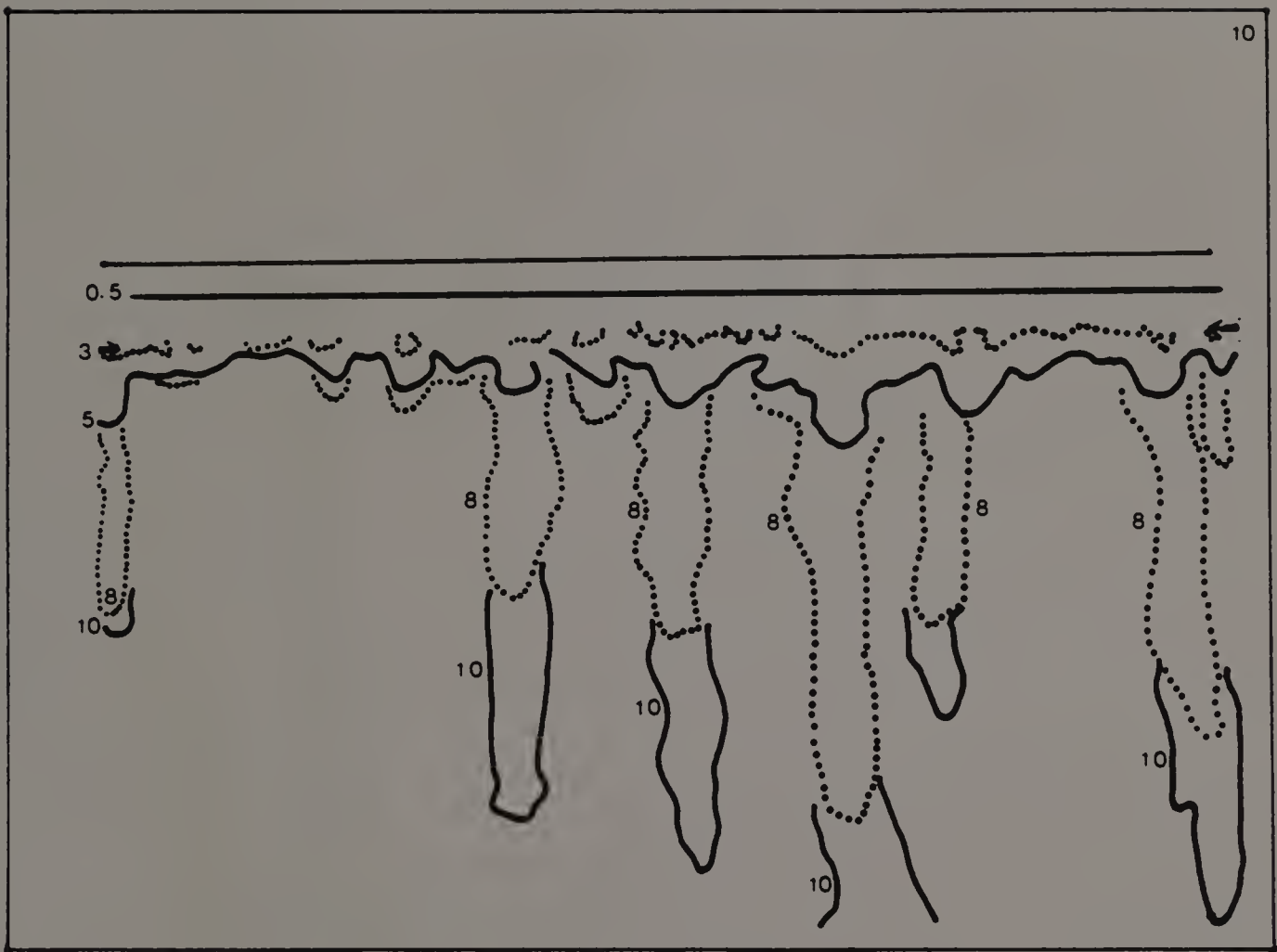


Fig. 4.10: Run 10, 19% of actual size. Straight line indicates soil surface. Arrows indicate position of interface. Numbers indicate time after ponding in minutes.

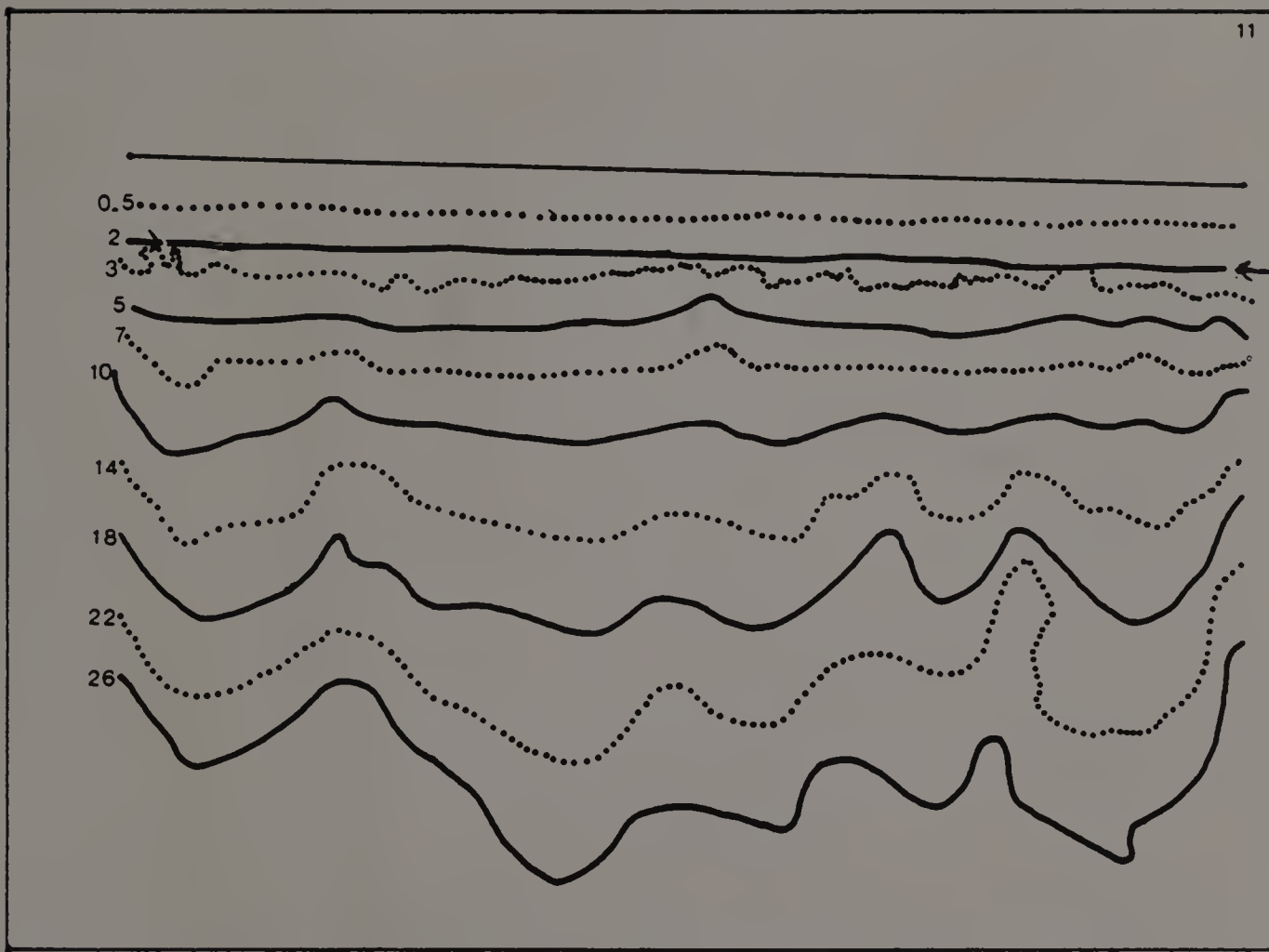


Fig. 4.11: Run 11, 19% of actual size. Straight line indicates soil surface. Arrows indicate position of interface. Numbers indicate time after ponding in minutes.

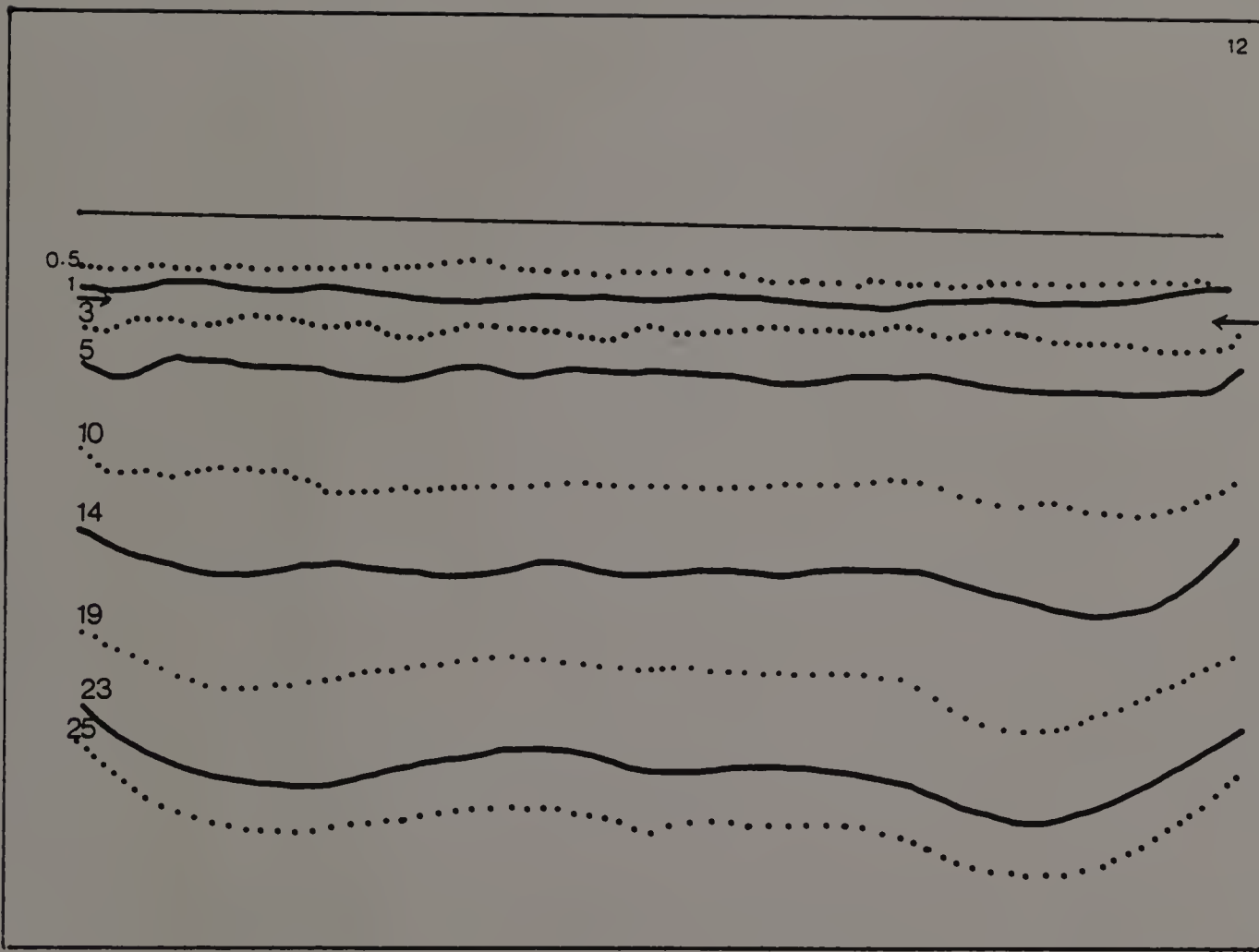
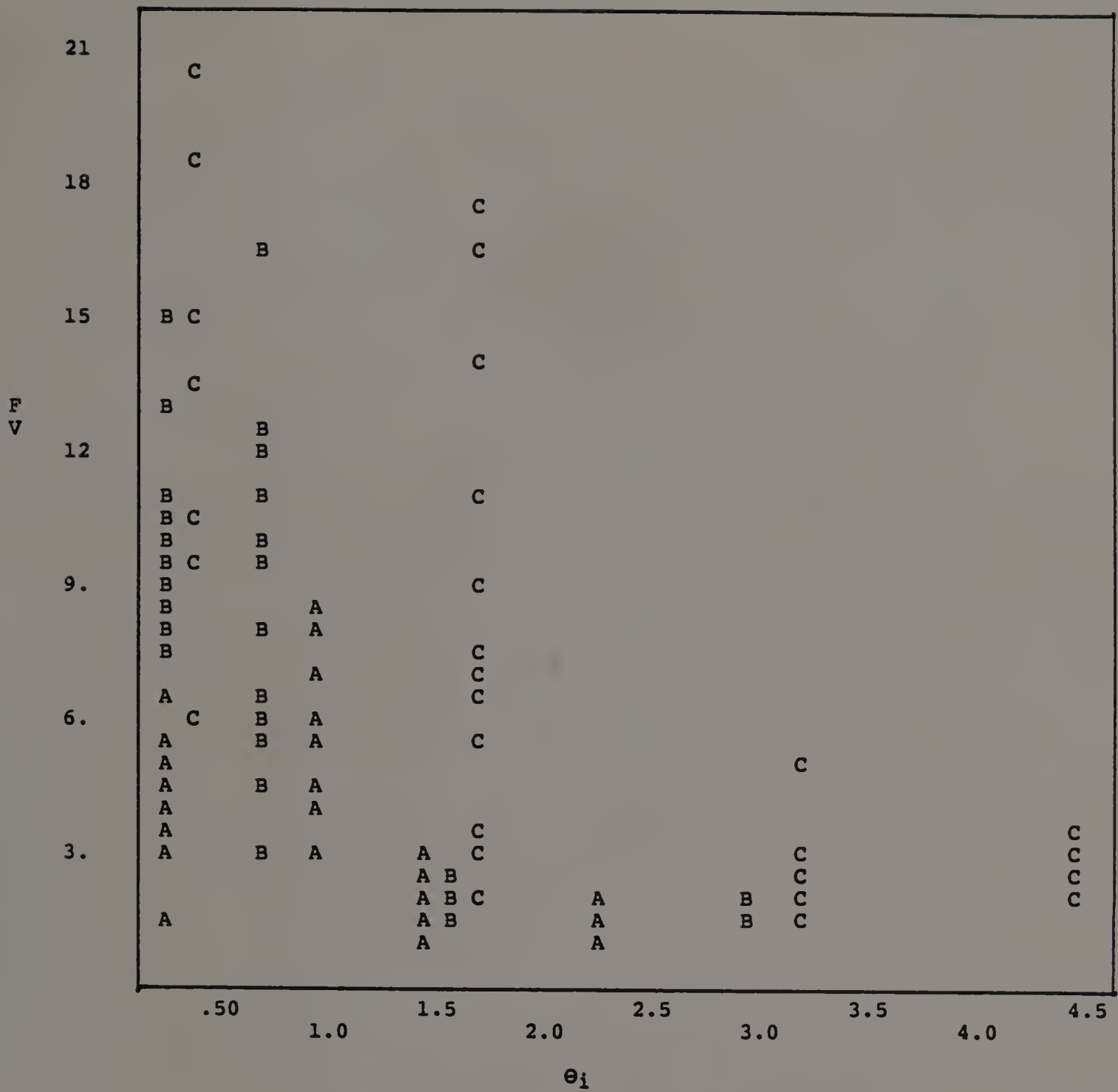


Fig. 4.12: Run 12, 19% of actual size. Straight line indicates soil surface. Arrows indicate position of interface. Numbers indicate time after ponding in minutes.







GROUP=\*425.000, SYMBOL=A  
 GROUP=\*600.000, SYMBOL=B  
 GROUP=\*1500.00, SYMBOL=C

Fig. 4.14: Initial wetness vs. finger speed, layered soil experiments. Initial wetness in percent volume, finger speed in cm/min. Points identified by mean particle size in microns.

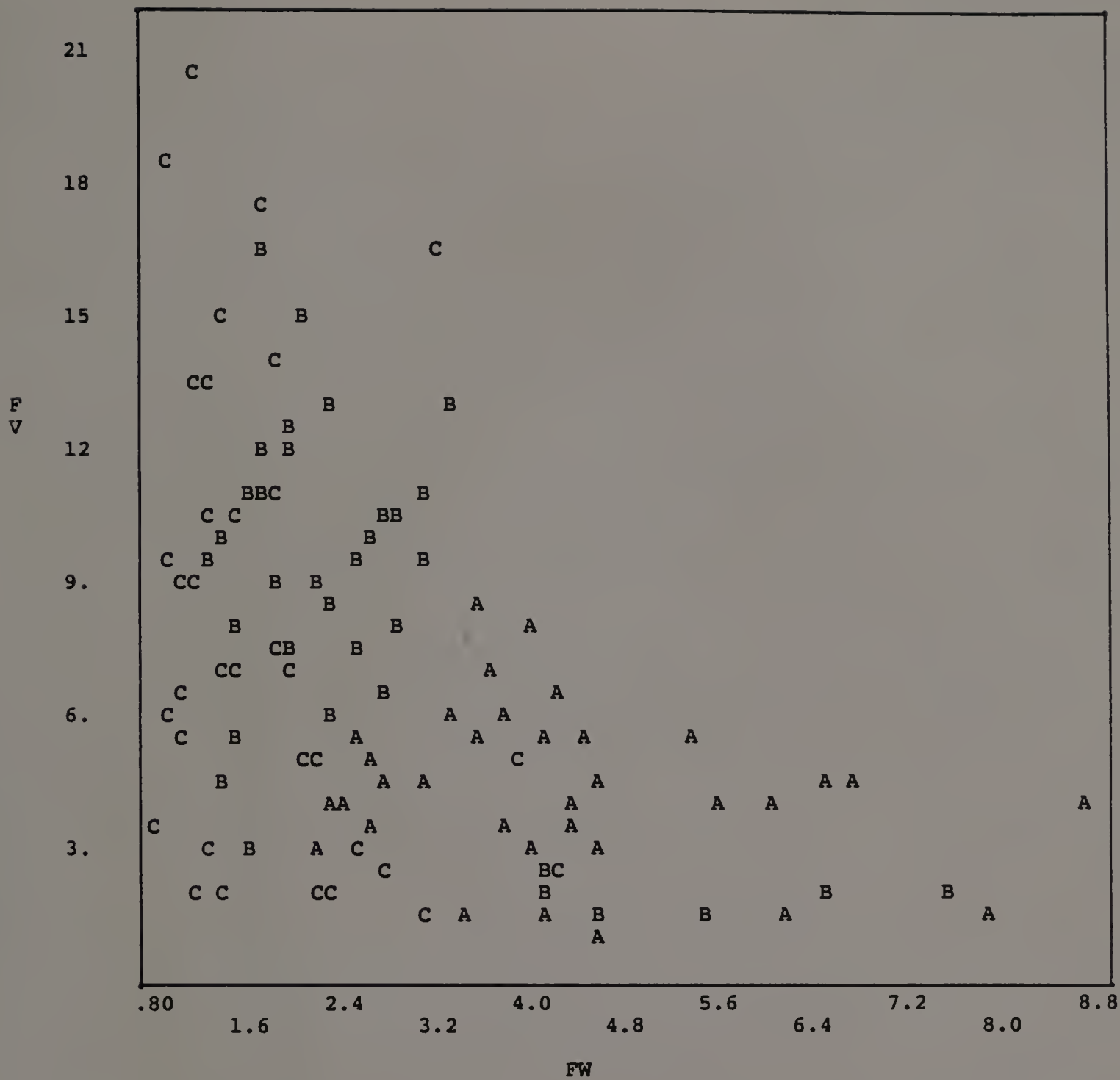


Fig. 4.15: Finger width vs. finger speed, layered soil experiments. Finger width in cm, finger speed in cm/min. Points identified by mean particle size in microns.

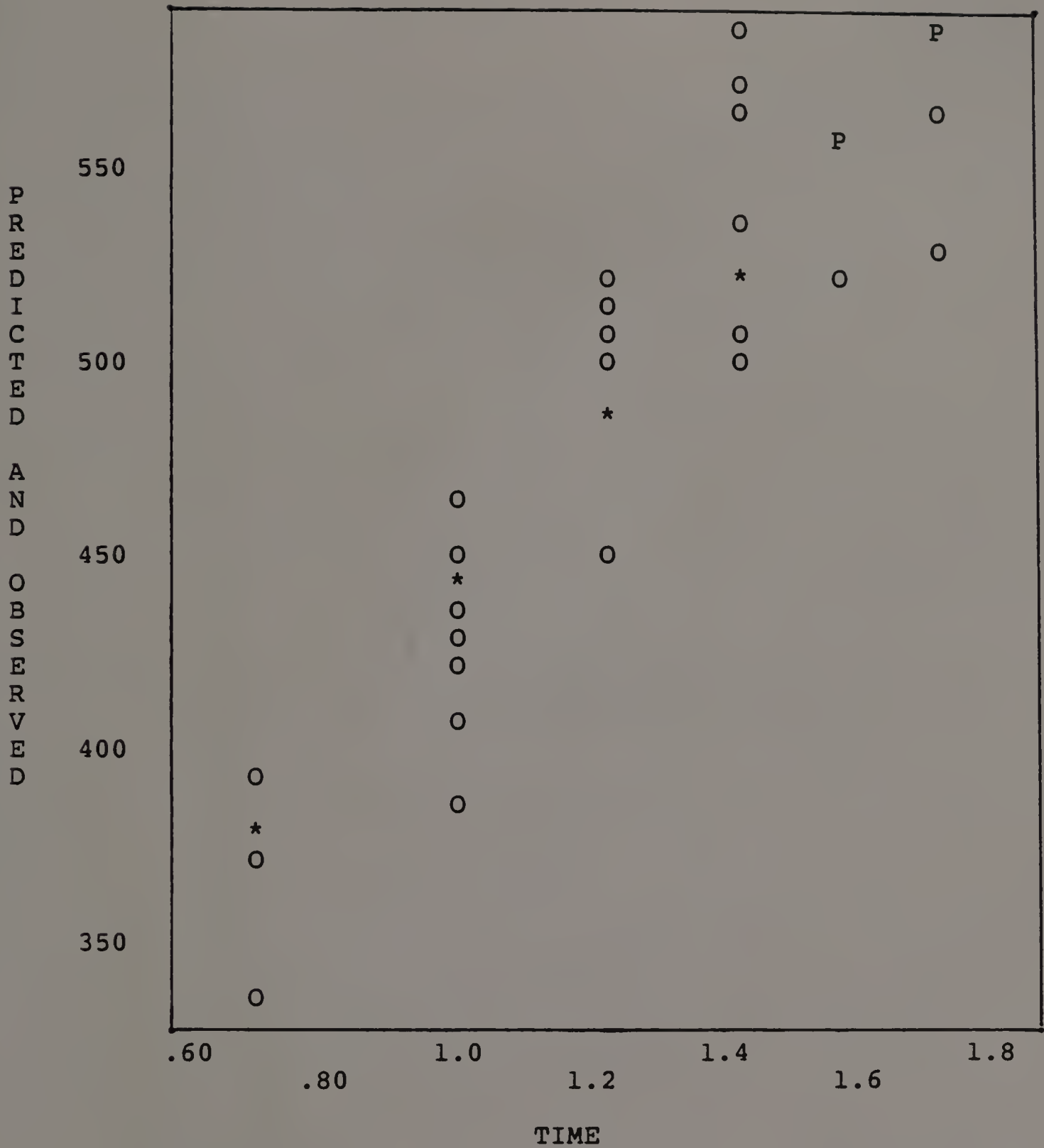


Fig. 4.16: Regression of  $(\text{time})^{1/2}$  vs. cumulative infiltration in layered soil experiments in an air dry condition. Evaluated on BMDP1R statistical program. Y intercept=174.4, coefficient  $(\text{time})^{1/2}$ =251.2, R=.901

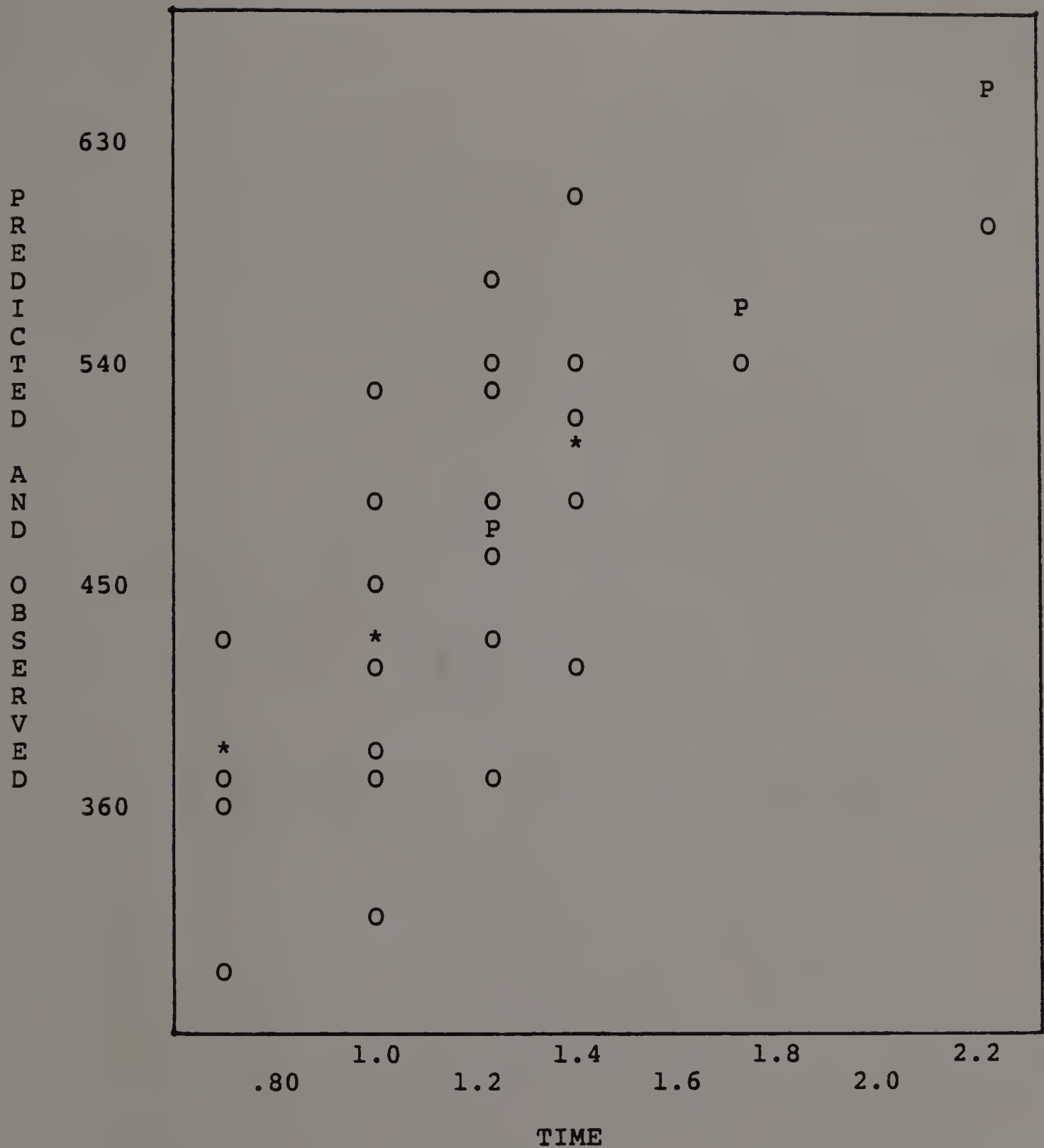


Fig. 4.17: Regression of  $(\text{time})^{1/2}$  vs. cumulative infiltration in layered soil experiments at first incremental increase in initial wetness. Evaluated on BMDP1R statistical program. Y intercept=238.4, coefficient  $(\text{time})^{1/2}$ =201.8,  $R=.91$



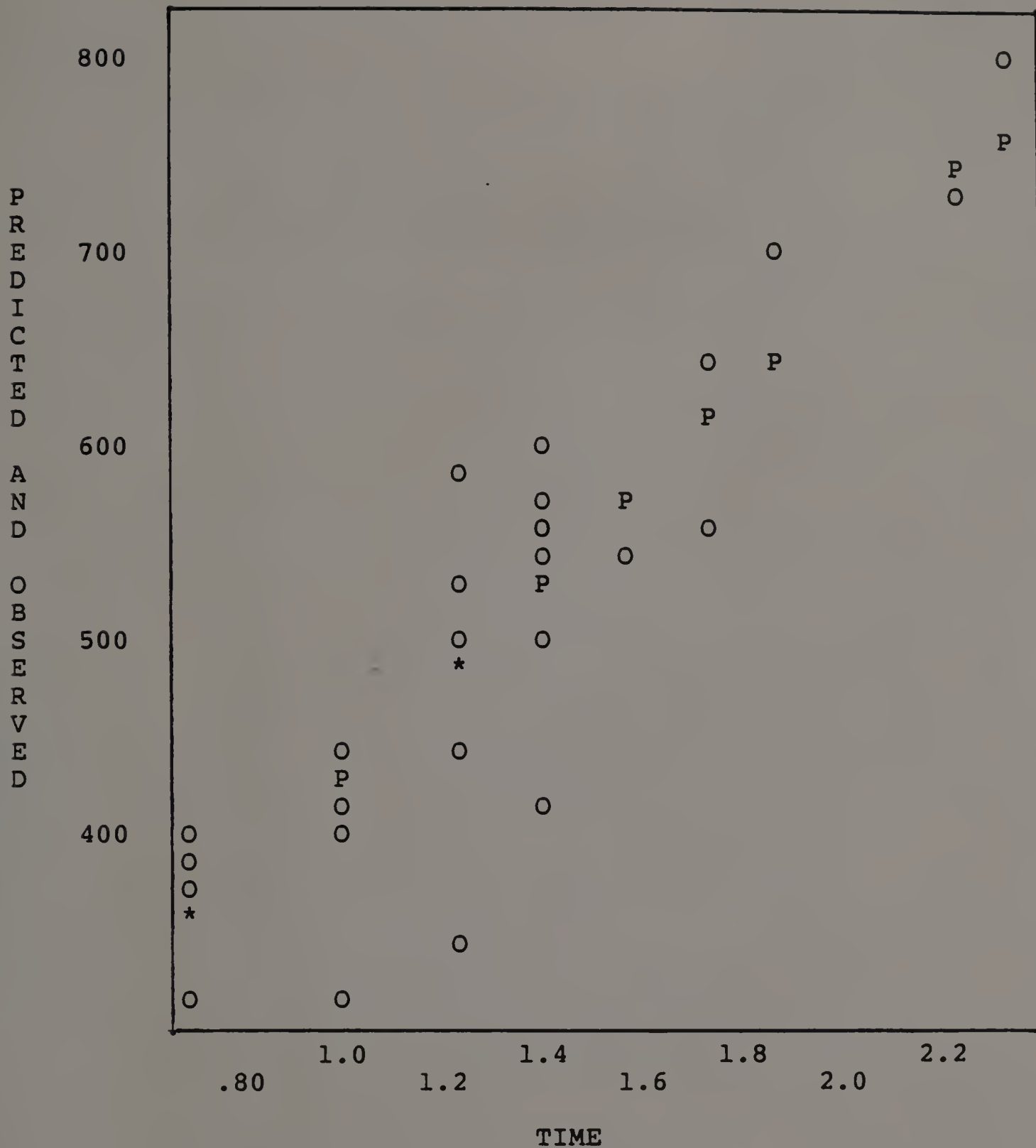


Fig. 4.18: Regression of  $(\text{time})^{1/2}$  vs. cumulative infiltration in layered soil experiments, second incremental increase in initial wetness. Evaluated on BMDP1R statistical program. Y intercept=253.5, coefficient  $(\text{time})^{1/2}$ =201.8,  $R=.919$



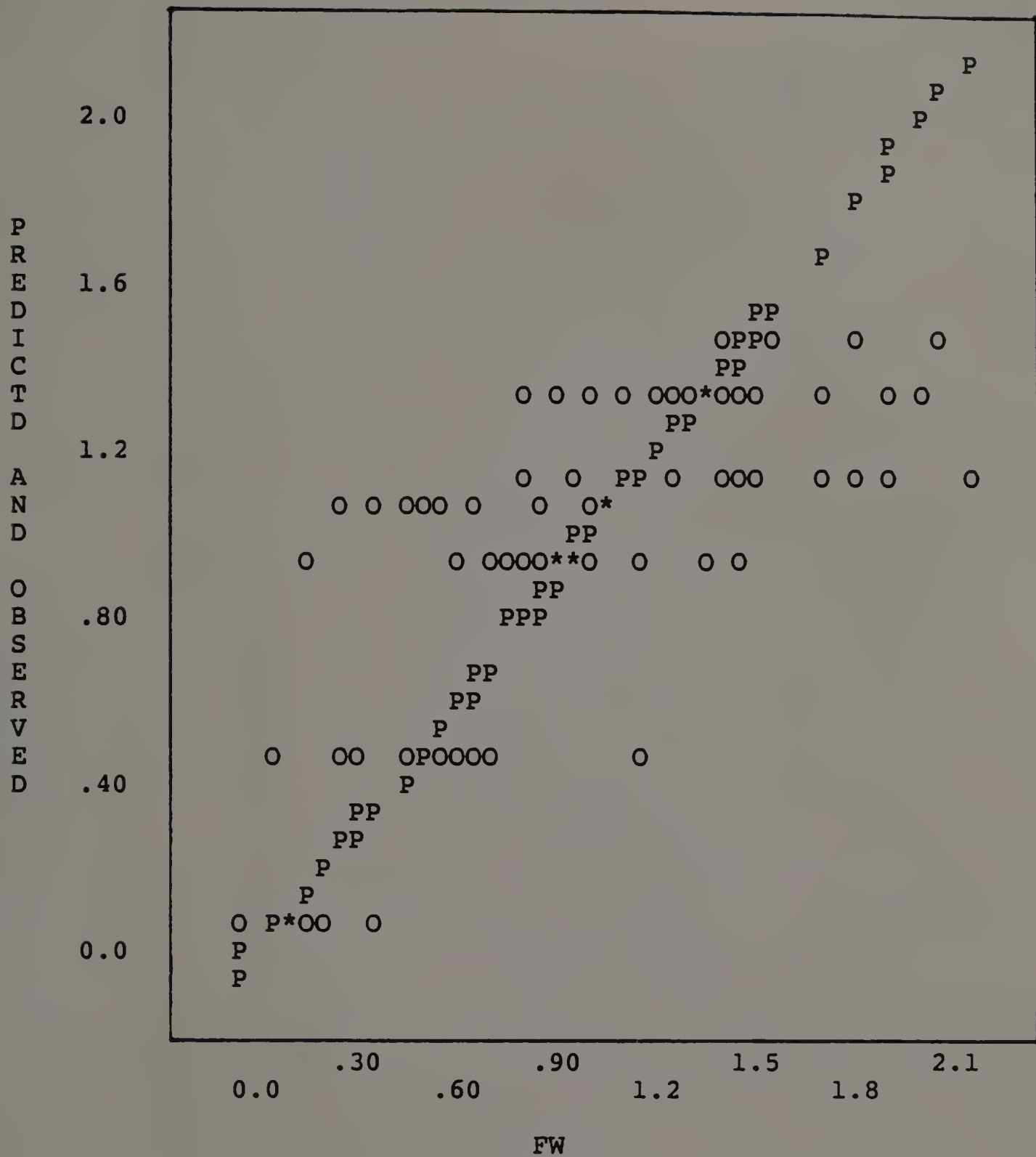


Fig. 4.20: Multiple stepwise regression,  $\ln(\text{finger width})$  in layered soil experiments. Evaluated on BMDP2R statistical program. Y intercept=1.47, coefficient(mps)=-.001, coefficient( $O_i$ )=.3165, Multiple R=.73

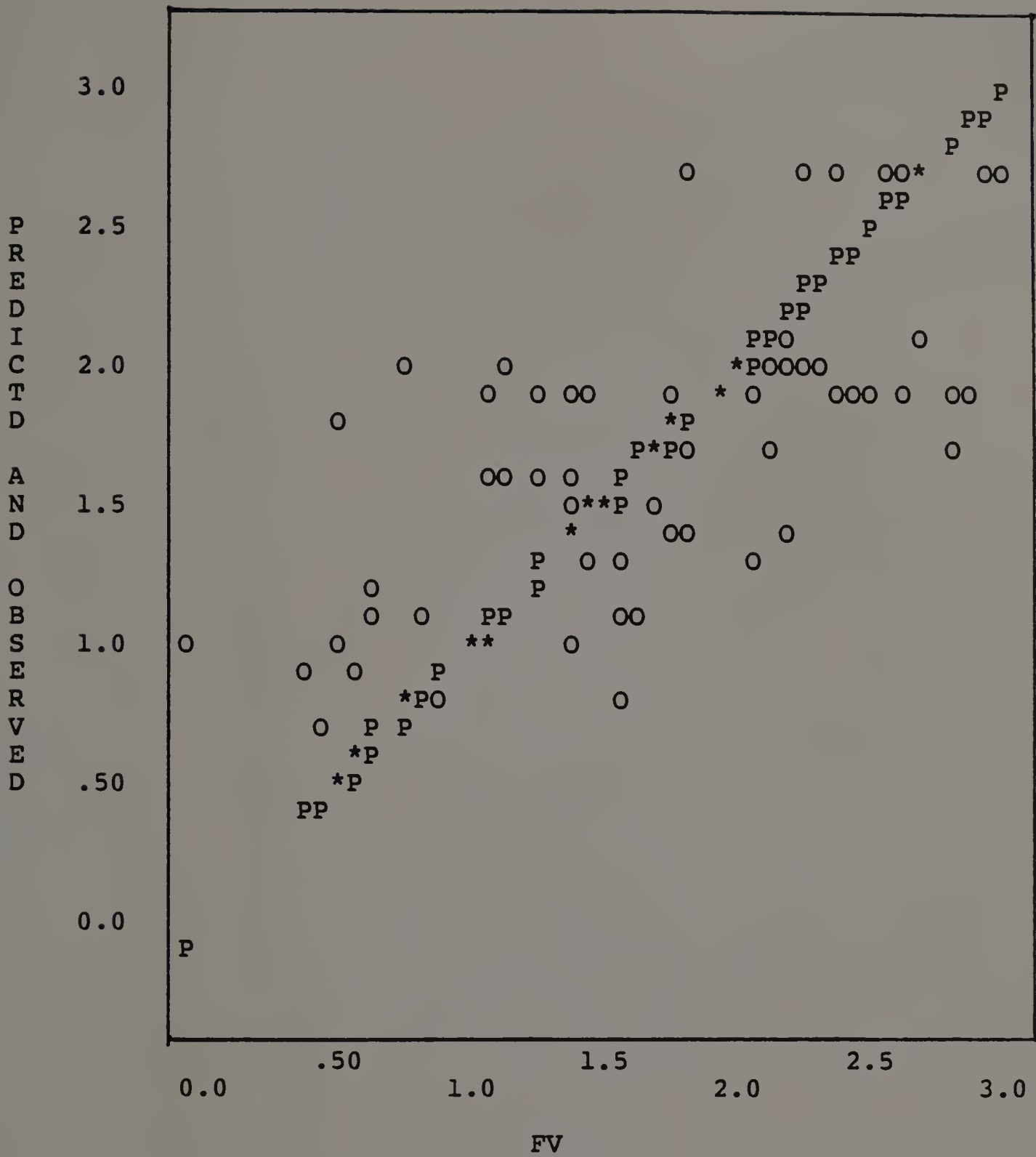


Fig. 4.21: Multiple stepwise regression,  $\ln(\text{finger speed})$  in layered soil experiments. Evaluated on BMDP2R statistical program. Y intercept=2.10, coefficient(finger width)=-.137, coefficient(mps)=.0007, coefficient( $\theta_i$ )=-.5372. Multiple R=.74

We found that fingering would stop in different underlying sands at differing levels of uniform initial moisture. Fingering ceased in the 1-2mm material at  $.045 \text{ cm}^3\text{cm}^{-3}$ , in the .500-.710 material at  $.030 \text{ cm}^3\text{cm}^{-3}$ , and in the .355-.500 mm material at  $.023 \text{ cm}^3\text{cm}^{-3}$ . It was clear that the increased wetness tended to decrease fingering. Smaller amounts of water were necessary to eliminate fingering in soils that exhibited wider fingers when dry. We did not observe fingers in any model beyond the limit of  $\theta_i = 0.45 \text{ cm}^3\text{cm}^{-3}$ .

For the 0.355 mm-0.500 mm and the 0.500 mm and 0.710 mm sand fractions, the initial increment of additional moisture reduced finger width. The second level of wetness, however, increased mean finger width and decreased mean finger speed. Wetting front speeds for the non-fingering wetnesses were considerably slower. The coarsest material did not exhibit this pattern, as fingers became wider and slower with every increase in wetness.

Saturation values behind the wetting front in each layer were occasionally determined. The overlying layer appeared to be saturated, but saturation values in the coarse sublayers did not exceed .50. This value was not measurably different in wet or dry sands. We were not able to determine whether fingers consisted of a saturated central core surrounded by an unsaturated region, as Hill and Parlange (1972) conjectured. By the time samples could



be taken, fingers appeared uniformly wet throughout their thickness, with no saturated zone evident.

In spite of the broader distribution of infiltrating water in initially wet experiments when compared to the dry cases, the correlation of infiltration to the square root of time was not significantly different from the most unstable to the most stable cases over the first six minutes of any experiment, as shown in the graphs in fig. 4.16-4.19. Experiments with sufficient moisture to eliminate fingering generally lasted far longer than experiments where fingering was evident, as the wetting front speed slowed with increased wetness. Regression lines drawn for infiltration against the square root of time did not differ significantly in terms of either their slopes or their Y-intercepts with changes in the experiments' level of initial moisture.

From the multiple linear regressions, it is seen that mean particle size and initial wetness are both significantly correlated to finger width. Mean particle size is negatively correlated to finger width, while initial wetness is positively correlated to finger width. Mean particle size is positively correlated to finger speed, however, and initial wetness is negatively correlated to finger speed. Finger width is also negatively correlated to finger speed.

## B. Variable initial wetness experiments

Experiments involving variations in initial moisture were run to determine how fingers may originate in layered soils, and how long they may persist, once formed.

Run 13 involved repeated infiltrations into the same cell, 20 minutes apart. The overlying layer was 1.5 kg of 0.047 mm to 0.105 mm sand, again 6 cm deep and packed to a bulk density of  $1.41 \text{ g/cm}^3$ , while the sublayer was 10 kg of 1.00-2.00 mm sand, packed to a depth of 40-42 cm. The second infiltration was run with water dyed with acid red, in an attempt to determine if fingers became preferred pathways for subsequent infiltrating water.

Run 14 examined whether fingers passed through regions of soil which were marginally wetter than others. The overlying layer was again 1.5 kg of 0.047-0.105 mm sand packed as in previous runs, while the underlying layer was composed of 5 kg of 0.500-0.710 mm sand at  $O_i=0.266\%$  in four vertical stripes alternating with four vertical stripes of the same sand at  $O_i=2.94\%$ , forming a total depth of 41 cm. Infiltration was carried out according to the standard procedure.

Run 15 examined the persistence of fingers as they passed through a dry soil layer into a wet soil layer. The overlying layer was a 6 cm depth of 0.047-0.105 mm sand overlying a 20 cm depth of 5 kg of 0.500-0.710 mm sand at

$O_i=0.266\%$ , which in turn overlay a 21 cm depth of 5 kg of the same sand at  $O_i=2.94\%$ .

Run 16 tested whether the wetting front was in fact fully stabilized by the presence of initial moisture. This run was the same as run 15, with the difference that in this case the coarse layer at the interface had a  $O_i$  of 2.94%, while the lower coarse layer was at air dryness ( $O_i=0.266\%$ ).

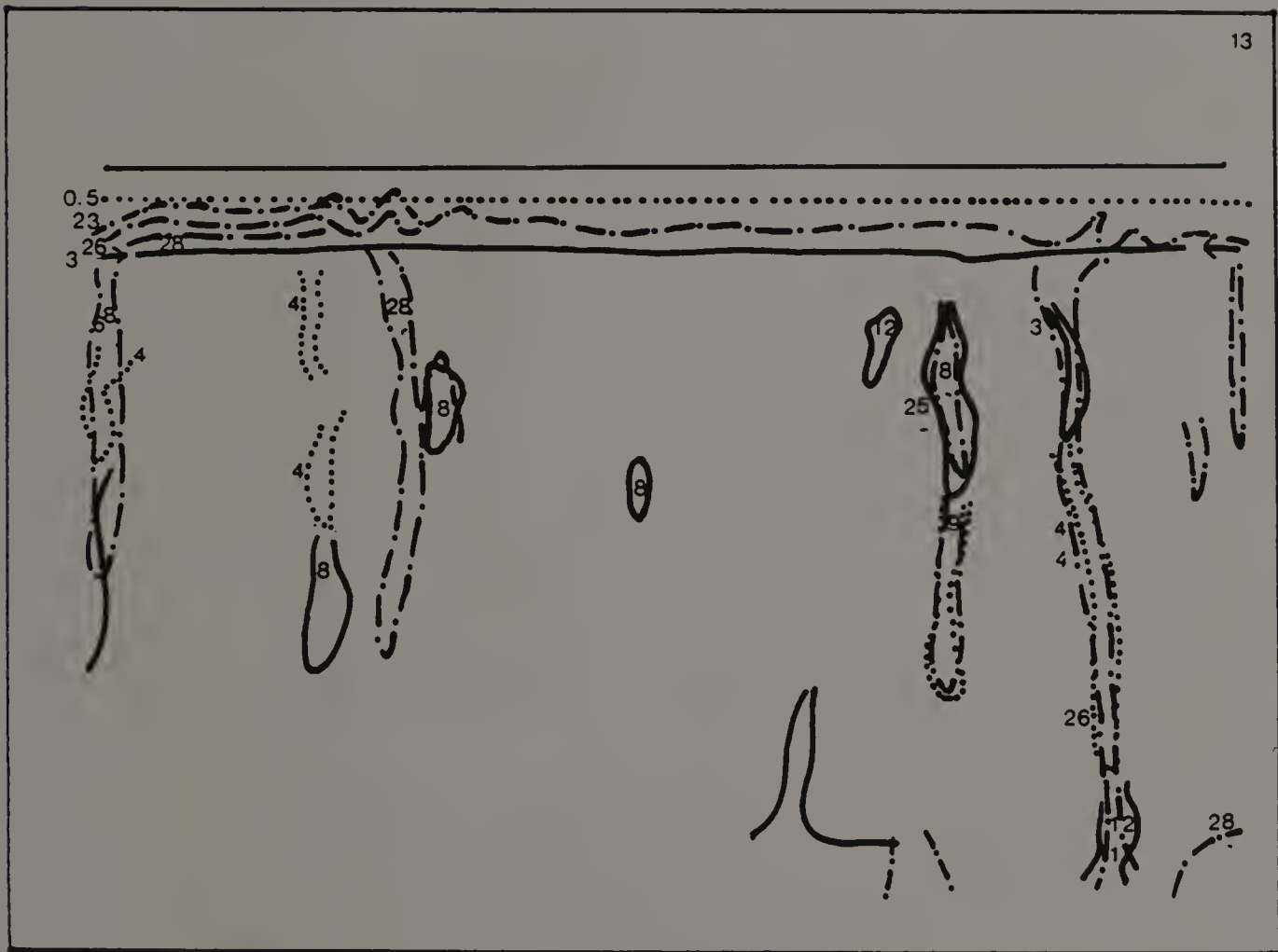


Fig. 4.22: Run 13, 19% of actual size. Straight line indicates soil surface. Arrows indicate position of interface. Numbers indicate time after ponding in minutes.

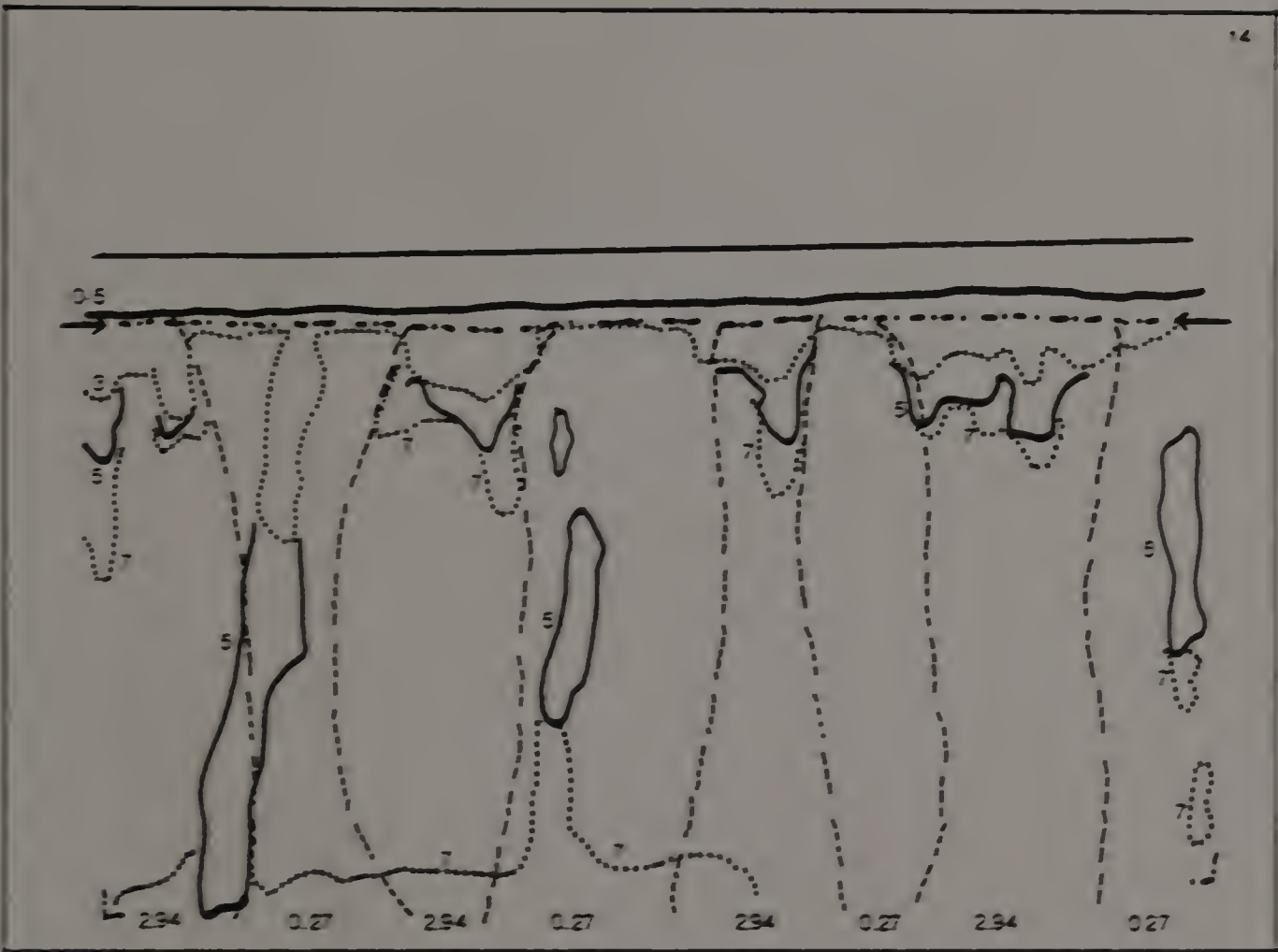


Fig. 4.23: Run 14, 19% of actual size. Straight line indicates soil surface. Arrows indicate position of interface. Numbers indicate time after ponding in minutes.

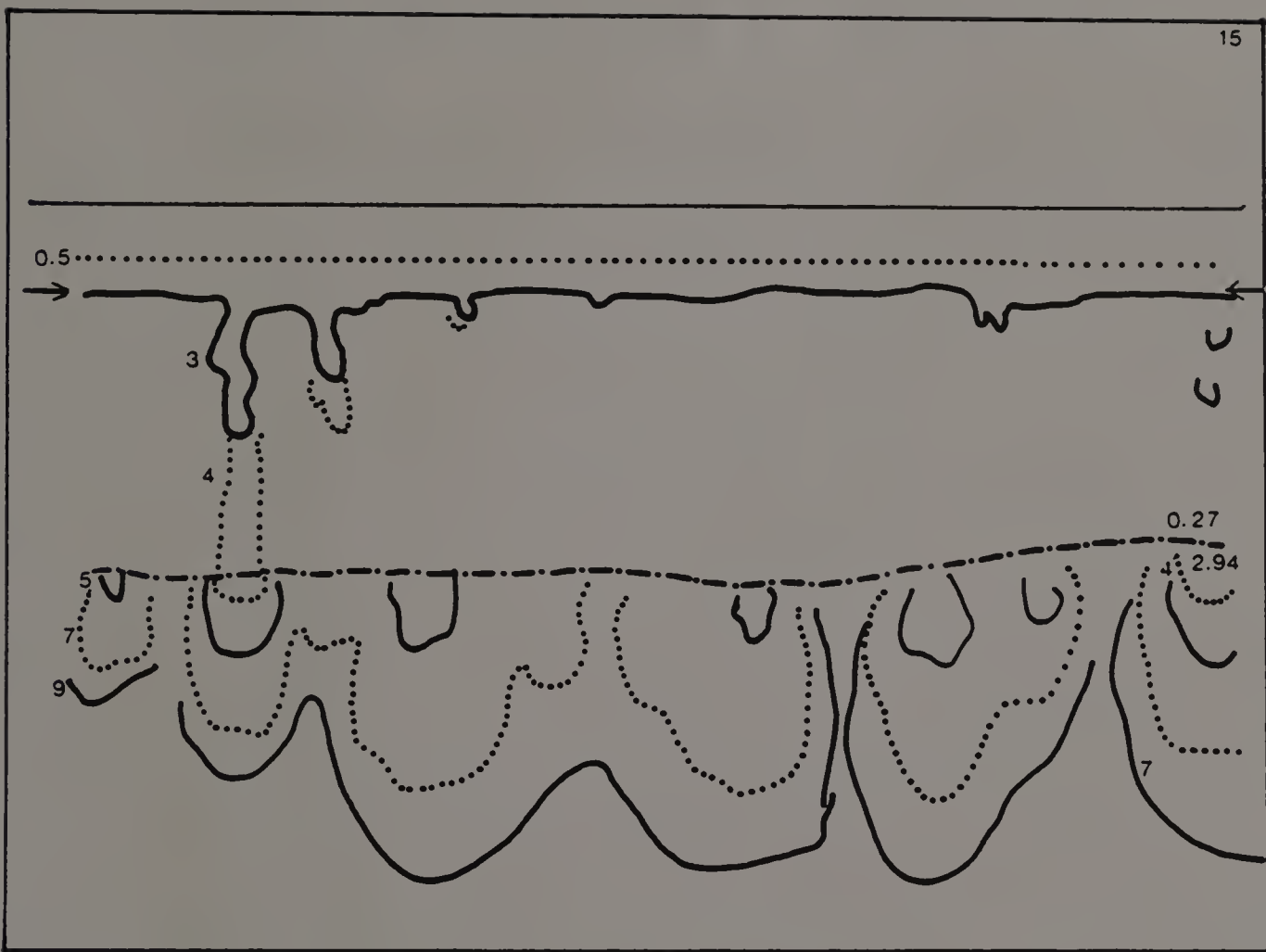


Fig. 4.24: Run 15, 19% of actual size. Straight line indicates soil surface. Arrows indicate position of interface. Numbers indicate time after ponding in minutes.



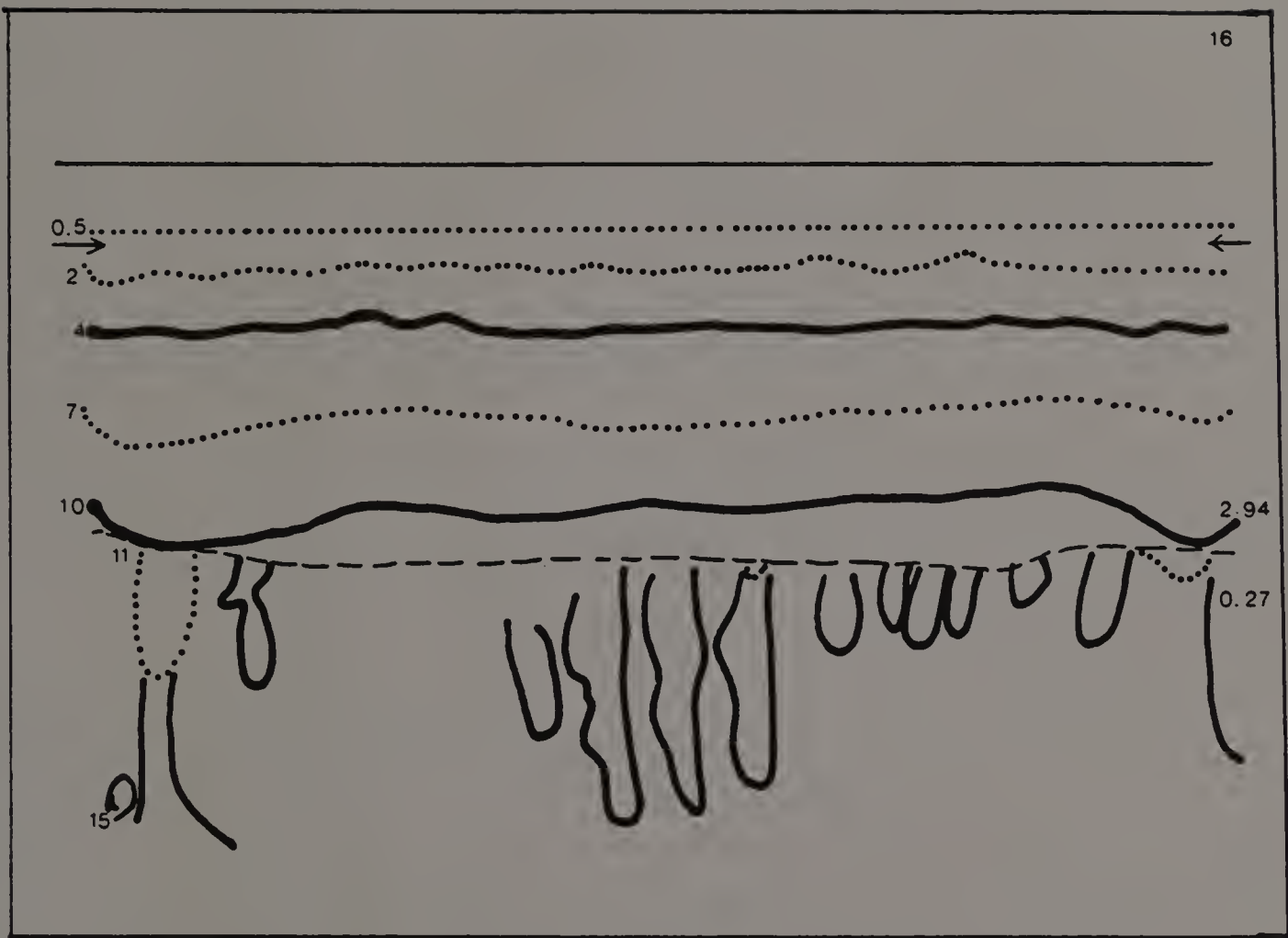


Fig. 4.25: Run 16, 19% of actual size. Straight line indicates soil surface. Arrows indicate position of interface. Numbers indicate time after ponding in minutes.

During run 13, fingers formed as usual in the dry sublayer during infiltration, and more fingers became apparent later as spreading occurred while ponded water infiltrated. A second infiltration with dyed water showed that water was moving almost exclusively through the fingers established by the previous infiltration.

Experimental run 14 demonstrated that fingering was occurring in the driest, rather than the wettest, regions of the soil. Water appeared to penetrate the moist soil first, spreading across the width of the moist vertical strips. After the water had moved some distance down these wet regions, fingers formed in the dry regions and soon overtook the wetting front in the moist strips, reaching the bottom of the cell before the wetting front in the moist strips had gone more than a few centimeters.

In run 15 where a fine layer overlay a layer of dry coarse material, with moist coarse material on the bottom, fingers formed as usual in the coarse, dry region. As the fingers reached the moist region they slowed considerably. Soon flow was almost as great in the horizontal direction as it was in the direction of the bottom of the cell. However, the fingers did not reach the point of overlapping completely.

In run 16, where a fine layer overlay a moist coarse layer with a dry coarse layer on the bottom, the wetting front entered the moist layer in the expected stable

fashion. Though the front was not perfectly planar, as it appeared to be in the upper layer, it moved slowly and no separate fingering zones formed. Upon reaching the dry region the front broke into distinct, fast-moving fingers which crossed the remaining distance to the bottom of the cell at a greater velocity than that of the wetting front as it had moved through the moist region.

### C. Point source infiltration experiments

Runs 15 and 16 indicated that the effect of destabilizing forces at the interface might be to cause the overlying layer to act as a series of point sources of water. The appearance of stability or instability in the lower layer might then depend on the degree of lateral spreading of fingers issuing from those point sources.

In experiments 17-26, water was released at a constant rate from a burette, which acted as a point source of uniform diameter. The stream flowed into the standard coarse lower layers used in the runs 1-12, and the full extent of lateral spreading of water from a point source could be seen without any overlap between fingers. Table 4.2 outlines the conditions and results of each experiment. Following the experimental tracings are graphs indicating

the relationships between the various experimental conditions and finger width and finger speed.

Table 4.2

## Point Source Infiltration Experiments

Run	date	Mean particle diameter (mm)	Volume wetness (%)	flux (ml/min.)	finger width (cm)	finger speed (cm/min.)
17	8/22/87	1.50	0.377	4	0.94	21.6
				4	1.24	18.2
18	8/23/87	1.67	1.67	1	1.36	5.42
				2	1.17	8.77
				2	1.23	11.52
				4	1.03	14.00
19	9/1/87	3.17	3.17	6	1.54	15.33
				4	5.15	12.2
				6	4.15	9.78
20	8/27/87	0.60	0.266	6	4.91	9.93
				1	1.43	3.31
				2	2.02	4.96
				4	2.03	9.05
21	9/2/87	1.56	1.56	6	1.93	10.43
				1	2.20	1.70
				2	3.00	1.77
22	8/26/87	2.94	2.94	6	2.27	5.37
				1	10.4	0.45
				4	11.9	1.29
23	8/24/87	0.425	0.267	6	13.05	1.62
				1	3.13	1.75
				5	3.68	4.98
24	8/28/87	1.46	1.46	9	4.32	7.25
				2	17.78	0.44
				6	13.52	1.28
25	8/25/87	2.27	2.27	2	17.75	0.46
				4	15.52	0.93
26	9/3/87	0.075	0.350	2	20.00	0.19
				6	33.4	0.30

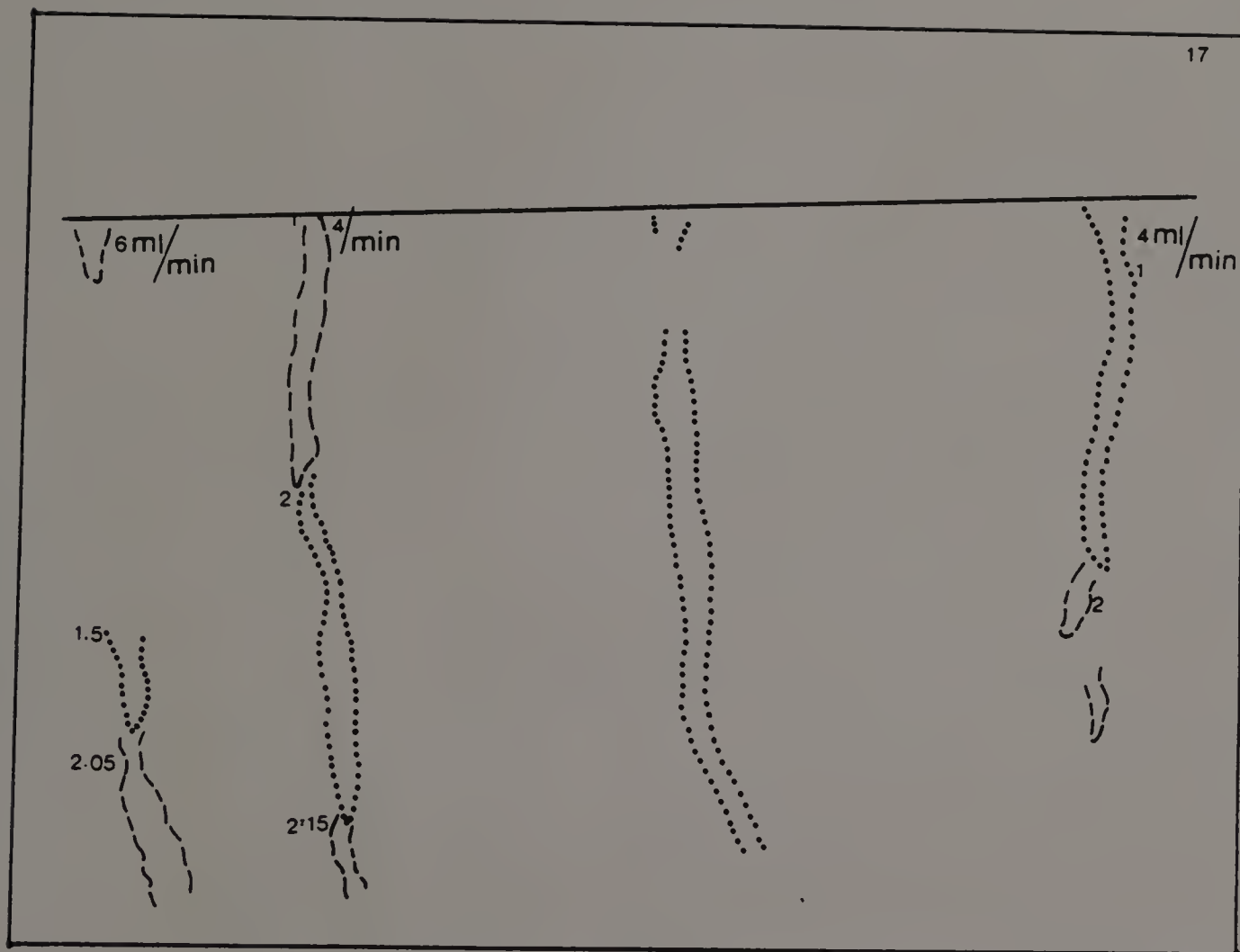


Fig. 4.26: Run 17, 19% of actual size. Straight line indicates soil surface. Numbers indicate time after opening burette in minutes.



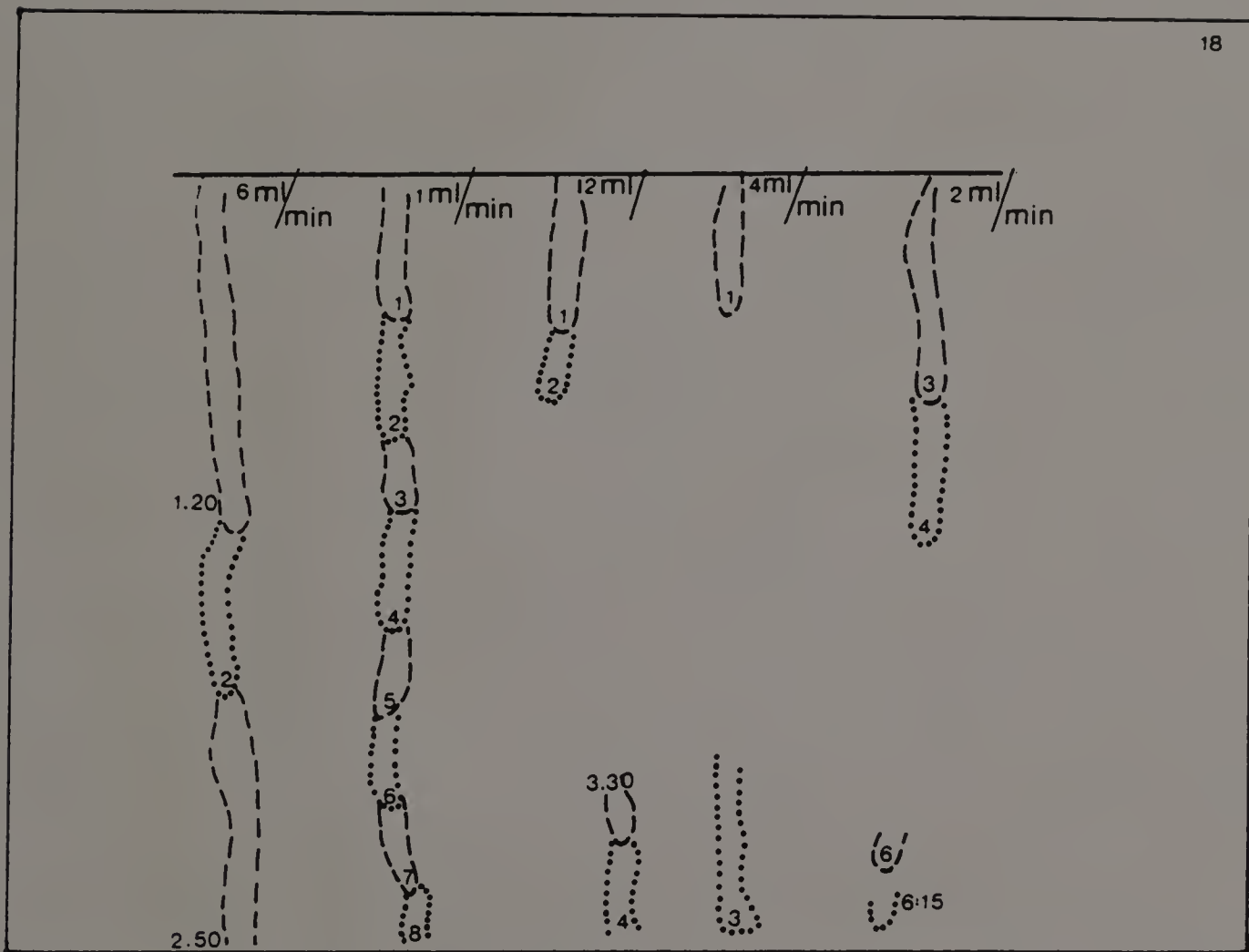


Fig. 4.27: Run 18, 19% of actual size. Straight line indicates soil surface. Numbers indicate time after opening burette in minutes.

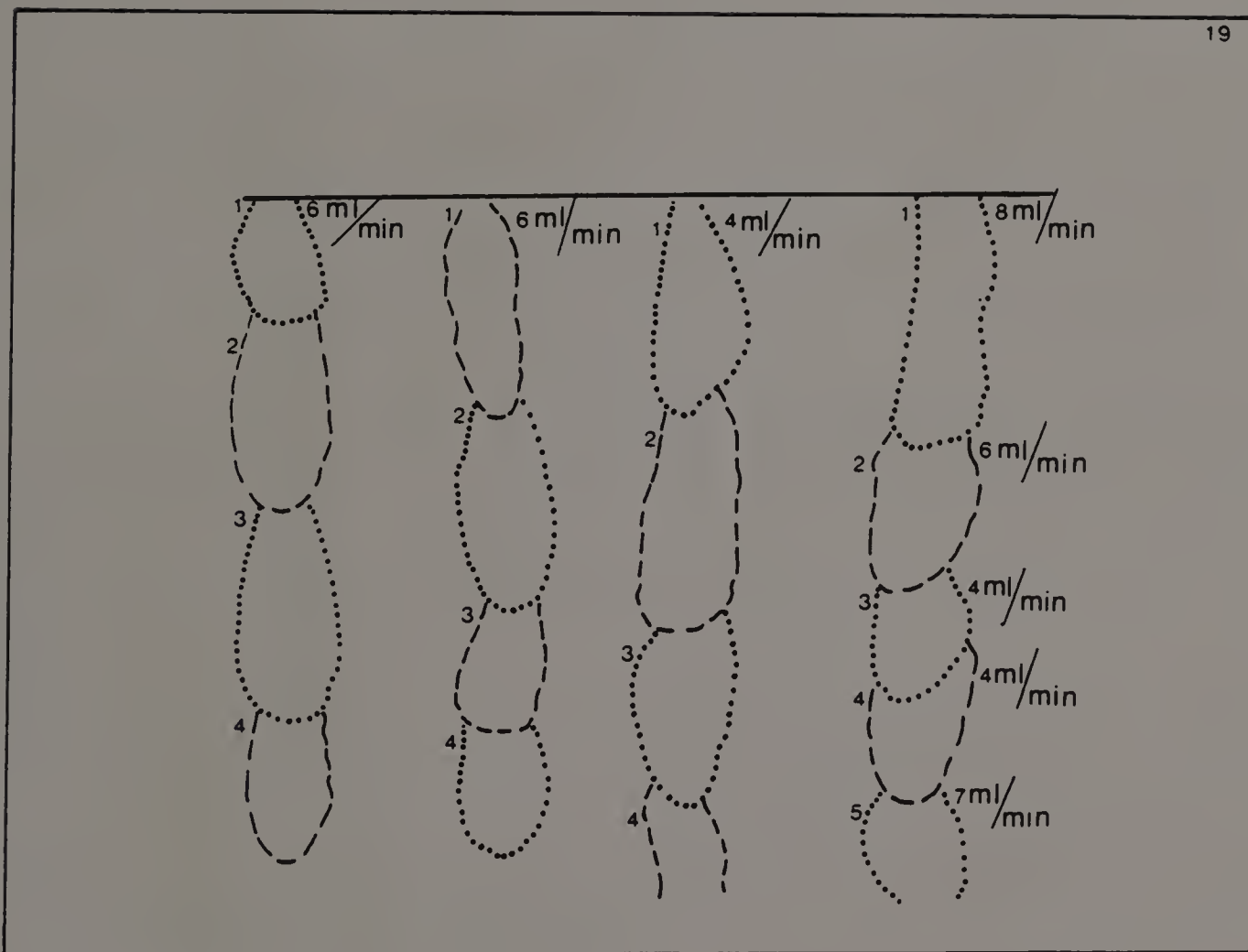


Fig. 4.28: Run 19, 19% of actual size. Straight line indicates soil surface. Numbers indicate time after opening burette in minutes.

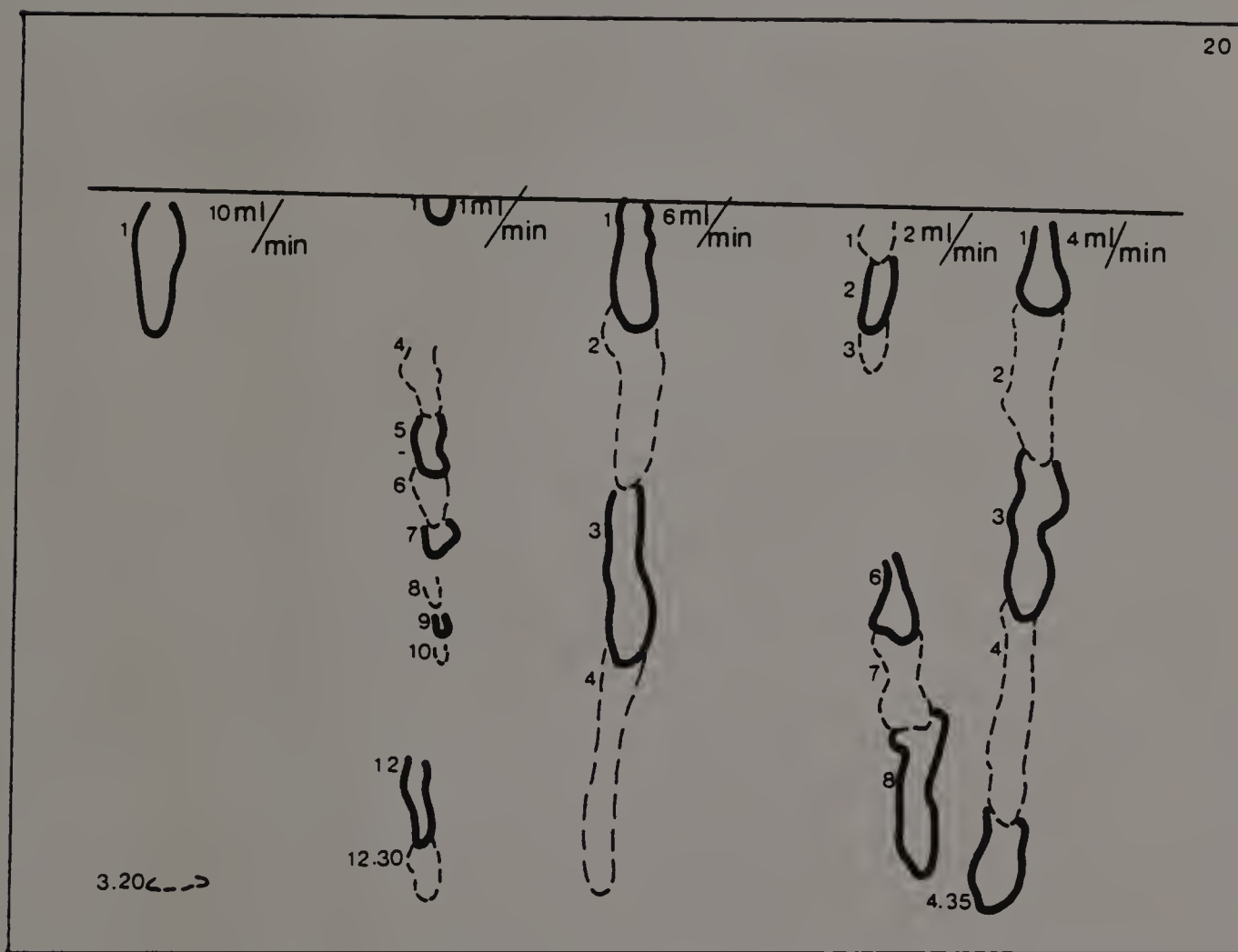


Fig. 4.29: Run 20, 19% of actual size. Straight line indicates soil surface. Numbers indicate time after opening burette in minutes.

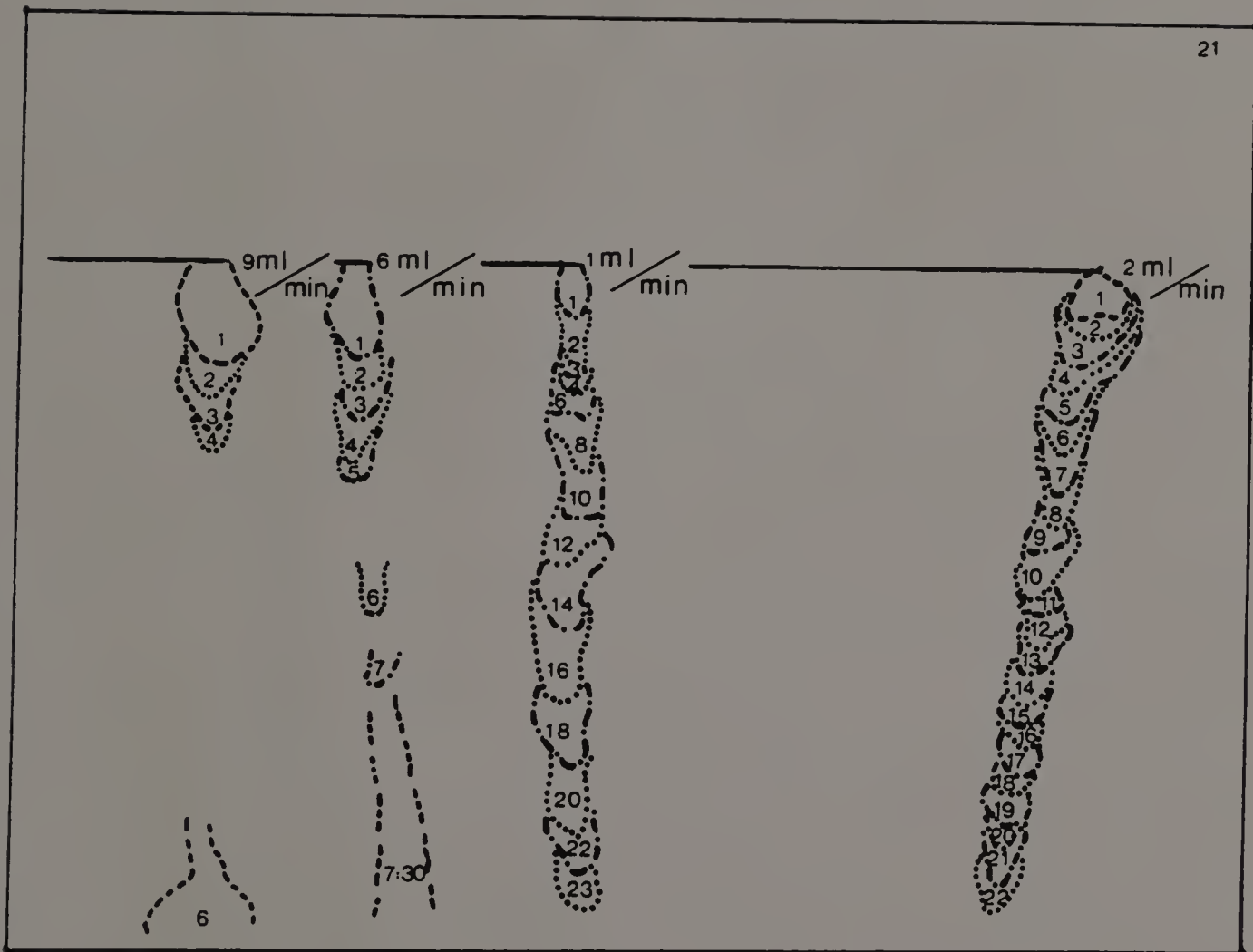


Fig. 4.30: Run 21, 19% of actual size. Straight line indicates soil surface. Numbers indicate time after opening burette in minutes.

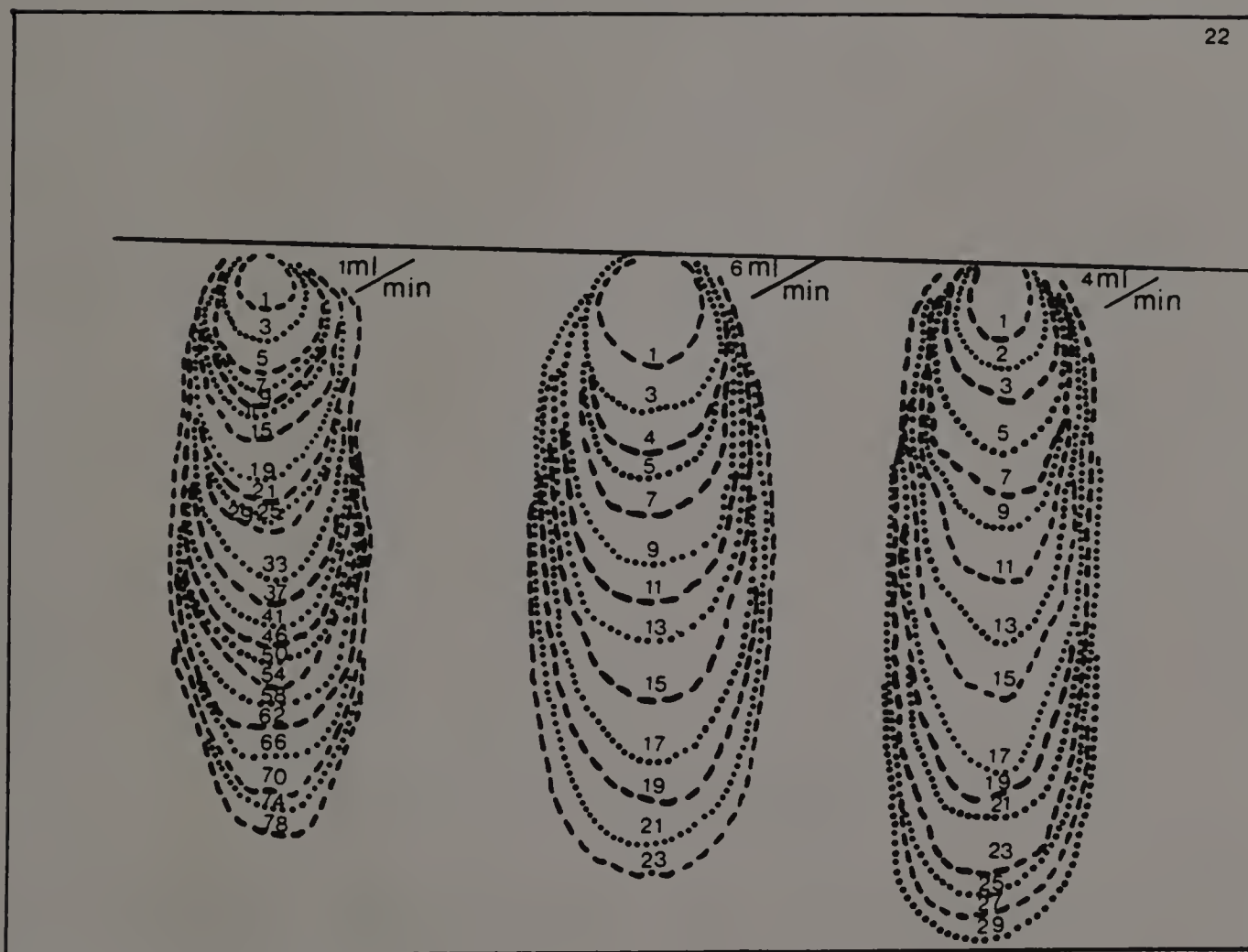


Fig. 4.31: Run 22, 19% of actual size. Straight line indicates soil surface. Numbers indicate time after opening burette in minutes.

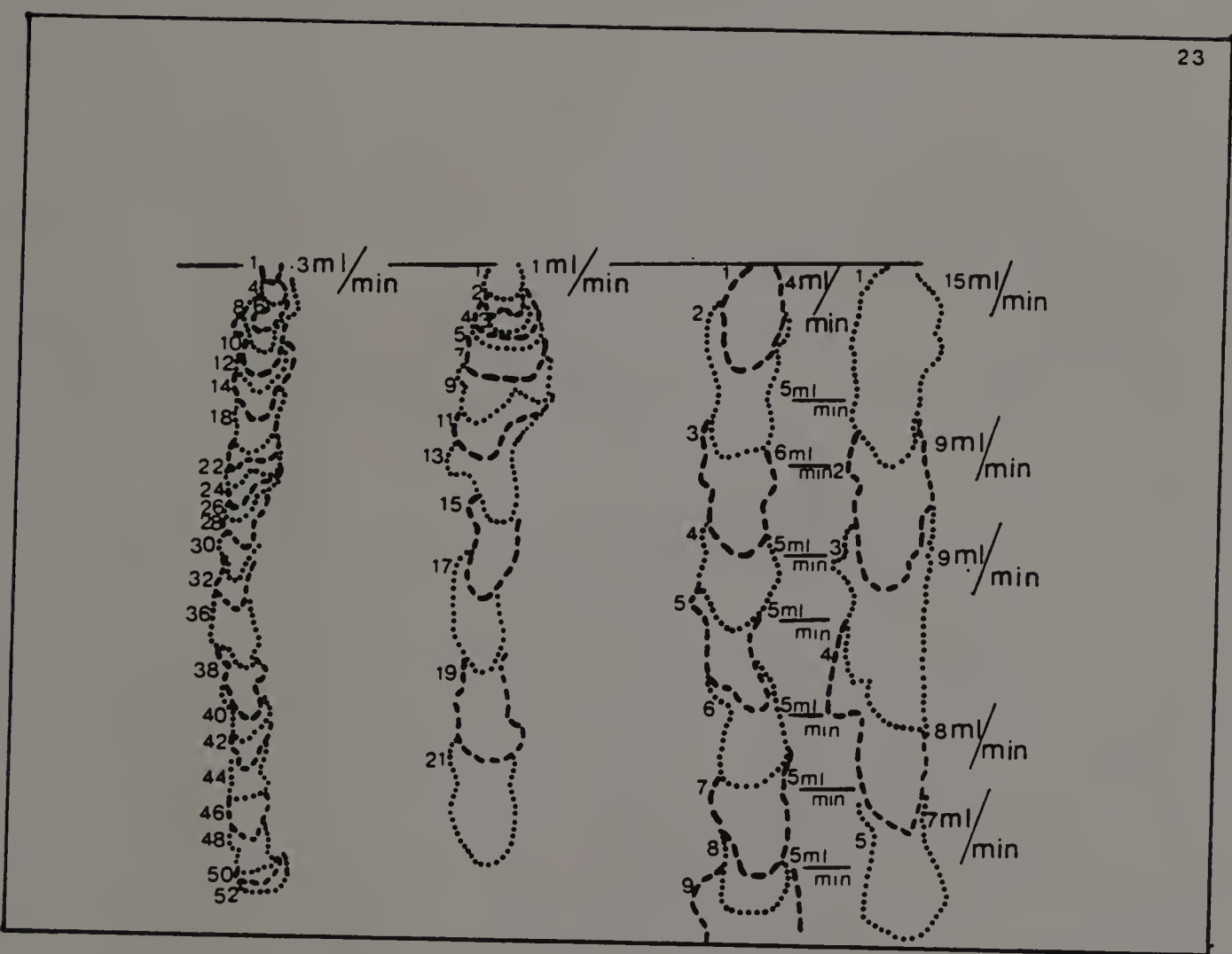


Fig. 4.32: Run 23, 19% of actual size. Straight line indicates soil surface. Numbers indicate time after opening burette in minutes.



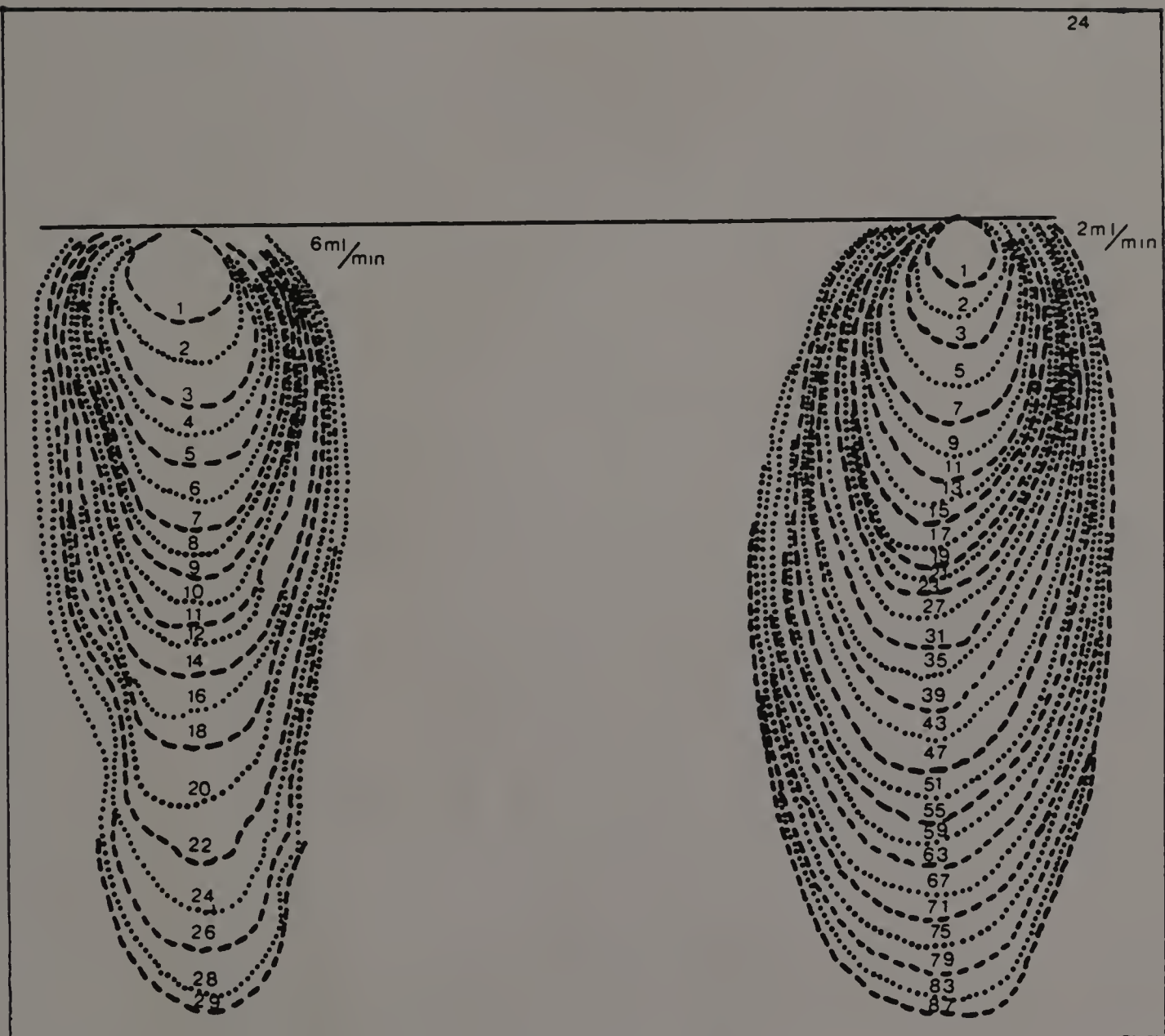


Fig. 4.33: Run 24, 19% of actual size. Straight line indicates soil surface. Numbers indicate time after opening burette in minutes.

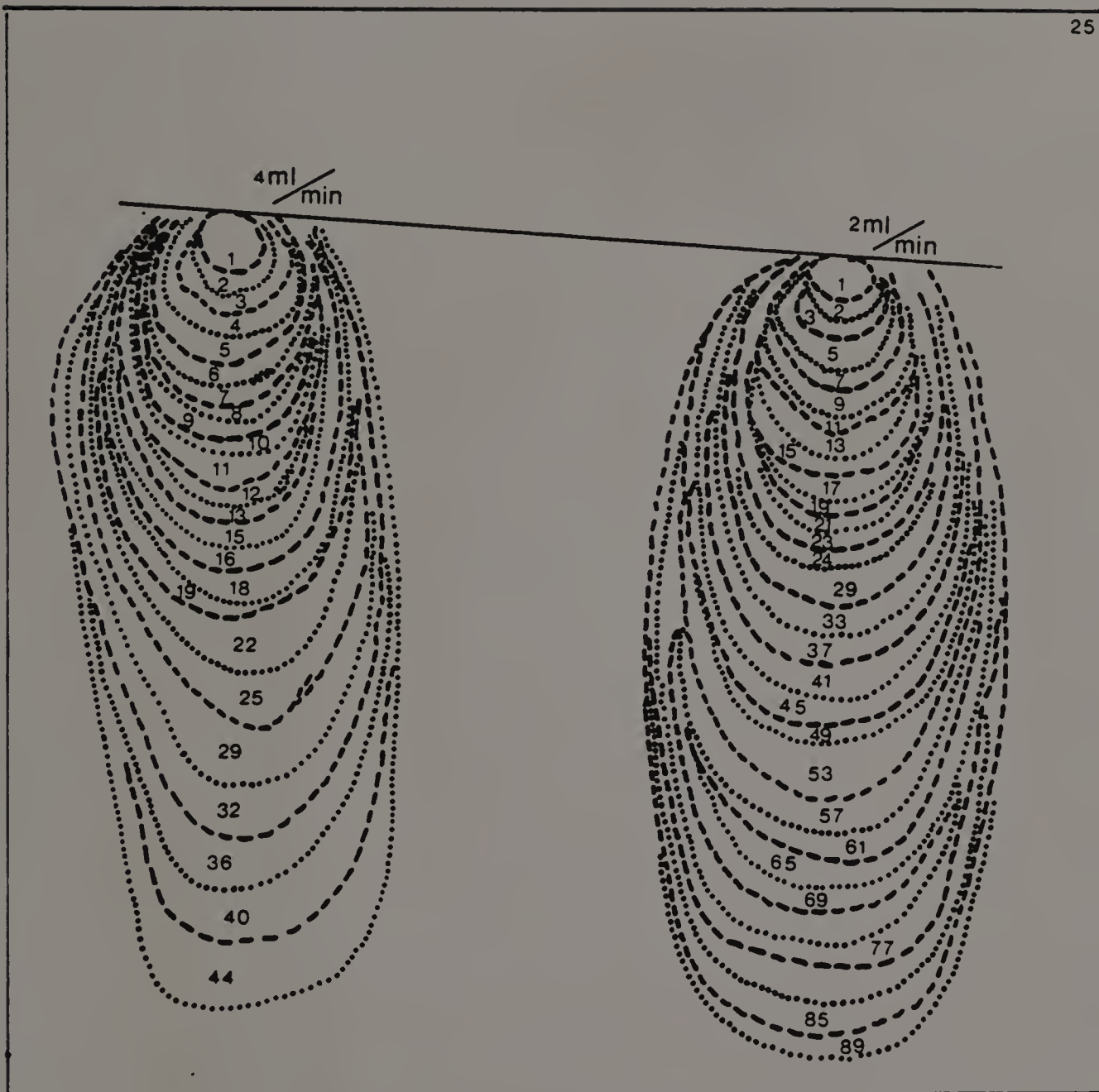


Fig. 4.34: Run 25, 19% of actual size. Straight line indicates soil surface. Numbers indicate time after opening burette in minutes.

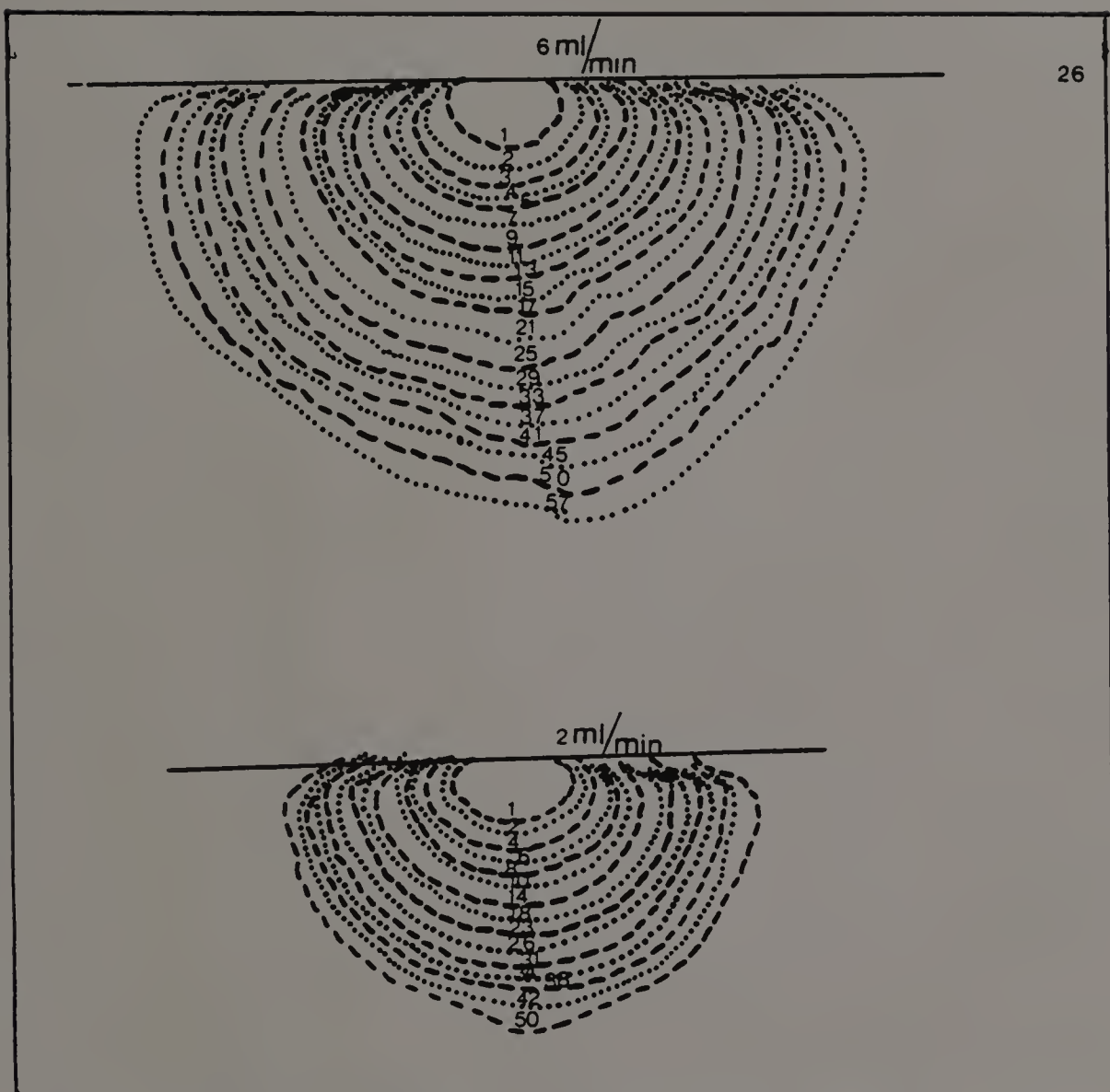
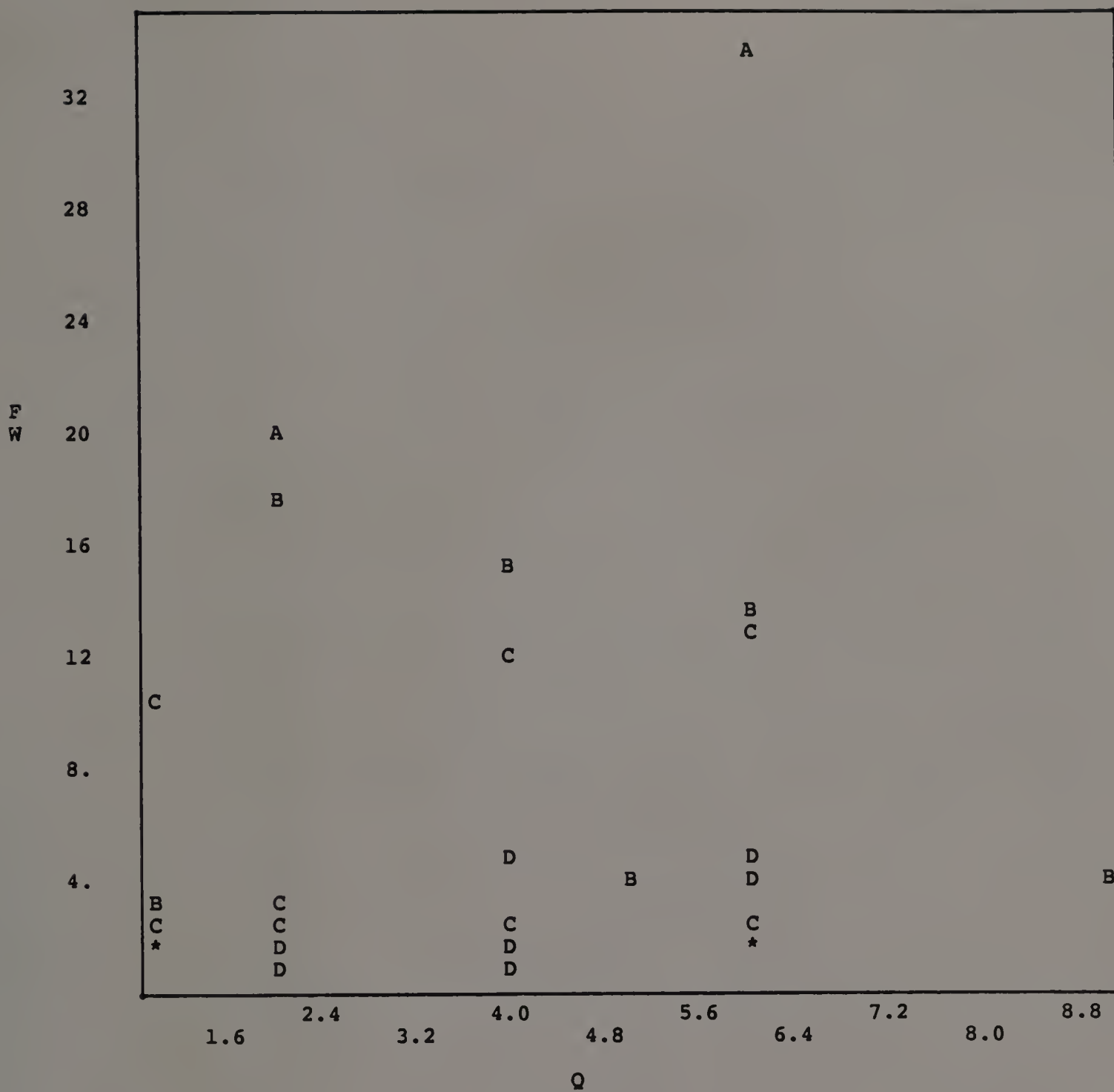
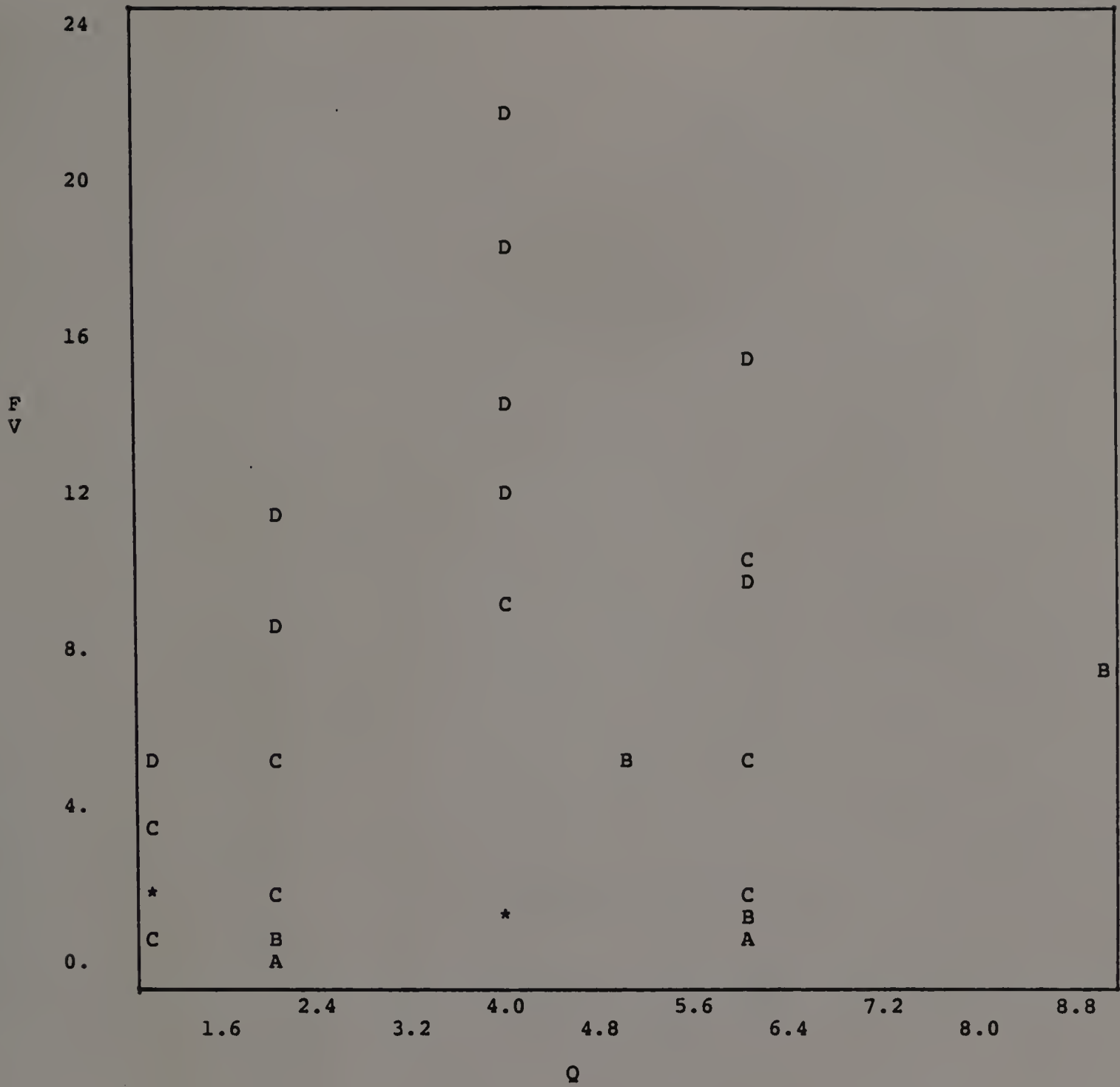


Fig. 4.35: Run 26, 19% of actual size. Straight line indicates soil surface. Numbers indicate time after opening burette in minutes.



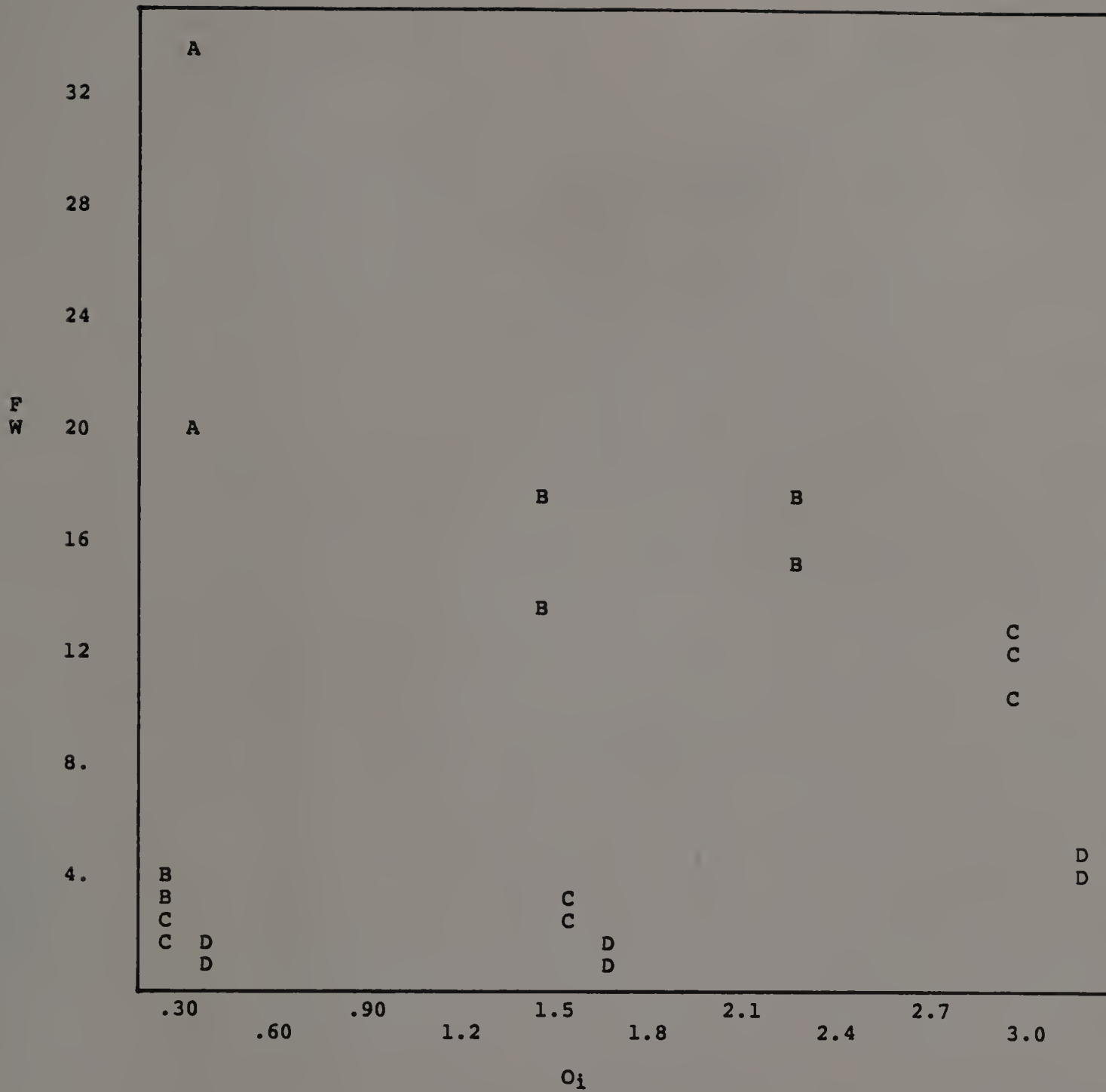
GROUP=\*76.0000, SYMBOL=A  
 GROUP=\*425.000, SYMBOL=B  
 GROUP=\*600.000, SYMBOL=C  
 GROUP=\*1500.00, SYMBOL=D

Fig. 4.36: Flux vs. finger width, point source experiments. Flux in ml/min., finger width in cm. Points identified by mean particle size in microns



GROUP=\*76.0000, SYMBOL=A  
 GROUP=\*425.000, SYMBOL=B  
 GROUP=\*600.000, SYMBOL=C  
 GROUP=\*1500.00, SYMBOL=D

Fig. 4.37: Flux vs. finger speed, point source experiments. Flux in ml/min., finger speed in cm/min. Points identified by mean particle size in microns.



GROUP=\*76.0000, SYMBOL=A  
 GROUP=\*425.000, SYMBOL=B  
 GROUP=\*600.000, SYMBOL=C  
 GROUP=\*1500.00, SYMBOL=D

Fig. 4.38: Intial wetness vs. finger width, point source experiments. Initial wetness in percent volume, finger width in cm. Points identified by mean particle size in microns.



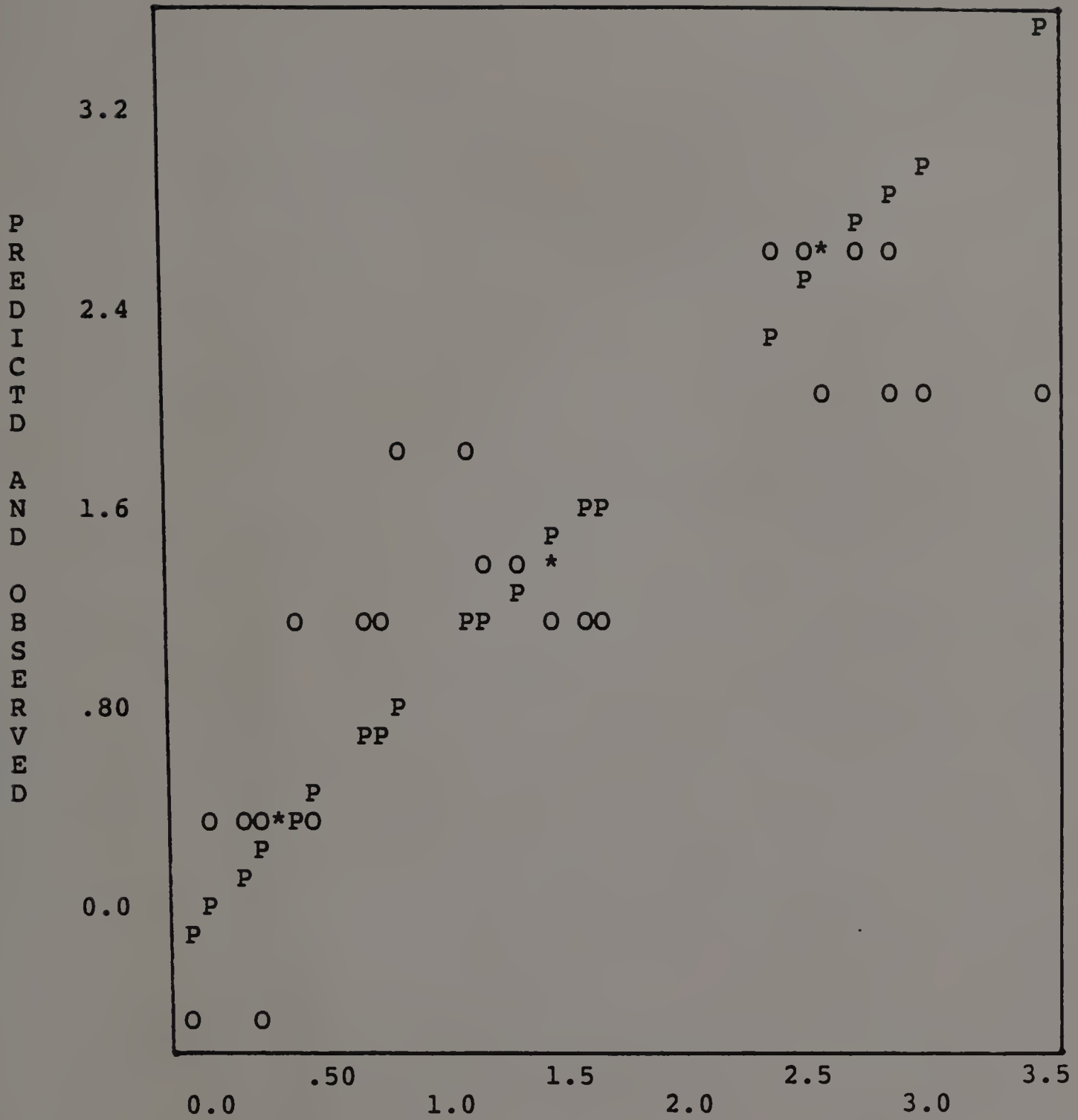
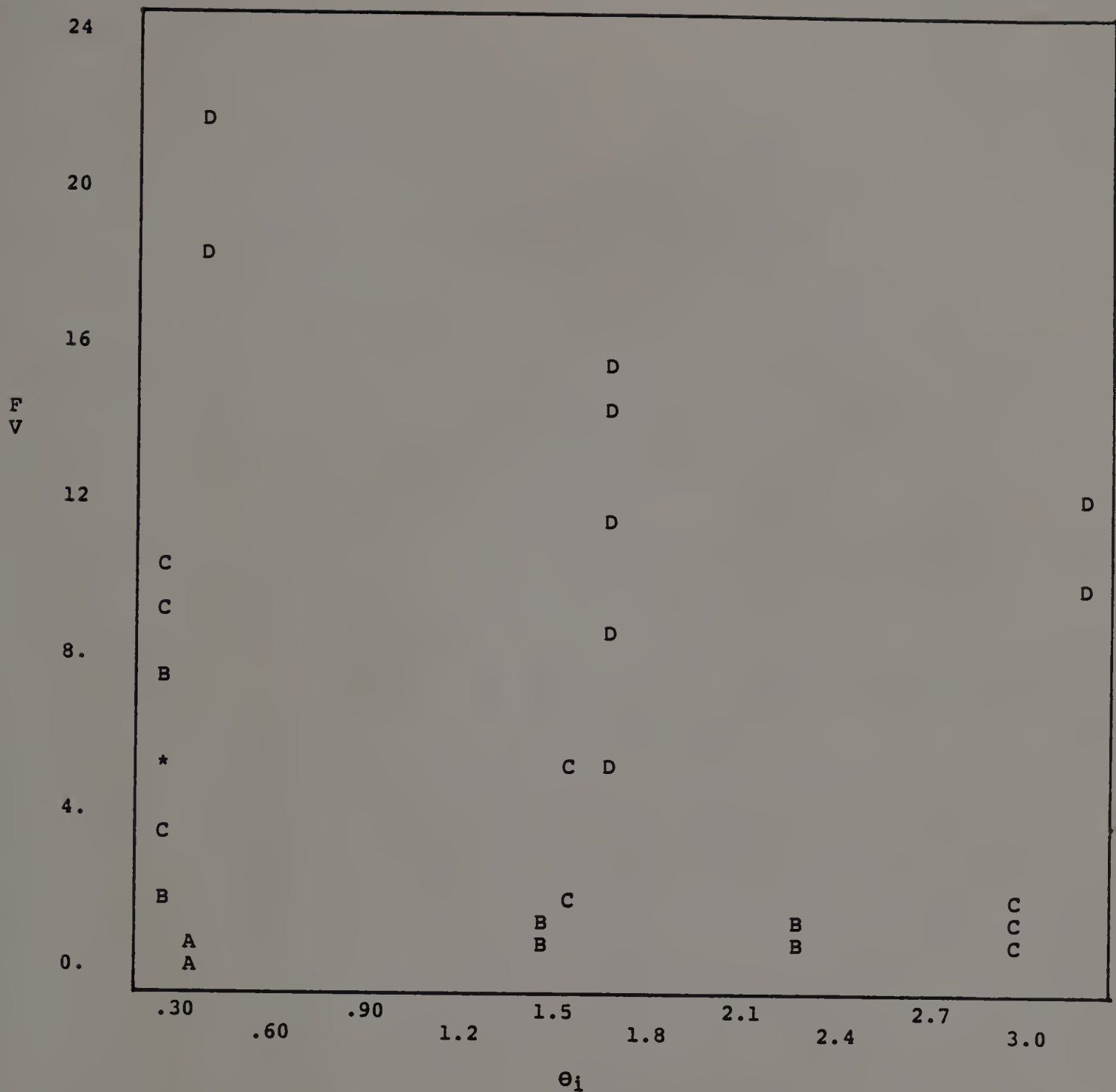


Fig. 4.39: Multiple stepwise regression,  $\ln(\text{finger width})$  in point source experiments. Evaluated on BMDP2R statistical program. Y intercept=2.01, coefficient(mps)=-.0018, coefficient( $\theta_1$ )=.5827. Multiple R=.85



GROUP=\*76.0000, SYMBOL=A  
 GROUP=\*425.000, SYMBOL=B  
 GROUP=\*600.000, SYMBOL=C  
 GROUP=\*1500.00, SYMBOL=D

Fig. 4.40: Initial wetness vs. finger speed, point source experiments. Initial wetness in percent volume, finger speed in cm/min. Points identified by mean particle size in microns



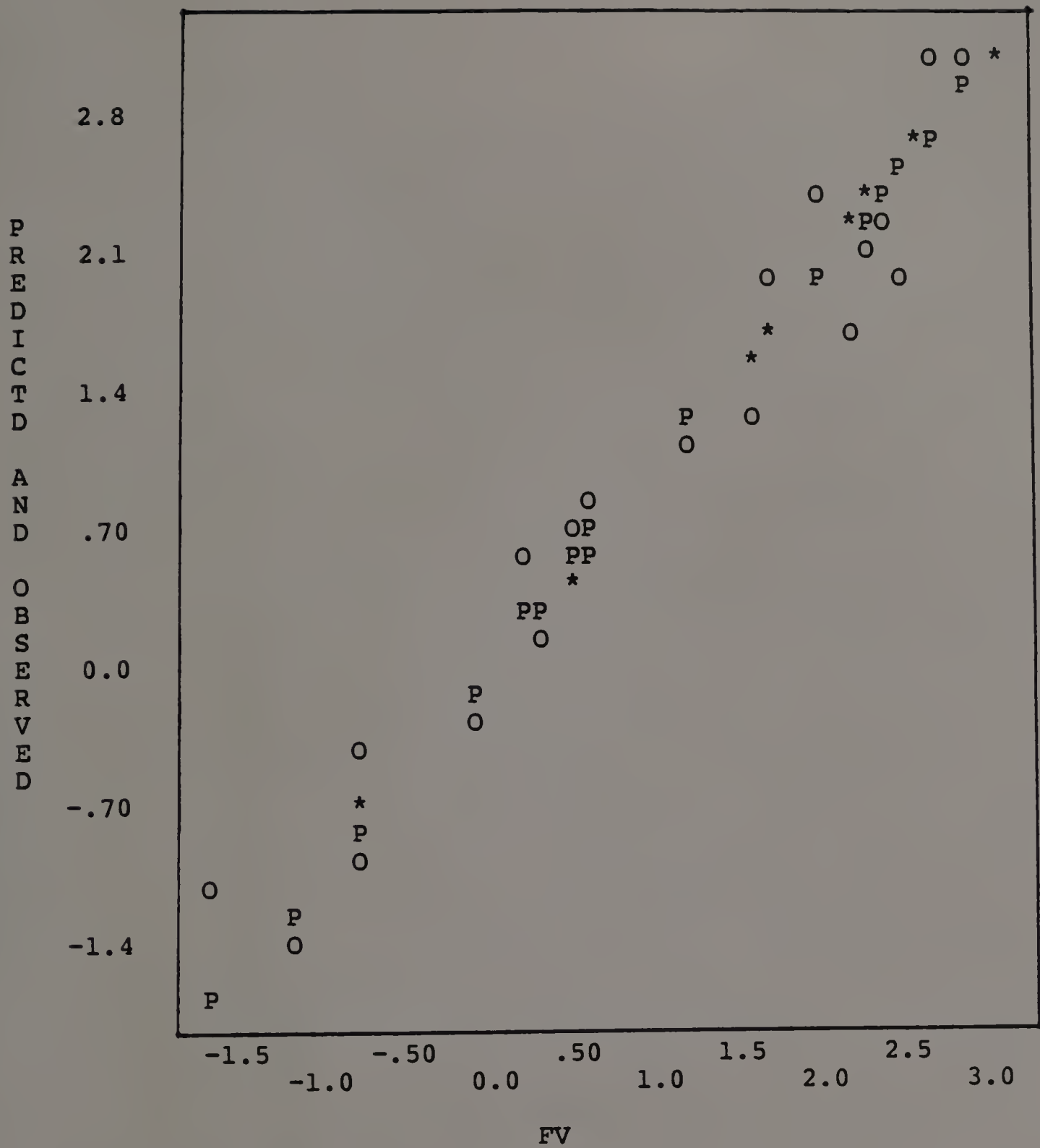


Fig. 4.42: Multiple stepwise regression,  $\ln(\text{finger speed})$  in point source experiments. Evaluated on BMDP2R statistical program. Y intercept=.1768, coefficient(mps)=.0014, coefficient( $\theta_1$ )=-.2722, coefficient(Q)=.2202, coefficient(finger width)=-.0881, Multiple R=.98

We infiltrated each sand material from a burette at several experimental wetness in order to model infiltration from a point source. The rate of flow was controlled manually at the burette. The resulting stream of water bore a qualitative resemblance to a finger. Graphs of finger width and finger speed indicate that the rate of flow made little difference in finger width (fig.4.36), but could make considerable difference in finger velocity (fig. 4.37). Changes in flux led to small changes in finger width, with the narrowest fingers resulting from the smallest flux.

As the wetness of the sands increased, finger width increased (fig. 4.38). Just as in the experiments involving layered soils (fig 4.13), finger width changed according to the amount of initial moisture present. Increases in introduced flux continued to result in increased finger velocity.

The multiple linear regressions again showed that mean particle size was negatively correlated with finger width and positively correlated to finger speed, while initial wetness was positively correlated to finger width and negatively correlated finger speed. Finger width was negatively correlated to finger speed. A property that could not be measured in layered soil experiments, namely the flux, bore no relationship to finger width, but was positively correlated to finger speed.

#### D. Hydraulic properties

Observations of the burette experiments and the layered soil experiments indicated that the appearance of a stable front in moist sands, as opposed to dry sands, was related to the lateral spreading of water from a point source. We examined a number of hydraulic properties of these sands in order to determine which properties might be correlated to this lateral spreading.

Soil moisture characteristic curves were obtained for the superlayer very fine sand, and the three sands used for the coarse sublayers. The hydraulic conductivity function from saturation to air dryness, which is a basic water transport property, was also obtained for each sand. Diffusivity and sorptivity, which are composite parameters which include conductivity and matric potential, had been conjectured as being correlated to finger width. Values for these properties were also obtained in an attempt to relate fingering flow to some standard hydraulic property of the sublayer.



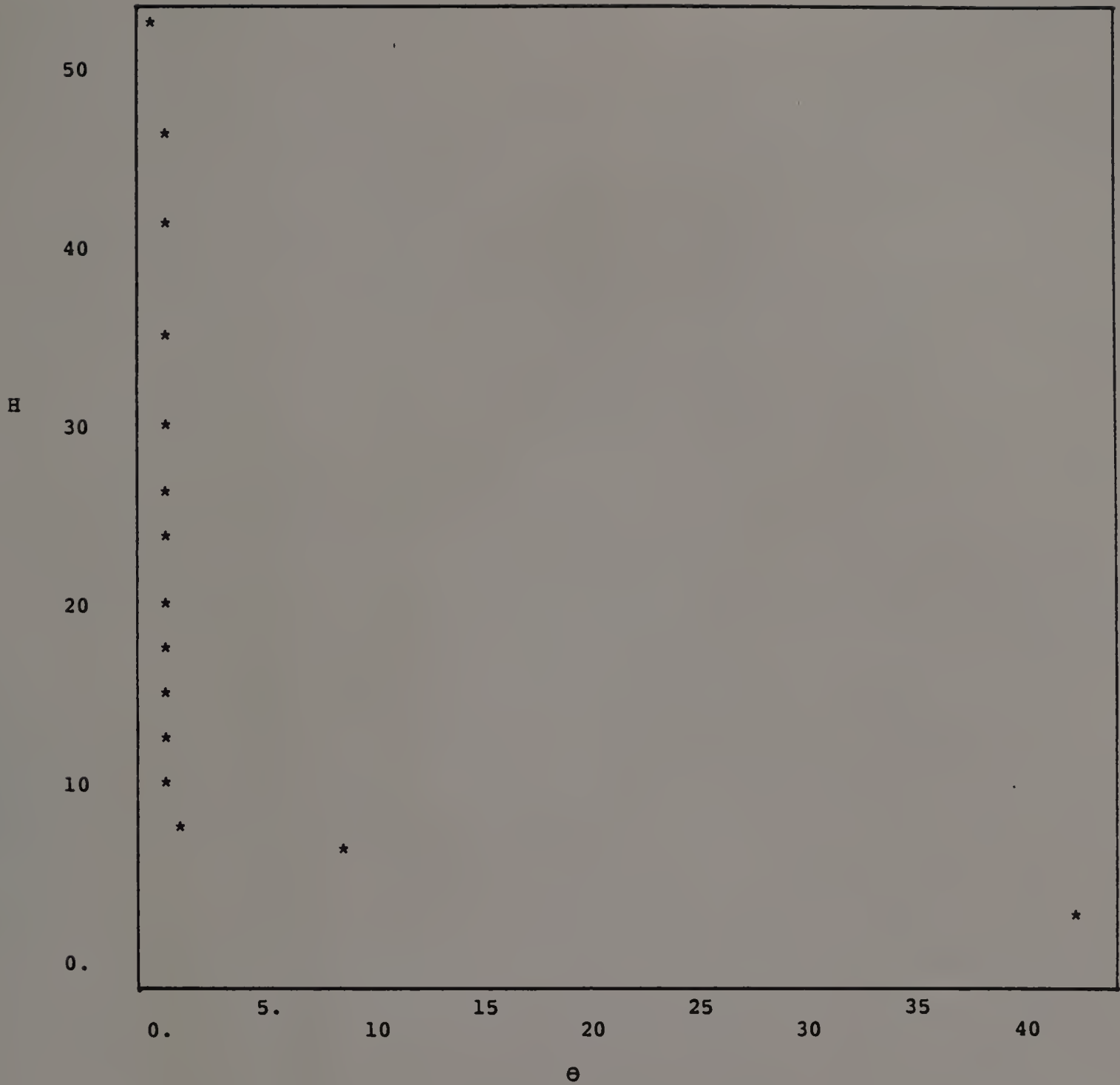


Fig. 4.43: Soil moisture characteristic curve for 1.00-2.00 mm sand. H is matric potential in cm of water.  $\theta$  is volumetric moisture content in percent.

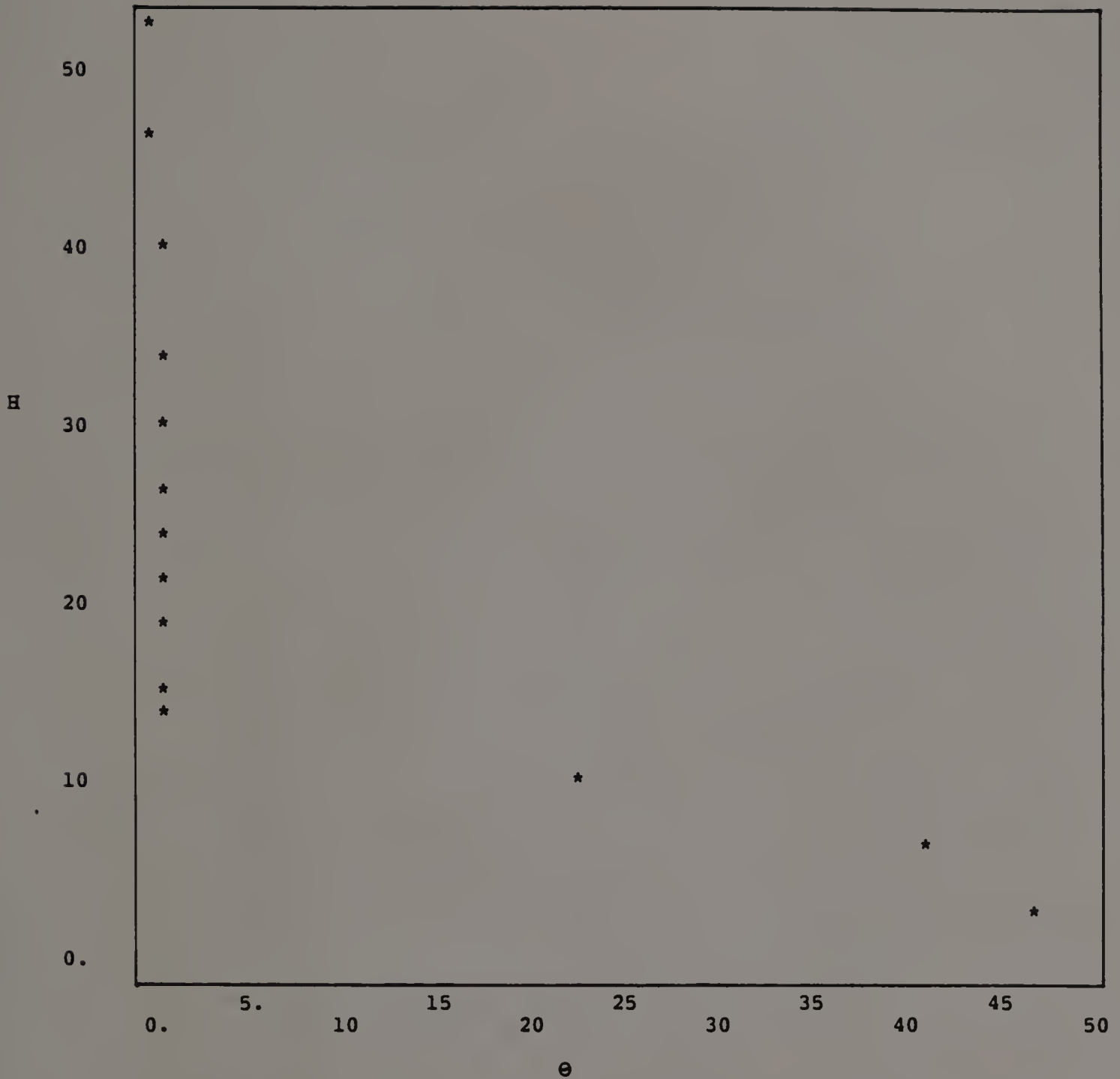


Fig. 4.44: Soil moisture characteristic curve for .500-.710 mm sand. H is matric potential in cm of water.  $\theta_v$  is volumetric moisture content in percent.

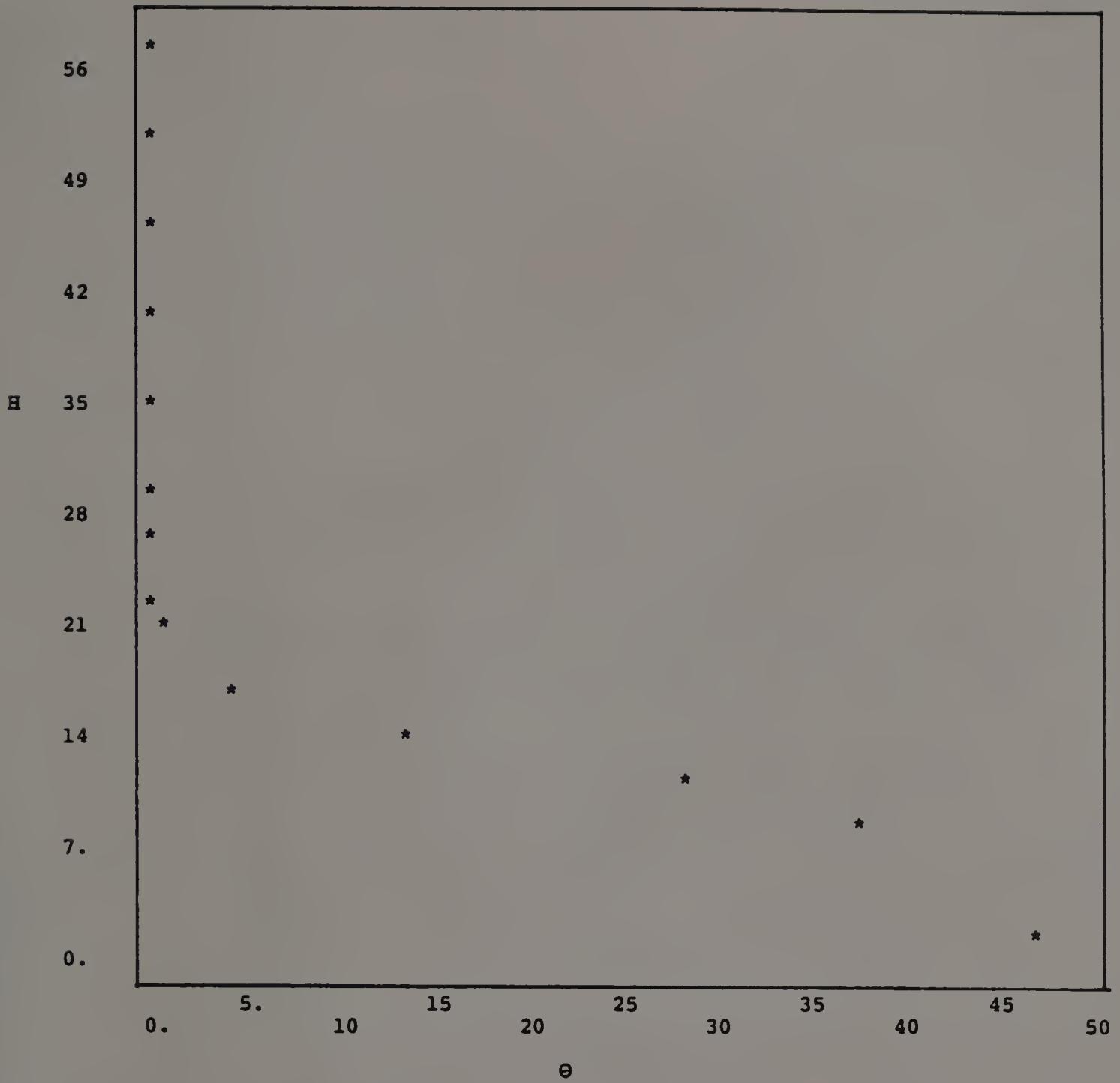


Fig. 4.45: Soil moisture characteristic curve for .355-.500 mm sand. H is matric potential in cm of water.  $\theta$  is volumetric moisture content in percent.

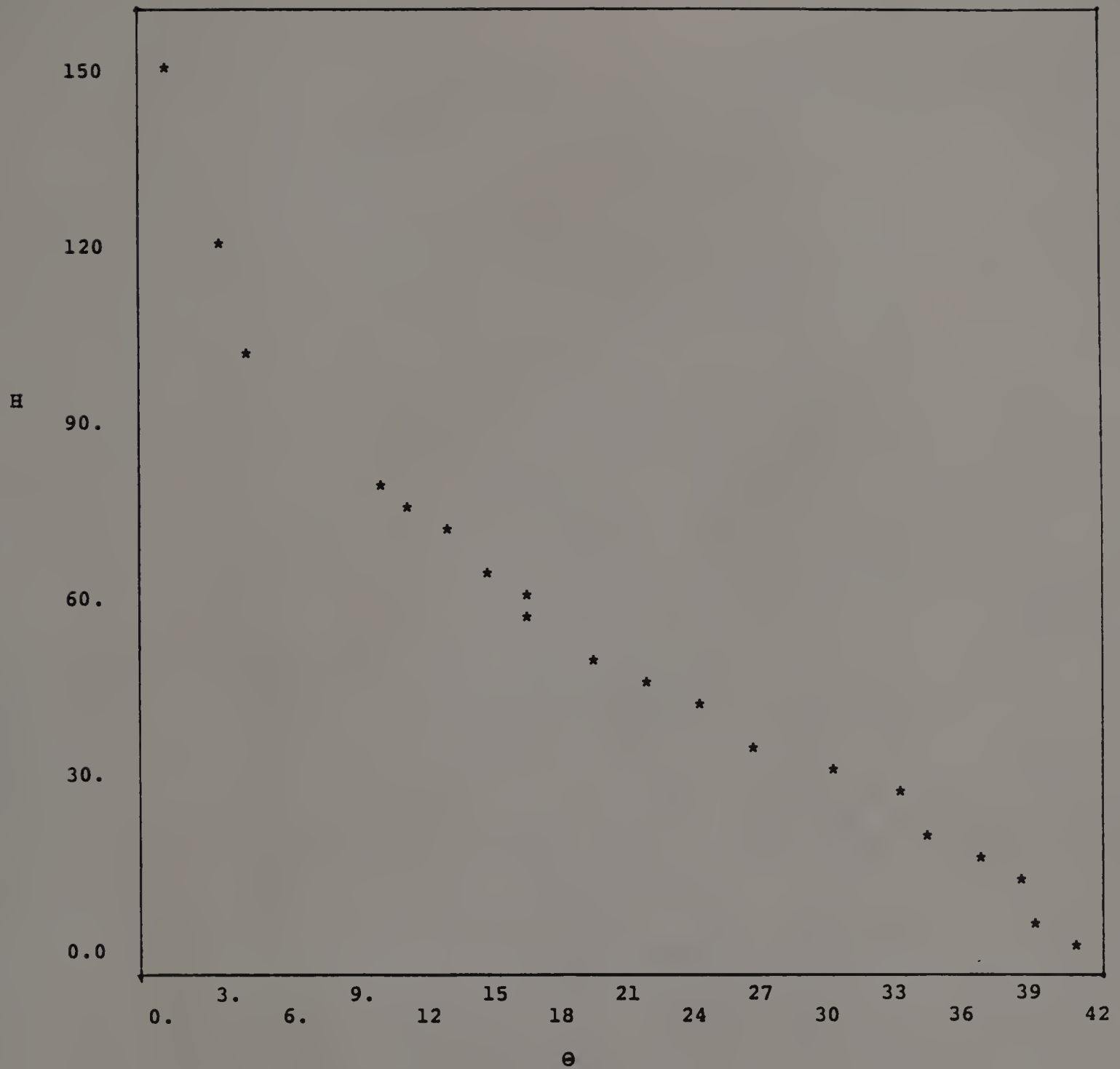


Fig. 4.46: Soil moisture characteristic curve for .047-.105 mm sand. H is matric potential in cm of water.  $\theta$  is volumetric moisture content in percent.

Table 4.3  
Conductivity

Mean particle size	Volume wetness	Matric potential	$K_{sat}$	$K(\theta)$
(mm)	(%)	(cm)		(cm/sec)
1.50	.377	10.0	.667	$5.64 \times 10^{-8}$
	1.67	7.5		$1.53 \times 10^{-5}$
	3.17	6.5		$1.34 \times 10^{-4}$
	4.41	6.0		$4.01 \times 10^{-4}$
.600	.266	12.5	.237	$1.82 \times 10^{-8}$
	.666	12.5		$3.34 \times 10^{-7}$
	1.56	11.5		$4.91 \times 10^{-6}$
	2.94	10.5		$3.67 \times 10^{-5}$
.425	.267	21	.102	$6.86 \times 10^{-10}$
	.931	19.5		$1.28 \times 10^{-7}$
	1.46	19.0		$6.63 \times 10^{-7}$
	2.27	18.0		$3.17 \times 10^{-6}$

Table 4.4  
Diffusivity and Sorptivity

Mean particle size (mm)	Volume wetness (%)	Matric potential (cm)	S(O) (cm/sec <sup>1/2</sup> )	D(O) (cm <sup>2</sup> /sec)
1.50	.377	10.0	1.49	3.20x10 <sup>-2</sup>
	1.67	7.5	1.42	.182
	3.17	6.5	1.34	.360
	4.41	6.0	1.28	.511
.600	.266	12.5	1.11	8.95x10 <sup>-3</sup>
	.666	12.5	1.09	2.25x10 <sup>-2</sup>
	1.56	11.5	1.06	3.94x10 <sup>-2</sup>
	2.94	10.5	1.02	.216
.425	.267	21.0	.935	5.24x10 <sup>-3</sup>
	.931	19.5	.914	2.48x10 <sup>-2</sup>
	1.46	19.0	.898	4.06x10 <sup>-2</sup>
	2.27	18.0	.873	6.53x10 <sup>-2</sup>
.075	.350	150.0	.242	6.54x10 <sup>-4</sup>



Diffusivity (Table 4.4) and unsaturated conductivity (Table 4.3) both increase with increasing soil moisture. Values for conductivity are extremely small at the wetness values employed in these experiments, while diffusivity values are several orders of magnitude larger. The rate of change for conductivity is much greater, however.

Coarse textured sands have greater sorptivities than finer textured sands, and dry sands have greater sorptivities than moist sands.

## V. Discussion

We undertook these experiments with the goal of answering three questions: 1) under what circumstances would fingers be produced in layered soil; 2) what effect would initial moisture in the sublayer have on flow instability; 3) if increasing the initial moisture of the sublayer had any effect on wetting front appearance, could the change be related to soil hydraulic properties?

### A. Uniform initial wetness experiments

In an effort to learn what textural contrast might be considered the minimum necessary to produce fingering, we ran several experiments (runs 1-12) using a series of well-washed sand fractions. With a constant overlying layer of .047-.105 mm sand, the finest fraction in which we observed fingering was the .355-.500 mm fraction. These fingers were considerably wider and slower moving than those in slightly coarser .500-.710 mm sand. Fingering could not be observed in a .250-.355 mm sand, though the wetting front in this sand was not completely planar. As a result, all experiments were performed with three sand fractions: 1) 1-2 mm sand; 2) .500-.710 mm sand; 3) .355-.500 mm sand. Since all of these sands were known to produce fingering flow in conjunction with the .047-.105 mm upper layer, any changes

in wetting front pattern in later experiments could be ascribed to effects other than particle size. It should be noted that values for the variable  $c$ , which had attracted the attention of Milly (1985), were 3.25 for the 1.00-2.00 mm sand, 3.17 for the 0.500-0.710 mm sand, and 3.37 for the 0.355-0.500 mm sand, according to the model of Mualem (1976). All of these values are greater than unity, which contradicts Milly's (1985) prediction that instability is restricted to materials where  $c \leq 1$ .

Experiments involving uniform initial wetness above air-dryness were meant to answer two questions: would moisture increase a soil's tendency to produce fast moving fingers as suggested by Raats (1973), or decrease that tendency, as suggested by Diment and Watson (1983), and at what wetness would this increase or decrease in fingering flow become indisputable?

The first experiments involving initial moisture (runs 2-4, 6-8, 10-12) were intended to determine whether the results of Diment and Watson (1985) would be duplicated. They had found that fingering behavior ceased at some moisture below  $0.02 \text{ cm}^3 \text{ cm}^{-3}$ . Our experiments focussed immediately on this moisture range in order to gain some understanding of what Diment and Watson had seen.

We found that the different underlying sands would stop producing fingers at differing levels of uniform initial moisture. Fingering ceased in the 1-2mm material at .045

$\text{cm}^3\text{cm}^{-3}$  (run 4), in the .500-.710 mm material at  $.030 \text{ cm}^3\text{cm}^{-3}$  (run 8), and in the .355-.500 mm material at  $.023 \text{ cm}^3\text{cm}^{-3}$  (run 12). It was clear that the addition of water tended to decrease fingering, confirming the result of Diment and Watson (1985), and that smaller amounts of water were necessary to eliminate fingering in soils that exhibited wider fingers when dry. Furthermore, we did not observe fingers in any model beyond the limit of  $O_i=0.5\text{cm}^3\text{cm}^{-3}$  postulated by Diment and Watson (1983).

In order to determine what was happening to the fingers between air dryness and the wetness which induced an apparent stabilization of flow, two intermediate levels of uniform wetness were examined for each soil. Each wetness was meant to divide the change in wetness from air dryness to the absence of fingering into three approximately equal increments. For the .355-.500 mm and the .500-.710 mm sands, the intermediate levels were  $.0075$  and  $.015 \text{ cm}^3\text{cm}^{-3}$ , while for the considerably larger 1-2 mm particles, the intermediate wetnesses were  $.015$  and  $.03 \text{ cm}^3\text{cm}^{-3}$ .

For the two 0.355 mm-0.500 mm (run 10) and the 0.500 mm-0.710 mm sand fractions (run 6), the initial increment of additional moisture actually reduced mean finger width and increased mean finger speed. The second level of moisture (runs 11 and 7), however, increased mean finger width and mean finger speed. Wetting front speed for the non-fingering wetnesses were considerably slower (runs

12 and 8). The coarsest material did not exhibit this pattern, as fingers became wider and slower with every increase in wetness (runs 2-4).

Saturation values behind the wetting front in each layer were occasionally examined to test for conformity to the Green-Ampt model. This model predicts that soil behind the wetting front will be uniformly wet. While the overlying layer did appear to be saturated, saturation values in the coarse sublayers did not exceed .50. This value was not measurably different in wet or dry sands. We were not able to determine whether fingers consisted of a saturated central core surrounded by an unsaturated region, as Hill and Parlange (1972) conjectured. By the time samples could be taken, fingers appeared uniformly wet throughout their thickness, with no saturated zone evident.

It was not possible to determine whether Philip's (1975a) equation correctly predicts the appearance of fingers. The sorbing arm of the soil moisture characteristic curve suggests that this model would predict fingering in cases where the soil is initially wet. However, if hysteresis plays a role in lowering the water entry tension of the soil's lower layer, then Philip's (1975a) model may prove to be correct. Controversy over this issue may well continue until an immediate response tensiometer is developed which can measure the precise rise and fall of soil water tension at the interface between soil layers.



## B. Variable initial wetness experiments

As part of our investigation into the effect of initial moisture on fingering, we attempted to determine where fingers were occurring. We considered it possible that they were occurring in the most conductive portion of the soil, in cases where they appeared. That is, that even in the dry sands where they seemed most prevalent, they were finding some preferred pathway of greater moisture to follow through the soil.

The first question was the persistence of instability fingers. Once these fingers had formed, would they then provide a preferred pathway of water movement, or would water move slowly through already wet fingers as it moved through uniformly wet soil?

An experiment was run in the usual fashion, and then repeated immediately in the same cell once ponding had dissipated. During run 13, fingers formed as usual in the dry sublayer during infiltration. A second infiltration with dyed water showed that water was moving almost exclusively through the pathways already established by the previous infiltration, confirming the results of Glass and Steenhuis, 1984.

This led to the question of whether fingers in dry soil were also following some preferred, more conductive pathway. If certain regions of the soil were marginally wetter than



others nearby, they might be the ones promoting fingering even though uniform wetness tended to reduce or eliminate fingers. We decided to observe the behavior of two regions of the same soil, one marginally wetter than the other, as in run 14.

Experiments of this kind demonstrated that fingering was occurring in the least conductive, rather than the most conductive, regions of the soil. While water readily penetrated the moist soil, it spread across the width of the moist vertical strips rather than forming fingers. When water penetrated the dry regions, fingers did form and soon overtook the wetting front in the moist strips, reaching the bottom of the cell without spread across the width of the dry region.

In runs 15 and 16, we studied variation of wetness in the vertical, rather than the horizontal, direction. An attempt was made to answer the following questions: if a soil demonstrated unstable flow in an initially dry region, would the fingers coalesce upon reaching a moist lower layer; and if flow were stabilized by moisture, would it remain stable upon reaching a dry lower layer?

In run 15 where a fine layer overlay a layer of dry coarse material, with moist coarse material on the bottom, fingers formed as usual in the coarse, dry region. As the fingers reached the moist region, however, they did not maintain their narrow width or high velocity. Flow was

almost as great in the horizontal direction as it was in the vertical direction. Although the fingers did not reach the point of overlapping completely, it was obvious that fast moving stream flow through the fingers had been interrupted by the moist layer.

In run 16, where a fine layer overlay a moist coarse layer with a dry coarse layer on the bottom, the wetting front entered the moist layer in the expected stable fashion. Though the front was not perfectly straight, as it appeared to be in the upper layer, it moved slowly and no separate fingering zones formed. Upon reaching the dry region, however, the front broke into distinct, fast-moving fingers which crossed the remaining distance to the bottom of the cell at a greater velocity than that of the wetting front as it had moved through the moist region.

The conjecture of increasing finger width ultimately unifying the wetting front is suggested by the results of these experiments involving change of moisture with depth. Where a front appeared to be stable as it flowed from the fine layer into the moist sand, fingers were observed as the front reached the dry sand. This suggests that even in the "stable" case, point sources are still being created. When the streams below these point sources reach a soil layer which is no longer capable of spreading them horizontally, they proceed through this layer as if they had never been stabilized. This perhaps supports the notion that the non-

fingering fronts observed in initially moist coarse sands are somehow unstable, although without the fast moving fingers characteristic of unstable flow, the environmental impact of flow instability becomes moot. Flow instability has been suggested as a source of accelerated environmental pollution. If flow instability does not cause pollutants to reach the groundwater more rapidly than stable flow, its impact cannot be distinguished from that of stable flow.

The implications of narrow streams of water flowing through the soil are also clear from Darcy's law (equation 3.1). When a stream enters a sand with little capacity to spread water laterally, due to either uniformly large pore sizes (leading to a low water entry value) or low conductivity, very little water will be moved in the horizontal directions  $x$  and  $y$ . With more water entering the sand from above, the stream will be conducted primarily in the vertical  $z$  direction. In a soil that is not limited by column walls,  $A$  (the cross-sectional area of water infiltration) is not a constant, but is determined by the flow of water in the  $x$  and  $y$  directions. In a case where such flow is small, water provided by the flux  $Q$  must be moving in the only remaining direction, down. Furthermore, the greater the conductivity in the  $z$  direction, the greater the speed of the wetting front. If water remains concentrated below a point source of flux, the conductivity of that region will become relatively high, as conductivity

increases with saturation. In other words, (eq. 3.1) suggests that small fluxes in the x and y directions, leading to low values of A, help to ensure that the conductivity of the soil in the z direction will be relatively great. This also ensures that the wetting front speed will be high.

The experiments with varying moisture content indicated that fingering flow might depend upon the inability of the sublayer to spread narrow streams of water arising from destabilizing forces at the textural interface. If the interface might be regarded as creating a number of point sources of water, perhaps fingering behavior could be modelled by water dripping from a burette at a controlled rate.

### C. Point source experiments

We infiltrated each sand material from a point source at several experimental wetnesses (runs 17-26). The rate of flow was controlled manually at the burette. The resulting stream of water bore a qualitative resemblance to an instability finger. Graphs of finger width and finger speed indicated that the rate of flow made little difference in finger width (fig. 4.36), but could make considerable difference in finger velocity (fig. 4.37). While the relationship between point flux and finger speed was not



linear, it was clear that a larger flux would cause a faster flow without that larger flux being apparent from finger width. Changes in flux led to small changes in finger width, with the narrowest fingers resulting from the smallest flux.

As the wetness of the sands increased, finger width increased (fig. 4.38). In some of the wetter sands, it was clear that as few as three or four point sources might overlap sufficiently to cover the entire cell. Just as in the experiments involving layered soils (fig 4.13), finger width changed according to the amount of initial moisture present. Differences in introduced flux continued to make a large difference in finger velocity.

The experiments involving uniform and variable wetness suggest the possibility that flow out of the upper layer could occur through point sources. At air dryness and at the first intermediate level of wetness, fingers are obviously separated and appear to "grow" directly out of the upper layer. At the next higher level of moisture, however, fingers may broaden and overlap. This creates the "rough front" appearance characteristic of these experiments: lobes of water proceed through the soil, while gaps between the lobes close some distance behind the greatest depth of finger penetration. These lobes can be pictured as ellipses growing below point sources at the interface. While the ellipses may not overlap sufficiently to eliminate any

impression of fingering, especially if one is growing more rapidly than another due to increased flux, they will also tend to overlap at some point near the middle of their long axis. At levels of wetness where fingering can no longer be observed, it may be conjectured that the ellipses described in the previous experiments are now growing even more rapidly along their horizontal axes in relation to their vertical axes, tending toward a more circular shape. Now the overlap will be even more complete. The results of the point source experiments bear out the idea that finger width can change with small (less than 5% by volume) increases in wetness.

Experiments 17-26 indicated that finger spreading could prevent unstable flow from resulting in distinct, rapidly moving fingers. Observation showed that fingers spread more in finer sands and in moist sands. This increased spreading is a function of some combination of soil hydraulic properties, so we attempted to correlate finger spreading to some combination of those properties.

#### D. Hydraulic properties

The soil moisture characteristic curves obtained for coarse sands capable of producing fingers when they underlay the fine sand used in these experiments show that they are



all resistant to water entry until very low tensions are achieved (fig. 4.43-4.45).

Once water enters these soils, the width of the stream bears a relationship to particle size. In the coarsest sand, the stream is at its narrowest, while in the medium sand, the stream spreads out. Since the sands are at approximately equal wetnesses when air dry, it seems likely that the stream width in this case is a function of the soil's height of capillary rise, rather than conductivity or diffusivity which are at their lowest when the soil is dry. At low initial moisture content, the data obtained for conductivity (Table 4.3), diffusivity (Table 4.4), and sorptivity (Table 4.4) indicate that these properties are all greater in the air dry 1.00-2.00 mm sand than in the air dry .355-.500 mm sand. Only the height of capillary rise in the finer sand is greater than that of the coarse sand, suggesting some correlation between this value and finger width.

Diffusivity (Table 4.4) and unsaturated conductivity (Table 4.3) both increase with increasing soil moisture, and could be responsible for the increase in finger width with the increase in initial soil moisture. Values for conductivity are extremely small at the wetness values employed in these experiments, while diffusivity values are several orders of magnitude larger. The rate of change for conductivity is much greater, however. The rapid increase

in finger width with increased initial moisture demonstrated by both layered soil (fig. 4.14, Table 4.1) and point source experiments (fig. 4.38, Table 4.2) suggests that the three to four orders of magnitude change in conductivity may be more significant than the two orders of magnitude change in diffusivity, even though the numerical values obtained for diffusivity are much greater than those obtained for conductivity.

Sorptivity seems to be inversely proportional to finger spreading, as coarse textured sands have greater sorptivities than finer textured sands, and dry sands have greater sorptivities than moist sands. This means that the sand with the greatest sorptivity has the narrowest stream. Lower sorptivities are associated with increased finger width.

The apparent correlation between mean particle size and initial wetness, as demonstrated by multiple linear regression, is clarified by the examination of the soil hydraulic properties. Mean particle size is negatively correlated with finger width, just as it is negatively associated with height of capillary rise. Conversely, mean particle size is positively correlated to finger speed, just as it is positively associated with the soil permeability, as indicated by saturated conductivity. Initial wetness is positively correlated to finger width, and is also positively associated with conductivity and diffusivity. It

may be conjectured that the immediate impact of enhanced conductivity and diffusivity is to cause water to spread throughout the soil in all directions, rather than concentrating the flow downward.

## VI. Conclusions

In order to study flow instability in layered soils, we built an approximately two dimensional model which contained a fine layer of sand overlying a coarse layer of sand. A series of experiments studied the effect of uniformly increased initial wetness in the coarse sand on flow instability during infiltration. These experiments were followed by experiments involving variable initial wetness in the sublayer and experiments where a point source modelled the upper sand layer. The results of these experiments lead to the following conclusions:

1) Fingering flow can be observed in systems of layered sands where a fine textured layer overlies a coarse textured layer if fine particles have been removed from the coarse textured layer. It appears that a minimum particle size ratio between the layers is necessary to induce fingering, but the minimum ratio necessary is still not known.

2) Uniformly increasing the initial wetness of the lower layer has the effect of smoothing and slowing the wetting front.

3) In cases of horizontally varying wetness, fingers occur in the driest regions of the soil.

4) Where water is applied from a point source, uniform initial wetness spreads incoming streams of water.

5) Height of capillary rise, conductivity, and diffusivity are associated with increased finger width. Increased sorptivity is associated with decreased finger width.

Appendix A.  
Quality Control

In order to ensure that packing was uniform in these experiments, 3 cells representing each sublayer at each experimental level of wetness was packed according to the procedure described in Materials and Methods III.A. The cells were then dismantled and sampled at four locations for bulk density and ten locations for wetness. Analysis of variance was carried out for density and wetness in relation to mean particle size, initial wetness, and location. The differences in density and wetness were both shown to be significant among experiments with different particle sizes at different initial wetnesses, but did not differ significantly from location to location within the cell.

ANOVA Table 1: Density

Source	Sum of Squares	df	F
Overall	330.4	1	$1.36 \times 10^{-5} **$
MPS	.0890	2	18.35**
Location	.0106	3	1.45
$\theta_i$ (MPS)	.7997	9	36.63**
ML	.0156	6	1.08
MØL	.0554	27	0.85
Error	.2305		



ANOVA Table 2: Wetness

Source	Sum of Squares	df	F
Overall	169.3	1	5249.4**
MPS	16.25	2	251.8**
Location	.0578	3	0.60
$\theta_i$ (MPS)	88.02	9	303.2**
ML	.0426	6	0.22
M $\theta$ L	.4687	27	0.54
Error	3.000		

Appendix B

Sorptivity Data and Programs  
Table A.1 Sorptivity Data

Mean Particle Size	.075		.425		.600		1.50	
	$\theta_i$	B	$\theta_i$	B	$\theta_i$	B	$\theta_i$	B
	0.00	46.2	0.00	42.9	0.00	45.1	0.00	42.2
	0.00	47.3	0.00	42.5	0.00	44.0	0.00	41.1
	0.00	45.1	0.00	43.3	0.00	44.0	1.85	38.4
	0.31	36.9	1.27	42.9	0.00	44.0	2.08	36.2
	0.34	36.8	1.35	44.5	0.00	41.8	2.21	39.1
	0.36	36.9	1.41	43.6	0.94	43.7	2.31	36.9
	0.37	39.0	1.48	43.8	1.09	43.1	2.39	39.9
	0.39	36.3	1.48	37.2	1.24	42.4	2.44	38.9
	0.42	36.9	1.56	41.9	1.37	43.8	2.55	33.9
	0.43	36.7	1.61	42.1	1.39	42.0	2.63	37.6
	0.43	38.6	1.63	42.7	1.50	41.6	2.65	36.3
	0.45	35.4	1.70	43.6	1.53	42.5	2.79	31.1
	0.46	36.0	1.74	43.9	1.58	40.8	2.87	37.1
	0.48	33.9	1.75	42.4	1.66	41.1	2.88	36.7
	0.48	39.0	1.81	41.8	1.69	42.4	2.91	28.9
	0.49	34.5	1.82	41.1	1.69	43.0	3.04	28.0
	0.50	32.2	1.84	39.2	1.69	43.6	3.04	33.1
	0.51	32.9	1.88	40.7	1.73	40.8	3.06	32.8
	0.52	31.4	1.90	43.1	1.79	40.7	3.16	28.2
	0.53	38.1	1.91	39.6	1.83	33.2	3.16	31.2
	0.53	29.2	1.96	42.4	1.84	42.0	3.18	30.8
	0.54	31.2	1.98	35.3	1.84	40.6	3.27	21.7
	0.55	25.1	1.98	40.0	1.84	45.1	3.31	29.3
	0.55	37.8	2.03	39.0	1.87	27.2	3.34	21.1
	0.56	5.82	2.04	38.8	1.91	23.6	3.39	27.2
	0.56	27.7	2.04	33.5	1.95	11.5	3.40	21.4
	0.57	0.79	2.09	33.6	1.97	39.5	3.44	30.0
	0.58	0.54	2.09	31.3	1.99	40.7	3.53	18.3
	0.58	24.3	2.10	30.8	1.99	0.22	3.53	26.2
	0.58	34.5	2.13	37.9	2.00	41.1	3.53	27.7
	0.59	7.65	2.13	29.1	2.05	40.8	3.59	22.2
	0.60	0.63	2.17	28.1	2.09	37.8	3.59	23.6
	0.61	35.7	2.17	30.2	2.10	34.1	3.60	27.8
	0.62	0.45	2.17	25.3	2.12	36.9	3.65	23.5
	0.62	33.9	2.20	26.0	2.13	39.7	3.67	26.5
	0.64	32.5	2.21	30.7	2.18	38.3	3.71	24.3
	0.66	27.3	2.21	20.4	2.18	35.0	3.73	25.5
	0.67	14.5	2.24	22.3	2.20	35.9	3.77	25.4
	0.69	1.24	2.24	28.3	2.21	39.2	3.79	24.5
	0.70	0.42	2.25	3.62	2.26	18.2	3.86	22.9
			2.27	11.9	2.27	38.8	4.07	14.5

Continued next page

Table A.1 cont.

Mean Particle Size	.425		.600		1.50	
	$\theta_i$	B	$\theta_i$	B	$\theta_i$	B
	2.28	2.36	2.28	34.4	4.85	0.32
	2.38	1.28	2.28	33.5	5.11	0.20
	3.10	0.73	2.32	31.0	5.19	0.22
	3.22	0.27	2.33	0.59		
			2.35	38.3		
			2.36	30.8		
			2.36	28.2		
			2.39	0.26		
			2.41	32.6		
			2.41	24.3		
			2.43	28.0		
			2.45	22.2		
			2.46	31.8		
			2.47	27.5		
			2.50	29.8		
			2.51	22.1		
			2.54	30.2		
			2.55	7.72		
			2.59	27.1		
			2.59	0.27		
			2.63	29.7		
			3.23	0.33		
			3.28	8.79		

Programs

Program Sorp, Ralph S. Baker and Robert Gonter

0010 program sorp

0020 dimension x(80),y(80),wk(1178),c(80,3)

0030 dimension f(80),u(100),s(100)

0040 dimension xk(2)

0050 real a,b,q

0060 ic=80

0070 open (5,file='tapes20')

0080 rewind 5

Continued next page

Program Sorp cont.

0090 rewind 10

0100 read (5,\*)nx

0110 print \*,nx

0120 do 20 i=1,nx

0130 read (5,\*) x(i),f(i)

0140 print \*,'firstbase'

0150 20 continue

0160 mode=0

0170 nxk=2

0180 xk(1)=x(1)

0190 xk(2)=x(nx)

0200 call icsfku (x,f,nx,mode,xk,nxk,y,c,ic,error,wk,ier)

0210 print \*,'secondbase,error=',error

0230 do 40 i=1,nx

0240 d=x(i)-x(1)

0250 s(i)=((c(1,3)\*d+c(1,2))\*d+c(1,1))\*d+y(1)

0260 40 continue

0280 do 60 i=1,nx

0290 write(unit=10,fmt=2000)i,x(i),f(i),s(i)

0300 2000 format(1x,i3,4f6.2)

0310 60 continue

0315 call icccu (x,s,nx,c,ic,ier)

0320 a=x(1)

0330 b=x(nx)

0340 call dcsqdu (x,s,nx,c,ix,a,b,q,ier) Continued next page

Program Sorp cont.

0350 print \*, 'thirdbase'

0360 print \*, 'q=', q

0370 stop

0380 end

Program sorpy

Robert Gonter

dimension x(80), y(80), wk(1000), c(80, 3)

ic=80

c

open(unit=10, file='tapel0')

call sm5sort(0)

call sm5from('tapel0')

call sm5key (17, 6, 'ascii6', 'a')

call sm5to('tape5')

call sm5end

c

rewind 5

c

knt=0

10 continue

read(unit=5, fmt=5000, end=20) by, ax

5000 format(4x, f6.2, 6x, f6.2)

knt=knt+1

y(knt)=by

x(knt)=ax

Continued next page

Program Sorpy cont.

go to 10

c

20 continue

c

print \*, 'no. of pts. ', knt

nx=knt

c

call icscu (x,y,nx,c,ic,ier)

80 continue

print 8, ' input a and b'

read (unit=\*,fmt=\*,end=400) a,b

call dcsqdu(x,y,nx,c,ic,a,b,q,ier)

c

print \*, ' a=', a, ' b=', b, ' q=', q

c

go to 80

c

400 continue

stop

end



## Appendix C.

### Conductivity Program

Program Etafit (input, output) ; By Ralph S. Baker

(\* Implements a golden section search to fit an eta value in the expression  $S = ((PSIB/PSI)**(1/ETA))$  to a given external set of S of PSI data \*)

(\* $\$I$ 'MATH' EXTENDED MATH DECLARATIONS. \*)

CONST NDATAPTS = 15;

TYPE DATAPTS = 1..NDATAPTS;  
PSILIST = ARRAY [DATAPTS] OF REAL;  
SLIST = ARRAY [DATAPTS] OF REAL;

VAR ETA1: REAL;  
ETA2: REAL;  
ETAMIN: REAL;  
ETAMAX: REAL;  
ETA: REAL;  
DELATMEAN: REAL  
DELTA1: REAL;  
DELTA2: REAL;  
PSI: PSILIST;  
S: SLIST;  
PSIB: REAL;  
SOIL: CHAR;  
I: DATAPTS;  
NITER: INTEGER;

FUNCTION SPRED ( ETA:REAL;  
PSI:REAL): REAL;

BEGIN  
SPRED : = POWER ((PSIB/PSI), (1/ETA))  
END;

PROCEDURE DELTACALC ( ETA: REAL;  
VAR DELTA: REAL;  
PSI: REAL;  
S : REAL);

(\* FOR A MEASURED VALUE OF PSI, CALCULATES CORRESPONDING VALUE OF DELTA, A MEASURE OF ERROR \*)

BEGIN (\* PROC DELTACALC \*)  
DELTA : = (S-SPRED(ETA,PSI))/SPRED(ETA,PSI)  
END; (\* PROC DELTACALC \*)

PROCEDURE DELTAMEANCALC (VAR ETA: REAL;

Continued next page

Program etaftit cont.

```
                                VAR DELTAMEAN: REAL);
(* GIVEN AN ETA VALUE THIS WILL YIELD A DELTA MEAN BY
READING THROUGH S OF PSI, REPEATEDLY CALLING DELTACALC, AND
STORING DELTA VALUES IN AN ACCUMULATOR; THEN IT CALCULATES
MEAN. *)
```

```
VAR      SPRED: REAL;
         DELTASUM: REAL;
         DELTA: REAL;
         I:      DATAPTS;
```

```
BEGIN (* PROC DELTAMEANCALC *)
```

```
    DELTAMEAN := 0;
    DELTASUM  := 0;
```

```
WRITELN;
WRITELN ('   ETA=',ETA:5:3);
WRITELN;
WRITELN ('   DELTA      PSI');
```

```
FOR I: = 1 TO NDATAPTS
DO BEGIN (* DELTASUM ACCUMULATION *)
    DELTACALC (ETA, DELTA, PSI[I], S[I]);
    WRITELN (DELTA:7:3, '      ',PSI[I]:5:2);
    DELTASUM := DELTASUM + DELTA
END; (* DELTASUM ACCUMULATION *)
```

```
DELTAMEAN := DELTASUM/NDATAPTS;
DELTAMEAN := ABS (DELTAMEAN)
END; (* OF PROC DELTAMEANCALC *)
```

```
PROCEDURE ITER (VAR ETA1 : REAL;
                VAR ETA2 : REAL;
                VAR ETAMIN: REAL;
                VAR ETAMAX: REAL;
                VAR DELTA1: REAL;
                VAR DELTA2: REAL);
```

```
(* EXECUTES REST OF ITERATIONS: COMPARES D1 AND D2;
RECOMPUTES ETAS AND DELTAS, CALLS DELTAMEANCALC, FOR
WHICHEVER OF ETA1 OR ETA2 IS REQUIRED *)
```

```
VAR DELTAMEAN : REAL;
    DELTA      : REAL;
    ETA        : REAL;
```

```
BEGIN (* PROC ITER *)
    IF (DELTA2>DELTA1)
```

Continued next page

Program etafit cont.

```
    THEN BEGIN (* IF D2>D1 *)
        ETAMAX := ETA2;
        ETA2   := ETAL;
        ETAL   := ETAMIN + (0.382)*(ETAMAX-ETAMIN);
        DELTA2 := DELTA1;
        DELTA1 := 0;
        ETA    := ETAL;
        DELTAMEANCALC (ETA, DELTAMEAN);
        DELTA1 := DELTAMEAN
    END      (* IF D2>D1 *)
ELSE BEGIN (* IF D1>D2 *)
    ETAMIN := ETAL;
    ETAL   := ETA2;
    ETA2   := ETAMIN + (0.618)*(ETAMAX-ETAMIN);
    DELTA1 := DELTA2;
    DELTA2 := 0;
    ETA    := ETAL;
    DELTAMEANCALC (ETA, DELTAMEAN);
    DELTA2 := DELTAMEAN
END;      (*IF D1>D2 *)
END;     (* PROC ITER *)
```

```
PROCEDURE ITER1 (VAR ETAL   : REAL;
                 VAR ETA2   : REAL;
                 VAR ETAMIN : REAL;
                 VAR ETAMAX : REAL;
                 VAR DELTA1 : REAL;
                 VAR DELTA2 : REAL);
```

```
(* EXECUTES FIRST ITERATION: CALCULATES ETAL, ETA2; CALLS
DELTAMEANCALC; DOES THIS FOR BOTH ETAL AND ETA2; COMPARES D1
AND D2; SETS UP FOR ITER. *)
```

```
VAR DELTAMEAN : REAL;
    DELTA     : REAL;
    ETA       : REAL;
```

```
BEGIN (* PROC ITER1 *)
```

```
    DELTA1 := 0;
    DELTA2 := 0;
    ETAL   := ETAMIN + (0.382)*(ETAMAX-ETAMIN);
    ETA    := ETAL;
    DELTAMEANCALC (ETA, DELTAMEAN);
    DELTA1 := DELTAMEAN;
    ETA2   := ETAMIN + (0.618)*(ETAMAX-ETAMIN);
    ETA    := ETA2;
    DELTAMEANCALC (ETA, DELTAMEAN);
    DELTA2 := DELTAMEAN
```

Continued next page

```
Program etafit cont.  
END; (* PROC ITER1 *)
```

```
BEGIN (* MAIN PROGRAM *)
```

```
  BEGIN (* INITIALIZING SOFPSI *)
```

```
    PSIB := 0;
```

```
    FOR I := 1 TO NDATAPTS DO BEGIN
```

```
      PSI[I] := 0;
```

```
      S[I] := 0
```

```
    END;
```

```
END; (* OF INITIALIZING SOFPSI *)
```

```
BEGIN (* READING IN PRELIMINARY DATA *)
```

```
  RESET (INPUT);
```

```
  READ (INPUT, PSIB, SOIL);
```

```
  READLN (INPUT);
```

```
  WRITELN;
```

```
  WRITELN;
```

```
  WRITELN (' SOIL NAME: ', SOIL:1);
```

```
  WRITELN (' PSI SUB B= ', PSIB:5:2);
```

```
  WRITELN;
```

```
  WRITELN ('PSI S')
```

```
END; (*READING IN SOFPSI DATA *)
```

```
BEGIN (* READING IN SOFPSI DATA *)
```

```
  FOR I := 1 TO NDATAPTS DO BEGIN
```

```
    READ (INPUT, PSI[I], S[I]);
```

```
    READLN (INPUT);
```

```
    WRITE (PSI[I]:5:3, ' ', S[I]:5:3);
```

```
    WRITELN
```

```
  END;
```

```
END (* READING IN SOFPSI DATA *)
```

```
BEGIN (* MAIN SEQUENCE *)
```

```
  ETAMIN := 0;
```

```
  ETAMAX := 1;
```

```
  ITER1 (ETA1, ETA2, ETAMIN, ETAMAX, DELTA1, DELTA2);
```

```
  NITER := 1;
```

```
  FOR NITER := 1 TO 9
```

```
    DO BEGIN (* ITERATION *)
```

```
      ITER (ETA1, ETA2, ETAMIN, ETAMAX, DELTA1, DELTA2);
```

```
      WRITELN;
```

```
      WRITELN (' ABS MEAN DELTA2=', DELTA2:7:3);
```

```
      WRITELN;
```

```
    END; (* ITERATION *)
```

```
  ETA1 := (ETA1 + ETA2)/2;
```

Continued next page

```
Program etafit cont.  
ETA := ETAl;  
DELTAMEANCALC (ETA, DELTAMEAN);  
WRITELN;  
WRITELN;  
WRITELN;  
WRITELN (' ETA OPTIMAL =', ETAl:5:3);  
WRITELN (' DELTA OPTIMAL =', DELTAMEAN:7:3);  
END; (* MAIN SEQUENCE *)  
  
END. (* OF PROGRAM ETAFIT *)
```



## Bibliography

- Bachmat, Y. and Elrick, D.E. (1970). Hydrodynamic Instability of Miscible Fluids in a Vertical Porous Column. Water Resources Res. 6: 156-171
- Bouma, J., Baker, F.G., and Veneman, P.L.M. (1974) Measurement of Water Movement in Soil Pedons above the Water Table. University of Wisconsin Information Circular Number 27.
- Brooks, R.H., and Corey, A.T. (1966) Properties of Porous Media Affecting Fluid Flow. Proc. Am. Soc. Civ. Eng., J. Irrigation Drainage Div., IR2: 61-68
- Bruce, R.R. and Klute, A. (1956) The Measurement of Soil Water Diffusivity. Soil Sci. Soc Am. Proc. 20: 458-462
- Clothier, B.E., Scotter, D.R., Green, A.E. (1983) Diffusivity and One-dimensional Absorption Experiments. Soil Sci. Soc. Am. J. 47: 641-644
- Corey, J.C. (1968) Evaluation of Dyes for Tracing Water Movement in Acid Soils. Soil Sci. 106: 182-187
- Diment, G.A., and Watson, K.K., and Blennerhasset, P.J. (1982) Stability Analysis of Water Movement in Unsaturated Porous Materials: 1. Theoretical Considerations. Water Resources Res. 18: 1248-1254
- Diment, G.A., and Watson, K.K. (1983) Stability Analysis of Water Movement in Unsaturated Porous Materials: 2. Numerical Studies. Water Resources Res. 19: 1002-1010
- Diment, G.A. and Watson, K.K. (1985) Stability Analysis of Water Movement in Unsaturated Porous Materials: 3. Experimental Studies. Water Resources Res. 21: 979-984
- Felt, E.J. (1958) Laboratory Methods of Compacting Granular Soils. Am. Soc. Testing Mats., 239, 89-110



Glass, R.J., and Steenhuis, T.S., (1984) Factors Influencing Infiltration Flow Instability and Movement of Toxics in Layered Sandy Soils. ASAE technical paper no. 84-2508

Hagoot, J. (1974) Displacement Stability of Water Drives in Water-wet Connate Water Bearing Reservoirs. Soc. Pet. Eng. J. 14: 63-74

Hanks, R.J., and Bowers, S.A. (1962) Numerical Solution of the Moisture Flow Equation for Infiltration into Layered Soils. Soil Sci. Soc. Am. Proc. 26: 530-534

Hill, E.D., and Parlange, J.-Y. (1972) Wetting Front Instability in Layered Soils. Soil Sci. Soc. Am. Proc. 36: 697-702

Hillel, D. (1980) "Introduction to Soil Physics" Academic Press, NY

Hillel, D. (1986) Unstable Flow in Layered Soils: a Review. Hydrologic Processes 1: 143-147.

Horton, R., and Wierenga, P.J. (1986) Preferential Flow of Water and Solutes in Structured Soils. Soil Sci. Soc. Am. workshop paper

Klute, A. (1965) Laboratory Measurement of Hydraulic Conductivity of Saturated Soil. in Black, C.A., ed. "Methods of Soil Analysis" American Society of Agronomy, Inc., Madison, WI

Lin, C.C. (1955) "Theory of Hydrodynamic Stability" Cambridge Univ. Press, London

Milly, P.C.D. (1985) Stability of the Green-Ampt Profile in a Delta-function Soil. Water Resources Res. 21: 399-402

Miller, D.E., and Gardner, W.H. (1962) Water Infiltration into Stratified Soil. Soil Sci. Soc. Am. Proc. 26: 115-118

- Mualem, Y. (1976) A New Model for Predicting the Hydraulic Conductivity of Unsaturated Porous Media, Water Resources Res. 12: 513-522
- Philip, J.R. (1957a) The Theory of Infiltration: 1. The Infiltration Equation and Its Solution. Soil Sci. 83: 345-357
- Philip, J.R. (1957b) The Theory of Infiltration: 2. The Profile at Infinity. Soil Sci. 83: 435-448
- Philip, J.R. (1957c) The Theory of Infiltration: 3. Moisture Profiles and Relation to Experiment. Soil Sci. 84: 163-178
- Philip, J.R. (1957d) The Theory of Infiltration: 4. Sorptivity and Algebraic Infiltration Equations. Soil Sci. 84, 257-164
- Philip, J.R. (1957e) The Theory of Infiltration: 5. The Influence of the Initial Moisture Content. Soil Sci. 84: 329-339
- Philip, J.R. (1975a) Stability Analysis of Infiltration. Soil Sci. Soc. Am. Proc. 39: 1042-1049
- Philip., J.R. (1975b) The Growth of Disturbances in Unstable Infiltration Flows. Soil Sci. Soc. Am. Proc. 39: 1049-1053
- Raats, P.A.C. (1973) Unstable Wetting Front in Uniform and Non-uniform Soils. Soil Sci. Soc. Am. Proc. 37: 681-685
- Saffman, P.G., and Taylor, G.I. (1958) The Penetration of Fluid into a Porous Medium of a Hele-Shaw Cell Containing a More Viscous Liquid. Proc. R. Soc. London Ser. A245: 312-331
- White, I., Colombera, P.M., and Philip, J.R. (1977a) Experimental Study of Wetting Front Instability in Porous Media. Second Australasian Conference on Heat and Mass Transfer, University of Sydney, pp. 107-113

White., I., Colombera, P.M., and Philip, J.R. (1977b)  
Experimental Studies of Wetting Front Instability Induced by  
Gradual Changes of Pressure Gradient and Heterogeneous  
Porous Media. Soil Sci. Soc. Am. J. 41: 483-489



